ABSTRACTS

NEVE ZOHAR 2007

ISRAEL GEOLOGICAL SOCIETY

Israel Geological Society, Annual Meeting

החברה הגיאולוגית הישראלית
Israel Geological Society

Abstracts

Editors: Onn Crouvi
Uri Malik
Orly Oren
Eyal Shalev
Vladimir Friedman
Yoseph Yechieli

NEVE ZOHAR **20-22.2.07**

Contents:

The geology of Timna copper mines

Alfaro R. M., Torres R. C., Mendoza T. C., Lopez D. G., Jimenez C. P.

Altos Hornos de Mexico, S.A. de C.V. (AHMSA)

ARAVA Mines is operating in the old mining area of TIMNA Copper Mines, the mines where closed since the early 80s. ARAVA Mines was granted by the government of Israel with exploration permit, prospecting license and certificate of discovery to conduct geological explorations including excavations, drillings and operating a copper pilot plant in an area of 12,620 dunams.

The mine is located in the Arava Valley, in the Southern part of Israel, 25 Km north of Elat. In the past two years the company conduct geological and geophysical studies and identified the directions and displacements of the faults affecting the zone, depending of the tectonic phase related, that is the case of the faults E-W, and NW-SE caused by the wedging of the openings of Dead Sea and Suez channel, with strikes N-S and NW-SE, secondary faults systems are result of different phases of tectonism.

As a consequence of the marine and continental hydrodynamics, there were deposited sandy sediments of different granulometry coming with finer sediments and clay, mainly containing manganese and iron. After, a hiatus related to a tectonic uplift because of younger intrusion inside the Precambrian igneous complex, followed by deposition of Cretaceous Rocks (sandstones, marls, shales, limestones). Once the geological column was formed, subsequently events were of fumarolic reactivation followed by the openning of Dead Sea where the hot solutions migrated affecting the minerals already existing of Cambric formation (Sasgon member) and more later to the cretaceous formations.

From the information obtained of old drilling and recent, geological and geophysical new data, we are performing a reinterpretation of mineral deposit in order to give a new geological model and determine the magnitude of mineral deposit.

An integrated model of the Lower Cretaceous sandy reservoir in the northwestern Negev from a combined well-seismic interpretation

Aksinenko T. [1], Grossowicz Y. [2], Weinberger G. [3], Reznikov M. [2], Sobolevsky L. [1].

1. Geophysical Institute of Israel, POB 182, Lod
2. Ecolog Eng. Ltd., Oppenheimer 5, Rehovot
3. Israel Hydrological Service, Jerusalem

Well log data and analyses of cuttings and cores (very few) were used to establish a petrophysical model of the Lower Cretaceous Kurnub Sandy Reservoir in the northWestern Negev. Model-based rock physics analysis of well-log data allows the recognition of reservoirs, clarify their lithology and relative mineral composition, and construction of salinity and sand isolith maps. This rock physics study provides the physical basis for understanding how changes in rock properties would affect seismic response. The inferred links between the elastic and bulk reservoir properties, combined with seismic impedance inversion allows to produce average porosity maps.

A number of reservoir parameters such as shale fraction, porosity, lithology, sonic times, bulk densities, salinity, water saturation were estimated. Then modeling and interactive seismic to well calibration was performed. These procedures allow mapping of interpreted horizons and building of a geological model of the reservoir. A relationship between porosity and acoustic impedance was documented. Seismically derived acoustic impedance data for each horizon was transformed to an average porosity. Such porosity prediction could improve reservoir characterization by providing information on the spatial variation of the reservoir away from existing well control.

The combination of geophysics, rock physics, and stratigraphy allows the recognition of structural and stratigraphic framework of the reservoir and establishing of the reservoir properties such as effective thickness and average porosity.

Using of high-frequency microtremor measurements for identification of fault zones and depth to reflector: Zevulun plain case

Aksinenko T. , Zaslavsky Y., Gorstein M., Kalmanovich M., Ataev G., Dan I., Giller D., Perelman N., Giller V., Livshits I., Shvartsburg A.

Seismology Division, Geophysical Institute of Israel, P.O. Box 182, Lod

The extensive database of H/V spectral ratios from microtremor over the Zvulun valley allowed reconstructing subsurface structure down to a basement and identifying faults.

H/V spectral ratios were calibrated and shear-wave velocity structure was derived at locations of the refraction survey and wells penetrating the hard basement (the fundamental reflector), which is the limestone of the Judea Group in the Central Horst; and limestone of the Ziqlag Fm. with or without gypsum of the Mavki'im Fm. in the Kishon Graben. At majority of the measuring sites intermediate a hard layer influencing the H/V ratio curve exists.

Based on the velocity model and spectral ratio analysis geological cross sections along reflection lines carried out in the study area were constructed. The location and vertical displacement of the inferred faults were compared with the results of geological interpretation of reflection lines. Some faults unmapped previously were detected and traced. Discrepancies in locations of the faults mapped by different authors are also revealed. Depths of the Top Judea Gr. at the Central Horst and the top Mavki'im/Ziqlag Fms. in the Kishon Graben were determined.

Our results show that high-frequency microtremors is effective for deducing geological structure from microtremor data recorded at a single site.

Interaction between smectite and oxalate

Amram K., Ganor J.

Department of Geological and Environmental Sciences, Ben-Gurion University of the Negev, 84105 Beer Sheva

Soil and ground water contain organic acids, which are both produced naturally by roots and microorganisms, and derived from anthropogenic sources. Any attempt to understand the effect of this compounds on the quality of water, must include the various interactions between the organic matter, the minerals and the soil. Cation release from clays significantly affects metal mobility and potential injection of toxic elements into these systems. The effects of organic acids on weathering in general and the mechanism, by which organic ligands enhance the dissolution of silicates in particular, have been the focus of scientific discussions for several decades.

As part of our on going attempt to describe the full rate law of smectite dissolution, the aims of this research are to study the effect of oxalate on the different dissolution mechanisms of smectite, to construct sorption isotherm of oxalate to smectite surface and to understand the effect of smectite surface on oxalate degradation.

Smectite dissolution rates were studied at pH 1.5-5 and temperature 50±0.1°C using a flow-through system. Oxalate sorption to smectite surface was studied at pH 1.5-5 and temperatures of 25 and 50±0.1°C using a batch experiments.

A fast decrease in oxalate concentration is observed during the first 15 minutes of the adsorption experiments. No further change was observed during the following 2 hours. Our results show that even with no smectite, oxalate is degraded or consumed over long period of time (several hundreds of hours). However, the insignificant change in oxalate concentration after the first 15 minutes verifies that the oxalate decomposition is negligible during the short period of the adsorption experiments. Oxalate adsorption on the smectite is higher at 50°C than at 25°C, and is independent of pH.

Most flow-through experiments at 50°C show stoichiometric dissolution. Preliminary results at pH 3 and 3.5 show that the dissolution rate is faster in the presence of oxalate than without oxalate. At pH 2, there are some inconsistencies in the results, and some experiments show even apparent inhibition effect of oxalate on the dissolution rate.

Infiltration processes and flow rates - monitoring environmental & artificial tracers in cave drippings - Mt. Carmel, Israel

Arbel Y.[1], Greenbaum N. [1], Lang J. [2], Inbar M. [1].

1. Department of Geography and Environmental Studies, Haifa University, Israel, 31905.
2. Hydrology Institute, Freiburg University, Germany.

The aim of the study is identification and quantification of the different infiltration processes in the carbonate, karst lithology of Mt. Carmel. Major ions concentration, temperature, EC, pH and water discharge were measured weekly in 14 cave drips, in two locations: "Yishach Caves" in the Yagur Dolomite formation and "Oranin cave" in the Muchraka limestone formation. Rainfall and soil moisture profile above the cave were monitored continuously using tipping buckets and FDR probes. In addition, an artificial tracer experiment was conducted: Uranine – a fluorescent dye tracer, was injected into the bottom of nearly saturated soil pockets at the surface above the cave (28m) before major rainfall event. Caves drips where sampled for chemistry and Uranine up to 4 times a day; discharge was monitored continuously by tipping bucket.

Based on the response characteristics to rainfall we distinguished among 3 types of cave drips: perennial, seasonal and post-storm drips, which also reflect differences in the relative contribution from the different infiltration processes. Seasonal drips and post-storm drips emerged only after cumulative seasonal rainfall of 180-530 mm. Fluctuation in water temperature, EC and ions concentrations, following major winter storms, serve as indicators to the fraction of preferential flow versus piston flow and wetting front infiltration. For example, the lag of 12-24 hours between the appearance of the Uranine tracer and the beginning of storm-dripping hydrograph, together with the higher salinity and temperature suggest a piston flow mechanism. The "Post-storm" drips, related to the intensive jointing in the rock above the cave start 12-48 hours after rainstorms. Discharge builds up to its maximum in a few hours, and completely decays after 2-3 weeks. The tracer breakthrough curve reinforces this hydrograph pattern. The perennial drips are characterized by stable discharge and higher salinities, nevertheless, post-storms discharge peaks were identified. The total preferential flow component in those drips was calculated using end member mixing analysis at 25-30% of the annual discharge. The maximum flow rates derived from the time of Uranine appearance was 57-70 cm/hr (in all drips). The typical (frequent) flow rates derived from the time to Uranine peaks were 15-23 cm/hr in the seasonal and perennial drips and 37-47 cm/hr in the post-storm drips. The difference between the mean flow rates of the various drip types is even larger as estimated from the late-appearance of the Uranine peaks in the seasonal and perennial drips.

Preliminary results indicate several possibilities: (1) Separate piston flow and preferential flow components of the infiltrating water (2) Calculate the contribution from the different infiltration processes as a response to rainstorms magnitude and distribution through the season; (3) Evaluate the maximal and typical flow rates in the unsaturated zone above the cave using the Uranine breakthrough curve.

Velocity model of the Levant basin using seismic and well data

Ariely R., Trachtman P., Gardosh M.

Geophysical Institute of Israel, Habaal Shem Tov 6, Lod, Israel.

This project was aimed to estimate the acoustic velocities and to build a 3D velocity model of the Levant basin-fill, offshore Israel. Velocity information was obtained from stacking velocities of 2D, seismic reflection profiles and from check-shot surveys in offshore wells. The sources of information were combined, considering the accuracy of the data and its compatibility with the geological interpretation. The velocity model includes eight layers that correspond to the main stratigraphic units identified on seismic profiles within the basin-fill.

Building the velocity model involved the following steps: (a) Acquiring all available velocity information and estimate RMS, stacking velocities at the interpreted horizons, (b) Construction of 2D RMS, stacking velocity sections, (c) Building RMS velocity 3D cube models that were manipulated from the data using interpolation and extrapolation and, (d) Converting these 3D models to average and interval velocities, 3D cube models. The results show an increase in the acoustic velocities from the margin in the east towards the basin in the west. This effect is explained by the increased depth of burial and degree of compaction of the various sedimentary units.

The velocity model was used in two applications. First, as a guide function for horizon velocity analysis that was performed in pre-stack depth processing of four selected lines. Second, in depth conversion of regional, time-structure maps derived from the seismic interpretation. The conversion incorporates the velocity variations within the sedimentary section and therefore produces a more accurate depth model of the subsurface of the Levant Basin.

Origin, mobilization and depositional processes of copper in the Timna area: Evidence from copper, strontium and lead isotope ratios

Asael D. [1,2], Matthews A. [1], Bar-Matthews M. [2], Halicz L. [2], Harlavan Y. [2], Segal I. [2], Ehrlich S. [2].

1.Institute of Earth Sciences, Hebrew University of Jerusalem, 91904 Jerusalem, Israel
2.Geological Survey of Israel, 30 Malkhe Israel St., 95501 Jerusalem, Israel

Copper, strontium and lead isotope ratios in copper minerals from the Timna Valley and Mt. Amram areas of Southern Israel were studied in order to understand the ore genesis. A whole range of copper mineralization processes occurs in the area including: altered primary ores in Precambrian quartz porphyries; Cu-sulphide deposition during Cambrian marine dolomite diagenesis and their oxidation to give malachite; epigenetic remobilization giving veins of paratacamite and copper silicates in Cambrian sandstones and shales; deposition of Cu-sulphide concretions and their oxidation in Lower Cretaceous sandstones. All isotope measurements were made using MC-ICP-MS after ion chromatographic separation.

In accord with experimental studies showing that there should be $^{65}Cu/^{63}Cu$ isotopic fractionation between reduced and oxidized Cu-minerals, $\delta^{65}Cu$ values of Cu-sulphides are significantly lower (-3.8 to -0.4‰) than Cu(II) minerals (-1.2 to 1.85‰). There are also regional variations in the Cu-isotope composition. Copper minerals from Lower Cretaceous Amir Formation at Timna have Cu sulphides with $\delta^{65}Cu = -2.4 \pm 1.1$‰ and Cu(II) minerals with $\delta^{65}Cu = -0.6 \pm 0.4$‰, whereas all values are shifted up by about 1.6‰ at Mt. Amram. This suggests different Cu sources at these locations. Cu(II) minerals, which constitute most of the Cu in the system, show $\delta^{65}Cu$ values of ~0.08±0.5‰, consistent with the fact that the ultimate source of copper in the Timna area was Precambrian igneous rocks. Cu-isotopic zoning in the Cu-sulphides from the Cambrian dolomite suggest they were precipitated from small disconnected Cu reservoirs. Mass balance modeling of the Cu isotope system in the Precambrian and Cambrian rocks of the Timna valley was made using Matlab software. The calculations indicate that the main copper reservoir is the Cambrian sandstone and shales and that the Cu sulphide reservoirs are very small. Most transport of Cu in the Timna basin therefore occurred in relatively oxidized conditions. Sr isotope values vary between $^{87}Sr/^{86}Sr = 0.7066$ to 0.7096 and fall into three groups. I. Cu sulphides from the Timna Formation dolomite with the lowest values (0.7066-0.7072). II. Cu silicates and malachite from the Timna Formation and Cu minerals from Amir Formation in the Timna valley with similar and intermediate values (0.7076-0.7086), thus suggesting the same sources for the copper –bearing solutions. III. Cu minerals from Amir Formation at Mt. Amram with the highest values (0.7086-0.7096), suggesting they were derived from a different source, possibly direct leaching of the underlying igneous rocks of Mt. Amram. A $^{207}Pb/^{204}Pb$ vs. $^{206}Pb/^{204}Pb$ plot for the copper minerals from the two exposures of the Amir Formation samples indicates two distinctly different compositional areas. Thus, all three isotopic systems point to different sources of the metallic elements in the Timna Valley and Mt Amran copper mineralization exposures.

Ambient vibration measurements for accurate interpretation of existing geological data in the Southern Sharon

Ataev G., Zaslavsky Y., Gorstein M., Kalmanovich M., Ezersky M., Aksinenko T., Giller D., Perelman N., Giller V., Livshits I., Dan I., Shvartsburg A.

Seismology Division, Geophysical Institute of Israel, P.O. Box 182, Lod, Israel

Seismic measurements of H/V spectral ratios of ambient vibrations were used for 1D modeling of the subsurface. We carried out ambient noise measurements at 580 locations within the area of the Southern Sharon and revealed the spatial distribution of the resonance frequencies of the soils and their respective H/V amplitudes. This information was added to the available geological, geophysical and bore-hole information in order to model the sub-surface. 1D sub-surface models were derived by way of fitting the limited information about the subsurface layers and seismic velocities, the analytical transfer function of the soil column and the observed resonance frequency and H/V amplitudes of the fundamental mode.

This study demonstrates, again, that the Top Judea Group is not always the main reflector of seismic waves that is responsible for the amplification effects but only its dolomite and limestone layers. The H/V technique has identified more accurately the major reverse fault, which divides the study area into the northWestern and southeastern parts, and the known Yarkon, Kfar Ganim faults. This technique has also identified several new east-west faults with a horizontal component of slip. These faults separate some structural blocks of different depth.

In the east of the study area, bordering the high velocity layers of Senonian-Eocene-Oligocene deposits (marl, chalk, limestone), we detected zones of possibly eroded terraces.

In the present study we do attempts to estimate accuracy of reflector depths determination in dependence on accuracy of resonance frequency and layer velocity.

Eocene-Oligocene tectono-sedimentary stages of rifting in the northern tip of the Red Sea and its environs: A key to the early breakup stages of the Arabo-Nubian plate

Avni Y. [1], Segev A. [1], Ginat H. [2]

1. Geological Survey of Israel, 30 Malkhe Israel St., Jerusalem 95501
2. The Arava Institute for Environmental Studies, Kibbutz Ketura,

Widespread intraformational Eocene conglomerates (Themed cgl.) were found in Sinai, the Eastern Desert of Egypt, Southern Israel and Southern Jordan. In places (Wadi Abura, Western Sinai, east of Temed, Eastern Sinai) these conglomerates are overlain by, and interfingered with, marine Eocene intercalations. Such Eocene conglomerates indicate tectonic activity and sedimentary instability that increased on a regional scale toward the south. Sporadic exposures point to vertical movements of up to several hundred meters. The Eocene conglomerate relics were preserved within Early Oligocene downfaulted blocks. The dispersed deformation of this extensional tectonics resulted in north-south, east-west and northwest trending fault systems, representing an early stage that pre-dated the Red sea rifting and pre-dated the localization of faults such as the present pattern exhibits. Later, the regional erosion surface, which developed during the Oligocene and the Early Miocene, emphasized the preexisting tectonic relief. Miocene conglomerates overlying this erosion surface include redeposition of much earlier materials, such as Cambrian quartzite and magmatic rocks from the Precambrian basement. This indicates an early (Oligocene – Early Miocene) uplifting of the regions bordering the Red Sea, south Sinai and some areas along the Dead Sea Transform. In other areas the pre-Miocene tectonic activity downfaulted large blocks, preserving the Eocene-Oligocene sequence. The major morphotectonic event, which uplifted the region and dictated most of the present day morphology (including the uplifting of the Sinai sub-plate to an elevation of more than 2500 m) occurred during the Middle – Late Miocene, after the deposition of the Hazeva Formation.

The distribution of the intraformational Eocene conglomerates and their expanded increase toward the south, where the Afar tectono-magmatic event caused the updoming centered in Ethiopia and Yemen, indicates mutual genetic relationships.

Rifting - Initiation by tension revisited

Bahat D.

Department of Geological and Environmental Sciences Ben Gurion University of the Negev, Beer Sheva, 84105

What are the mechanical principles for this concept? Why aren't they supported by seismic data? What are the dozen examples that demonstrate this concept?

Principles: 1. Griffith's observation (1924) that "in such tests of stone and like materials as are available the crushing strength is from 7 to 11 times the tensile strength". This distinction (as supported later by others) requires earlier fracture by tension than by shear when stresses are applied. 2. When shear (mode II) is applied on a uniform body and overcomes its strength, only mode I fracture can be produced, compared with another situation when mode II is applied along a straight contact between two bodies that are strongly compressed together. Only in the latter case a mode II fracture may be formed. When this principle is translated to earth dimensions, an early earthquake fault that has been completely healed and sealed can fracture again only by mode I, compared to partly healed fault, which can be parted by mode II fracture, caused by an earthquake. Hence, the degree of healing and sealing determines the type of early rifting. Long intervals between subsequent earthquakes along the Dead Sea Rift would require tensile rejuvenations of the rift. Ignoring: These arguments and expectations are not backed by scientists whose research rests on focal mechanism methods that do not include exclusive mode I readings, and therefore they "do not see evidence for ''pure'' tensile fracturing''.

Representative examples: For instance, fault bifurcations that were induced by the 1968 earthquake along the San Jucinto fault zone (a branch of the San Andreas) display surface tensile characteristics (Bahat, 1982). Additional examples: At the meeting.

A new effect of sub-critical multi-scale tensile/shear alternating fracturing

Bahat D. [1], Rabinovich A. [2], Frid V. [1], Brosch F.J. [3]

1. Department of Geological and Environmental Sciences Ben Gurion University of the Negev, Beer Sheva, 84105
2. Department of Physics, Ben Gurion University of the Negev, Beer Sheva, 84105
3. Institute of Engineering Geology and Applied Mineralogy, Technical University Graz, A-8010 GRAZ, Austria

Fractured surfaces of PMMA glass display plumes that are similar to those which decorate joints cutting rocks in geological outcrops. The PMMA plumes show under the microscope, a regular division into curved couples of dark-smooth tensile zones, alternating light-ragged shear zones. Magnification reveals that the primary ragged zones are further sub-divided into secondary smaller alternating, curved tensile smooth, and shear ragged zones. The secondary shear zones are again subdivided into smaller tertiary couples of tensile and shear zones. On the other hand, the primary, secondary and tertiary tensile zones remain smooth and undivided. Silicate glass ceramic fractured by uniaxial compression reveals under the microscope a multi-scale tensile/shear alternating fracturing similar to the one observed in the PMMA glass, but, with certain deviations from the regularity exhibited by the PMMA. These deviations from the regularity are attributed to the higher fracture velocity in the glass ceramic than in the PMMA. Microscopic examination of plumes that decorate joints found in rock outcrops, discloses the same multi-fracture phenomena, which are seen in the PMMA and glass ceramic. However, the graininess of the rock seems to camouflage the exact pattern of the secondary division. Thus, the fractography of these sub-critical plumes is not an indication of merely a tensile, mode I fracturing as has hitherto been thought. It is in fact a product of a complex mixed mode I and III loading, which is greatly conditioned and enhanced by the fracture boundaries of each material.

Reactivation and reshaping of the central Israel continental margin in Late Eocene - Early Oligocene

Bar (Farago) O. [1,2], Gvirtzman Z. [2], Zilberman E. [2], Feinstein S. [1]

1. Department of Geological and Environmental Sciences, Ben Gurion University of the Negev, 84105 Beer Sheva
2. Geological Survey of Israel, 30 Malkhe Israel St., 95501 Jerusalem

The highland of central Israel and Jordan is separated from the Levant Basin by three NNE oriented structural steps: 1. The eastern step – the western mountain front (WMF), ca. 500 m high, separates the Judea mountain plateau from the foothills and the Coastal Plain. 2. The middle step – the Coastal Plain step (CPS), which separates the Coastal Plain from the marine Jaffa Basin, is buried under Oligocene to Pleistocene sedimentary section and has no morphological expression at the current surface. 3. The western step, extends along the present shelf edge.

We suggest that the separation of the highland of Israel and Jordan from the Levant Basin began in the time range between Late Eocene to late Early Oligocene, by tectonic reactivation of the two eastern steps, and possibly also the western one.

The constraints for the earliest age of reactivation of the two eastern steps are somewhat circumstantial: 1. Similar stratigraphic sections of the Senonian to Middle Eocene Mt. Scopus and Avedat groups are present on both sides of the WMF and CPS. 2. Fragments of Judea and Mt. Scopus groups are not found anywhere within the Mt. Scopus and Avedat groups in the piedmonts of the WMF, suggesting that the WMF was still not exposed during their sedimentation. 3. Previous studies showed that a gentle ramp existed during deposition of the Avedat Group. 4. Angular unconformities indicate that only one third of the WMF structure was formed during the deposition of the Mt. Scopus Group. 5. Deep submarine canyons crossing the CPS did not exist during the deposition of the Mt. Scopus and Avedat groups, but were formed soon afterward. Thus, although these steps might have earlier roots, we argue that their present structure postdates the Early to Middle Eocene Avedat Group.

Constraint on the youngest possible age of the reactivation is derived from the late Early Oligocene Ashdod Clasts, deposited in the Jaffa Basin. These Clasts contain fragments derived from the Judea Hills, and probably record the erosion that shaped the mountain plateau, which truncates the folded layers of the WMF. Moreover, these clasts were also deposited in the bottom of the deep submarine canyons that cross the CPS, and cover the CPS piedmont. Those relations indicate that the formation of the WMF and CPS predate the late Early Oligocene, although they may have continued to develop later.

The influence of dairy farm on ground water quality in the Coastal aquifer: Preliminary results

Baram S.[1], Dahan O.[1], Arnon S.[1], Shore L.[2], Gross A.[1], Ronen Z.[1], Cohen K.[2]

1. Department of Environmental Hydrology & Microbiology, Zuckerberg Institute for Water Research, Blaustein Institutes for Desert Research, Ben-Gurion University of the Negev, Sede Boqer Campus, Israel
2. Kimron Veterinary Institute, Bet-Degan, Israel.

Concentrated animal feeding operations such as dairy farms have recently been shown to be a source of contaminants, such as nitrates, brines, organic matter, hormones and antibiotics. Although dairy farm-operations are currently undergoing critical revisions in order to reduce their potential negative impact on water resources, little is known about the long-term impact of pollutants stored in the vadose zone. Considering the importance of the Israeli coastal aquifer, and the relatively high number of dairy farms situated on top of the coastal plain, there is an urgent need to better understand pollutant transport from dairy farms to groundwater.

A typical dairy farm in the 'Beer Tuvia' region was chosen to study the impact of dairy farms on ground water quality. The farm has been operating in the same way for the last 40 years, releasing manure and effluents from the feeding lots and shelters to a storage lagoon, which was regularly drained to a stream channel. It should be emphasized that until recently this was the common waste disposal practice that used by all dairy farms.

The lithology in the study site consists of 8 m of clay layer on top of sand and calcareous formation. The ground water table is situated at a depth of 46m. Contaminant distribution under the dairy farm was estimated from ground water samples, sediment samples and by using a novel vadose zone monitoring system (VZMS), which allows us to quantify continuously water and contaminant fluxes from the land surface down to the groundwater. The VZMS is installed under the waste lagoon to a depth of 40 m, and it consist of 10 units of Flexible TDR probes (FTDR), EC probes, thermocouples and water sampling cells.

Preliminary results of the ground water chemistry underneath the farm, show a high concentration of Cl^- (1114.4 mg/l), NO_3^- (192.1 mg/l), as well as the presence of testosterone and estrogen, while the concentrations up stream are much lower, with Cl^- (585.9 mg/l), NO_3^- (59 mg/l, and no detectable hormones. In addition, sediment and poor water samples from the vadose zone suggest direct contribution of contaminants from the dairy farm to the underlying groundwater. Integrated assessment of contaminant leaching from dairy farms will support the estimation of the risk to groundwater quality in areas with dense dairy farm operation above the Israeli Coastal Aquifer, and will also support the development of remediation strategies to minimize the legacy from dairy farm wastes.

Temporal changes of variance in radon time series from the Elat granite, Israel

Barbosa S. M. [1,2] Steinitz G. [3], Piatibratov O. [3], Silva M. E. [1], Lago P. [1].

1. Dept. of Applied Mathematics, University of Porto, Portugal
2. Danish National Space Center, Copenhagen, Denmark
3. Geological Survey of Israel, Jerusalem, Israel

High-rate radon monitoring is being carried out in the geogas of a homogeneous, massive, jointed granite body at Elat, Israel. The collected time series display a compound temporal pattern, which includes long-term (multi-year) variations, seasonal variations, non-periodic (multi-day) variations and periodic diurnal variations (Steinitz et al, 2006). Furthermore, the radon time series exhibit temporal variability in variance (heteroscedasticity).

Here, heteroscedastic features of radon time series are investigated through the analysis of radon measurements over 2 complete years (2003-2004) from two boreholes at the Elat Granite. The variance of radon counts is computed for consecutive 7-days segments spanning the entire 2 years record. Constancy of variance is assessed through a nonparametric test of randomness, the runs test. Furthermore, the association between the variance of each segment and the overall mean radon level is investigated by linear regression.

For comparative purposes, a similar analysis is carried out for 6-hour time series of other geophysical variables for the Elat area, obtained from the NCEP/NCAR reanalysis dataset, specifically: air temperature, atmospheric pressure, precipitation rate, precipitable water (for the entire atmospheric column), net long-wave radiation, net short-wave radiation, cloud forcing net solar flux and ground heat flux.

The results show that air temperature, precipitation, and long-wave radiation time series exhibit constant variance over the analyzed period, while radon time series, atmospheric pressure, short-wave radiation, ground heat flux and net solar flux exhibit temporal changes in variance. Furthermore, for radon and radiation time series the variability is associated with the overall mean radon or radiation level, while for atmospheric pressure such an association is not present. These differences in the statistical characteristics suggest that air temperature and atmospheric pressure are not driving the radon signal in the subsurface.

Discriminating quarry blasts and natural seismicity at local distances by pattern recognition: Case study from the Northern Dead Sea fault region

Barzilay S. [1,2], Wust-Bloch G. H. [1], Ben-Horin Y. [2], Ben-Avraham Z. [1]

1. Dep. of Geophysics and Planetary Sciences, Tel Aviv University, Tel-Aviv 69978, Israel
2. Israel National Data Center (NDC), SOREQ Nuclear Research Center, Yavne 45832, Israel

The performance of pattern recognition-based seismic detectors (Joswig, 1999) was evaluated at local distance with natural and man-made sources. These weak (ML 1.5 - 3.0) events were discriminated by SparseNet (Joswig, 1999), a sonogram analysis software integrating broadband self-adaptive filters for signal energy (Joswig, 1990). The Northern Dead Sea fault region was selected for this case study because it has a remarkable record of both local seismicity and of blasting activity, which is recorded by the MMAI (Mount Meiron) array.

A reference catalog of 90 events (earthquakes, explosions and possible explosions) generated between January 2004 and January 2006 within a 30 km radius from MMAI array was designed for the analysis. The vertical channels of five sensors (MMA0, MMC1, MMC4, MMB2 and MMA3) were picked for the analysis. Blast events from five active quarries were sampled to have a complete azimuthal coverage. One single master pattern (MP) was selected for each quarry. Despite the variability of natural seismicity, it was also possible to select a single representative MP for weak earthquakes.

Results confirm that path dependency is negligible at local distances (< 30 km) and that discrimination performance remains strongly distance sensitive. Using two MPs at MMA0, MMC1, MMC4, MMB2 and MMA3 gave a successful recognition rate for blast event of 95%, 75%, 86%, 86% and 89% respectively. Using additional MP's can further improve the recognition rate. One single MP at MMA0 produced a recognition rate of 95% for earthquakes. No misclassification was found between earthquakes and quarry blasts. Although the MMAI array functions under optimal SNR conditions, our analysis shows that recognition performance decreases when MP's are imported from one sensor to another. It is optimal to sample a MP and use it for discrimination analysis at the very same sensor.

The geochemical cycle of ^{10}Be in the Dead Sea drainage system: Towards the use of Lake Lisan sediments as a high -resolution production rate archive

Belmaker R. [1], Lazar B. [1], Beer J. [2], Stein M. [3]

1. Institute of Earth Sciences, Hebrew University, Jerusalem 91904, Israel
2. Swiss Federal Institute of Environmental Science and Technology (EAWAG), Ueberlandstrasse 133, CH-8600, Dübendorf, Switzerland
3. Geological Survey of Israel, Jerusalem 95501, Israel

The potential use of the Dead Sea and Lake Lisan sediments (the Pleistocene precursor of the Dead Sea) as archives of ^{10}Be production rate was evaluated by analyzing ^{10}Be concentrations in detrital and chemical aragonite material from Lake Lisan and by constraining the geochemical behavior of ^{10}Be in the modern Dead Sea hydrological-limnological system. Analyses included modern dust, terra rossa soil (eolian in origin), loess from the Negev desert, flood suspended load and waters along a rain-flood evolutionary pathway.

The terra rossa soil yielded ^{10}Be concentration of $1.24\pm0.07\times10^{9}$ atoms$\times$gr^{-1} an order of magnitude higher than in modern dust ($1.6\pm0.8\times10^{8}$ atoms$\times$gr^{-1}) indicating long (100-500y) residence time of the terra rossa soil on the Judea Mt., that enables continuous absorption of ^{10}Be from rainwater. The removal of ^{10}Be by the soil particles is demonstrated by the continuous decrease in ^{10}Be concentration throughout the flood profile (from 8.2×10^{3} atoms$\times$gr^{-1} in the runoff to $\sim1\times10^{3}$ atoms$\times$gr^{-1} in the Dead Sea water). Overall, it appears that during periods of fast dust-fine detritus turnover (e.g. short residence of the dust on the Judea Mt.) ^{10}Be is rapidly transported from its atmospheric source to the Dead Sea basin and stored within the fine detrital and aragonite sediment inventories of the lacustarine formations where its concentration reflects a mixture between the annually produced and recycled ^{10}Be components. This situation characterized the high-stand period of Lake Lisan when fine-detritus eolian material was annually transported into the lake. During low stands of the lake (e.g. the Holocene Dead Sea), terra rossa inputs increased and ^{10}Be reflects mixing between soil and local dust. Additional support towards this mechanism is evident in the significant ^{10}Be concentration peak during the Laschamp excursion where enhanced production of cosmogenic isotopes is expected. These observations lay the foundations for the use of Lake Lisan sediments as a high-resolution low latitude production rate archive.

Composite digital database of the Yarqon-Taninim aquifer and its applications on an industry-standard oil exploration expert system

Ben-Gai Y. [1], Steinberg J. [1,2], Fleischer L. [1], Goldberg I. [1], Gendler M. [1], Dafny E. [2], Gvirtzman H. [2]

1. Geophysical Institute of Israel, POB 182 LOD 71100
2. Institute of Earth Sciences, Hebrew University, Givat Ram, JERUSALEM 91904

The Yarqon-Taninim aquifer is spread over a large area in central Israel and is one of the major sources of fresh water in the country. Its operation is subject to many factors, and one way of dealing with operational scenarios is through a computerized flow model. Such model requires a detailed database to support, among other parameters, its structural and lithological skeletons.

The task of constructing such skeleton is similar in nature to oil exploration workflow, which requires an "expert system" to manage a database and run specific programs that apply analytical procedures on its content. These programs are used for presenting and analyzing seismic data, lithologic data and geophysical borehole measurements.

We selected an industry-standard PC-based system, the Kingdom Suite, to handle this task. The database currently holds few tens of seismic sections, key structural maps and about 70 wells that were reconstructed for missing lithological information at the Judea Group and upper Kurnub Group interval, and were analysed to extract petrophysical attributes. The system can combine this information, all in digital form, into composite presentations that strongly enhance spatial correlations and allow construction of statistical analysis of a variety of parameters over user-specified subsurface intervals. The process of constructing this database involves, among other tasks, retrieval of old analog borehole data and reformatting into digital form. This process ensures long-lasting and easily accessed archive of an important source of subsurface data.

Evolution of talus chronosequences in extremely arid regions

Boroda R. [1,2], Amit R. [1], Eyal Y. [2], Porat N. [1]

1. Geological Survey of Israel (GSI),30 Malkhe Israel St.,95501 Jerusalem
2. Geological and Environmental Sciences, Ben-Gurion University, 84105 Beer Sheva

Talus-flatirons are characteristics landforms in arid and semi-arid zones. Their origin corresponds initially to slopes covered by debris, which later are incised by fluvial erosion while some relicts remain isolated in the drainage basin. The relict slopes have a triangular shape with their apex toward the scarp. The repetition of several alternating such stages leads to the generation of several sequences of talus flatirons with the more ancient ones located further from the scarp. Such talus chronosequences located in extremely arid areas in the Negev and Judea desert enable us to test the control of climate change parameter on their formation and to model their formation process. The most accepted conceptual model of their origin is the one related to climatic changes.

Several talus chronosequences in the Judean Desert, Zuk Tamrur area, were geologically and geomorphologically mapped (1:10,000). All the sequences have similar lithology of hard rock capping soft rocks. Talus profiles were measured by SOCET SET and the topographic profiles of the rock below the colluvium were detected by GPR. The different age groups (A-C) of the talus relicts were trenched exposing the colluvial sediments including the soil catena. The colluvial sediments and soil catena were described, analyzed and dated by OSL.

The mapping results and the longitudinal topographic profiles analysis of the talus sequences at the study sites stress the fact that no much scarp retreat occurred during the talus flatiron chronosequence formation. High number of continuous beside discontinuous taluses were detected and several reconstructed talus relicts show that they are related to the recent cliff position with no any indication for significant cliff retreat. All the talus relicts which were analyzed showing gypsic-salic soil catena with no indication to calcic paleosols or any intense biogenic activity or buried organic material which can point at previous vegetation cover of these taluses.

These results can not support a climatic change as a main control of their formation. The process of their formation must be searched at the balance between the production - deposition – and removal of particles under similar climatic conditions with no severs cliff retreat.

The Denya cave project for dating paleo-seismic activity in the Quaternary

Braun Y.[1,2], Bar-Matthews M.[2], Ayalon A.[2], Kagan E.[1,2], Agnon A.[1]

1. Institute of Earth Sciences, Hebrew University of Jerusalem, 91904 Israel
2. Geological Survey of Israel, Malkhei Israel, Jerusalem 915509 Israel

A study conducted in the Mount Carmel region at Denya Cave suggests that examination of broken speleothems enables precise dating of damage related to ancient earthquakes. Following the work of Kagan (2002) in the Judean Hills, in which dates were consistent with independent evidence for strong earthquakes, we present here initial results obtained in the Denya Cave project.

The region of Mount Carmel has many karstic features, which can be used in a comprehensive paleo-seismological study of the fault system that defines it. The Denya neighborhood of Haifa is situated on the south side of the mountain on a spur sloping to the west from the summit of Mount Carmel, toward the town of Tirat Ha-Carmel. Circa 500 m northwest of the cave opening we found evidence of a previously existing cave and faulting, which seems to have caused the collapse of that cave.

Work in Denya Cave to date includes initial collection of speleothem samples suspected of being seismites (broken or deformed speleothems that could result from seismic activity) and their dating using the $^{230}Th/^{234}U$ method. Use of this method has a 350 to 500 kyr limit, which can vastly increase the seismic record of the Quaternary in this region. Measurements for dating are conducted on the Multiple Collector Inductively Coupled Plasma Mass Spectrometer (MC-ICP-MS), which gives results of high analytical precision (ca. 1% or less).

The collection of samples and processing of findings is in its initial stages. Nevertheless, the study has given results of some significance. Two distinct growth phases were detected in two samples, while several additional samples clearly show either pre-seismic or post seismic phases. A preliminary conclusion based on the dating of one of the seismites, shows that ca. 22.5 kyr ago, an event occurred which broke a stalagmite. Its re-growth occurred only 10 kyr later. Other results show damage to speleothems occurring ca. 40 kyr and 70 kyr ago. These results suggest that further studies of this type may be diagnostic of seismic activity on the Carmel Fault during the Quaternary, which has eluded paleoseismic investigations thus far.

Mapping ranks of potential denudation along the Mediterranean Israeli coastal cliffs

Calvo R., Ilani S., Zilberman E.

Geological Survey of Israel, 30 Malkhe Israel St., Jerusalem

Some 45 km of the total Israeli coast line (225 km long) have a Kurkar (eolinite) cliff within 250 m of the seashore. The longest continues cliff, 11 km long, is located north of Herzliyya, in a high populated area.

The Kurkar coastal cliffs of Israel are continuously destroyed by erosive forces (winter storms and waves) and by gravity instabilities (related to height and slope of the cliff). Thus, denudation of the cliffs is widespread, particularly along the "Sharon cliffs", extending between Herzliyya and Bet Yannay.

The denudation rate is influenced by the cliff morphology and lithological characters such as: the degree of the Kurkar cementation, the position of paleosols (the Netanya and Nachsholim Hamra) in the exposed cliff, and the relief of the unconformity surfaces between the stratigraphic units that build the cliff. However, the dominant factor that determines the rate of cliff retreat is its distance from the coast line.

In the current study we applied GIS software in measuring morphological parameters (height, slope and distance to the shoreline) along the Mediterranean coast. All measurements were made based on the digital elevation model (DEM) of Israel with cells having a spatial ground resolution of 25 m (Hall, 1997), and using ArcGIS Geoprocessing tools written especially for the study (Calvo et al., 2006).

Using these parameters, we established a ranking of relative risk. These ranking levels allow an awareness of the more dangerous segments of the cliff. Our GIS analyses found that the cliff extending between Herzliyya and Nahal Poleg has the highest risk rank, in accord with previous field observations. The second problematic section is located between Nahal Poleg and Bet Yannay. Here, the risk rank is also high, and in addition, it is located within a short distance of neighborhoods in Netanya.

Isotopic concentration of Carbon in pore-water of the unsaturated zone: implications for improved dating of groundwater with ^{14}C

Carmi I. [1,2], Kronfeld J. [1], Yechieli Y. [2], Yakir D. [3], Stiller M. [2], Boaretto E. [3]

1. Tel-Aviv University, Tel-Aviv, Israel
2. Geological Survey of Israel, Jerusalem, Israel
3. Weizmann Institute of Science, Rehovot, Israel

Dissolved inorganic carbon (DIC), $\delta^{13}C$(‰), ^{14}C(pMC) and tritium were measured in pore water of the unsaturated zone (USZ) above the Coastal Aquifer of Israel in the nature reserve park of Nitzanim. The DIC and water were extracted from the sediments of the USZ by vacuum distillation. The vertical velocity of water in the USZ, 0.5m/year, was determined by the pulse of tritium from the thermonuclear tests of the 1960's. Thus, for each depth in the USZ an equivalent travel time of water,θ, from the surface to that depth can be assigned. The DIC showed a clear decreasing gradient with depth, suggesting carbonate precipitation in the USZ. The high DIC close to the surface is probably the result of soil CO_2 dissolution in the infiltrating water. The rate of carbonate precipitation (2.8%/year) was estimated by assuming first order reaction kinetics, as follows:

$$\frac{dQ_\theta}{d\theta} = \rho(Q_\theta - Q_{eq})e^{-\rho\theta}$$

where Q is the DIC concentration and ρ is the rate constant. The $\delta^{13}C$ of the DIC showed no variation with depth in the USZ and is very similar to that of groundwater in the Coastal Aquifer and of the solid carbonate fraction of the sediment in Nitzanim. The ^{14}C data also shows the effect of the thermonuclear tests of the 1960's. In the case of ^{14}C, the parameter Q_θ at each depth of the USZ is defined as the ratio between the measured ^{14}C to the atmospheric ^{14}C, θ years before sampling time. Presenting the ^{14}C data by the parameter Q_θ shows a clear gradient with depth, which suggests exchange between ^{14}C in pore water and the sedimentary carbonate of the USZ. The rate of exchange calculated as a first order reaction (by the above equation) is 4.1%/year. The gradient of Q_θ in the USZ indicates that at the entrance to the aquifer its value is 0.54. This value is the correction factor for the transfer of ^{14}C from the atmosphere to the aquifer. Thus a new tool to solve the long standing problem of dating groundwater with ^{14}C is added to the arsenal of the hydrologist.

Sediment transport by flashfloods: a comparison of wadis across the semi-arid/arid environmental spectrum

Cohen H. [1], Alexandrov Y. [1], Reid I. [2], Laronne J. B. [1]

1. Ben Gurion University of the Negev, Department of Geography and Environmental Development, P.O.B. 653 Beer-Sheva 84105, Israel.
2. Loughborough University, Department of Geography, Loughborough, England, United Kingdom.

Semi-arid desert margins are amongst the most sensitive environments to global/regional climatic fluctuations and desertification. A comparison of transport rates/processes in wadis along an arid to semi-arid environmental gradient is used ergodically to predict one impact of environmental change during aridification.

Continuous sediment transport observations for more than fifty flashfloods in four gravel-bed wadis in Southern Israel (Eshtemoa, Yatir, Rahaf and Qanna'im) reflect a range of climatic conditions from semi-arid to hyper-arid.

These wadis have produced the highest recorded bedload transport rates and the bedload/suspended load ratio is shown to increase with aridity. Bedload transport rates are correlated with reach characteristics such as channel width, slope and bed texture, but there is no apparent correlation with climatic gradient.

On the other hand, suspended transport rates and processes vary with the climatic gradient because of differences in soil and vegetation cover and storm type. Although maximum suspended sediment load is similar across the environmental gradient (>200 000 mg l^{-1}), the duration of exceptionally high loads is greater in semi-arid channels, giving higher unit yields. The relations between suspended sediment and discharge are generally complex and hysteretic in semi-arid channels, whilst those in arid-zone channels are usually simpler.

Long-term sediment yields are very high for semi-arid environments. The number of case studies in arid- and hyperarid-zone catchments is doubled by this study, confirming that the low frequency of events is not offset by higher sediment loads and results in low average yields.

Regional pedo-sedimentary stratigraphic units in the primary eolian loess of the Negev desert, Israel

Crouvi O. [1,2], Amit R. [1], Enzel Y. [2], Porat N. [1], McDonald E. [3]

1. The Geological Survey of Israel, 30 Malkhi Israel St., Jerusalem, 95501
2. The Institute of Earth Sciences, The Hebrew University, Jerusalem, 91904
3. Division of Earth and Ecosystem Sciences, Desert Research Institute, Reno, NV 89512, USA

Terrestrial loess deposits are widespread in desert margins. Since their transport, deposition, and accumulation are related to climate, they are used in studying past climates. Yet, many dated loess sequences, especially from the Negev desert in Israel, are not of primary origin but of secondary fluvially reworked loess. This makes the regional paleoclimate reconstructions complicated as the loess exhibits a complex history of eolian, fluvial and colluvial processes that reflect local conditions and the direct climatic signal can be masked. Separating primary from secondary loess deposits prior to their analysis is therefore crucial for regional paleoclimatology and for detecting temporal patterns in dust sources, deposition and transport.

In the Central and Northern Negev desert we located five primary eolian loess sequences on mountain tops and plateaus along a climatic transect from ~100 to ~250 mm/yr. They consist of two main pedo-sedimentary stratigraphic units separated by an unconformity: The lower, fine-grained (30-40% clay), brown, 0.3-2 m thick unit is overlying a thick weathered calcretes developed within the pre-Quaternary bedrock. It contains stage I-II calcic B buried soil horizons. OSL ages indicate that this unit was accumulated during the middle Pleistocene, with a relatively high average accumulation rate of 0.1-0.2 mm/yr. The upper, 0.1-3 m thick, coarser-grained (silt to clay loam; 20-30% clay), light brown loess unit overlies the lower unit with a noticeable tens of thousand years hiatus/erosion phase. It contains stage I-III calcic B-buried soil horizons. This upper unit was accumulated during the Late Pleistocene (90-14 ka) with accumulation rate ranging from 0.05-0.08 mm/yr at its lower part to 0.02-0.04 mm/yr towards the end of the Pleistocene.

The spatial and temporal characteristics of these primary loess units across the Negev desert, which are up to 150 km apart, show that they can be used as stratigraphic markers and that they differ from the secondary, reworked loess. We found that an earlier loess deposition episode, during the middle Pleistocene, preceded the well-documented Late Pleistocene loess. In addition, during the late Pleistocene there was almost continuous loess accumulation in contrast to several loess episodes which are characteristic of the reworked valley fill loess. The pedologic character of the buried soils supports an arid to semi-arid climate without strong indication for much wetter phases during the deposition of the loess in the Negev. These results highlight the possibility that the source of the dust, and the deposition rate accordingly, was changed with time and space. Part of the loess is coarser than the dust capable of long-distance transport and probably indicates the importance of the local sources such as floodplains, dunes, and the exposed shelf of Northern Sinai versus distant sources such as the Sahara or Arabia.

Building a semi-automated geological model from remotely sensed data for GIS mapping and analysis: A case study of the Danna reserve in Jordan

Dadon A.[1], Piters A. [2], Karnieli A. [1]

1. Remote Sensing Laboratory, Department of Solar Energy and Environmental Physics, J. Blaustein Institutes for Desert Research, Ben-Gurion University of the Negev, Israel
2. Desert Architecture and Urban Planning Unit, Department of Man in the Desert, J. Blaustein Institutes for Desert Research, Ben-Gurion University of the Negev, Israel

In recent years, remote sensing (RS) has become a prime data source for Geographic Information Systems (GIS) mapping and analysis. The option to introduce a global view that enables to recognize spatial patterns, enhance ground-collected data, acquire high-resolution spatial and spectral data and incorporate this data into a GIS system has been recognized by the geological community as well. This has resulted in a wide range of applications, e.g. groundwater and mineral exploration and environmental geoscience. In addition, novel image processing techniques have been integrated into the RS-GIS framework, making it possible to classify rock and mineral features in a faster and more accurate way. Remotely sensed digital geodata has enhanced also the use of 2.5 and 3D modelling of surface and subsurface objects and phenomena, not only for the purpose of representing and visualizing the third dimension, but also for interpreting and analyzing geological objects.

This paper presents the development of a semi-automated model for geological mapping and 3D geodata investigation based on a set of image processing and GIS techniques. The aim of the developed methodology is to extract lithological and morphological information by combining geological object recognition and GIS data mining and analysis. The output is stratigraphic information that can be used for mapping and constructing a 2.5D / 3D model of the subsurface or for geological spatial analysis.

The Danna national park reserve, located in Western Jordan, on the eastern edge of the Dead Sea Transform Rift, was chosen as a case study. Input data consisted of a digital geological map of the area and of remotely sensed geodata: a Digital Elevation Model (DEM) and a hyperspectral satellite image. This data served as the basis for a supervised classification of the geological units and for extracting geomorphological data. To conclude, an example application for the use of the extracted information to construct a physical model is demonstrated.

By applying the developed automated model, remote sensing and GIS can be integrated to create one framework into which raw spatial data in the form of images is transformed in the process into spatial information. This information can be used for surface and subsurface modelling or, in conjunction with additional thematic layers, for geospatial analysis.

The salinization mechanism and the resulted discharge-salinity relationships at the Taninim Springs, Israel

Dafny E. [1], Gvirtzman H. [1], Burg A.[2]

1. Institute of Earth Sciences, Hebrew University, 91904 Jerusalem, Israel.
2. Geological Survey of Israel, 30 Malkhe Israel St., 95501 Jerusalem, Israel.

The Taninim Springs are the north-Western outlet of the Yarkon-Taninim basin. Its discharge decreased gradually during the last six decades from about 90 MCM/y to 30 MCM/y in response to increased pumping. During the same period, the salinity of the springs varied between 700 and 2500 mgCl/l. This unexpected salinization of the springs gave rise to different theories regarding the flow system as well as the springs' salt source (Mandel, 1961; Golani, 1971; Bar-Yosef, 1974, 1975, 1976, 1978; Smoller, 1975; Mercado, 1980; Bar, 1983; Guttman and Zukerman, 1995; Paster, 2004; Schilman and Almogi-Labin, 2003; Starinsky and Katz, 2006).

We examined all the data sets (1949-2005) of discharge and salinity from the hydrological stations located at the lower Taninim basin. Subsequently, we re-calculated mass balances of water and salt and built a unified cell model to calibrate salt input. By analyzing annual averaged data of the springs' discharge and salinity together with heads at nearby wells, a multi-annual trend was detected. We then inspected the possible sources of salts to the Taninim Springs. Among them was the saline water body at the lower part of the aquifer, which was detected and sampled at a few deep wells at the north western part of the aquifer. From these analyses a thoroughly revision of the previous conceptual models of the salinization mechanism was achieved.

We conclude that:

The salty source that feeds the Taninim Springs is the saline water body at the north-Western part of the mountain aquifer. The theory of a marine 'toe' penetrating from the Carmel shore landward to the aquifer was discarded.

The mixing between saline and fresh water is taking place few kilometers east of the springs, at depth of a hundred meters, forming brackish water of 1000-2000 mgCl/l. The brackish water is found at shallow wells in the Taninim - Binyamina area.

The annual cycles of discharge and salinity, recognized until the late 1960's, are explained as a result of a seasonal head difference between the saline and fresh water bodies at both sides of the Binyamina fault. Higher head difference in the winter leads to increase discharge and salinity, and which is reversed in the summer.

The natural, undisturbed dynamic equilibrium that persisted until the mid 1950's, had replaced by the current 'disturbed' dynamic equilibrium, resulting from continuous pumping at the basin. At first, the salinity of the springs' water was not affected, but later the salinity increased in response to a decrease in discharge (~18 mgCl/l per 1 MCM/y on the average).

At the current rate of discharge of 20-30 MCM/y, the stable salinity of the Taninim Springs water is about 1300-1400 mgCl/l.

New geological cross-sections across the Yarkon-Taninim basin

Dafny E. [1], Gvirtzman H. [1], Burg A.[2]

1. Institute of Earth Sciences, Hebrew University, 91904 Jerusalem, Israel.
2. Geological Survey of Israel, 30 Malkhe Israel St., 95501 Jerusalem, Israel.

Geological cross-sections are a fundamental tool in hydrogeology research. We present five new accurate geological cross-sections across the Yarkon-Taninim basin ('YT') that improve the understanding of the groundwater flow regime and clarify several uncertainties. The new cross-sections are:

A1: Taninim coast - Giv'at Ada (E-W); A2: Taninim coast - Zichron Ya'akov - Yizre'el valley (SW-NE); B: Tel Aviv (North) - Yarkon Springs - Tapu'ach (E-W); C: Ga'ash - Ra'anana monitoring wells - Ram'alla anticline - Na'ama (NW-SE); D: Tel Aviv (Center) - Zafaria monitoring well - Ma'ale Ha'Chamisha - Muntar (NW-SE); E: Yatir ridge - Hatrurim Junc. at Arad Valley (NW-SE)

The cross-sections were plotted with a horizontal scale of 1:100,000 and a vertical scale of 1:20,000. Topography and Top Judea horizons were extracted from DEM grids (Hall et al., 1997 and Fleischer and Gafsu, 2003, respectively) using the GIS system. Post-Turonian outcrops were compiled from the Geological Map of Israel, 1:200,000 sheets (Sneh et al., 1998). Judea Group outcrops were compiled from 1:50,000 sheets of published and unpublished geological maps. Subsurface geology (down to Late Aptian) was determind using stratigraphic data from water and oil wells. The Data reveal that:

Neither the saltwater of the Mediterranean Sea nor the saltwater deep below the Taninim area is the source of the salt in the Taninim Springs; both of these are confined by thick impermeable geological units.

Tirely basin is separated from the Ramot Menashe area by a prominent fault and by impermeable units that lie beneath it.

The Yagur Fault is the north-eastern boundary of YT basin, because it puts the Judea Group rocks next to the relatively impermeable alluvial fill of the Yizre'el Valley. Hence, the Yagur fault is a hydrogeological boundary which prevents groundwater flow toward the Yizre'el Valley.

At the Samaria Mountains the basin boundary is a water divide line. At the north-Western part of the Ram'alla Anticline, the aquifer is usually dry over the inclined impermeable base. However, at the south-western part of Ram'alla anticline, a thin saturated section is preserved at the bottom of the aquifer. The water level of the En-Karem elevated sub-basin is slightly higher than the aquifer bottom and feeds the thin saturated section.

High groundwater levels (up to +120m asl.) at the Arad Valley are maintained by both flow from the Hebron Mts. and recharge at the E'fe ridge.

There is no division between the upper and lower sub-aquifers in either the Arad valley or the Samaria Mts.; the recharge to the upper sub-aquifer is percolates downward and feeds the lower sub-aquifer. At the Samaria Mts., this indicated by similar groundwater levels in the deep and shallow wells.

Using of environmental isotopes to identify the groundwater in Tucson basin, Arizona

Dody A. [1], Estoe C. [2]

1. NRCN, P.O.Box 9001, Beer Sheva, 84190
2. Geosciences Department, University of Arizona, Tucson, AZ

The hydrogeology of Tucson basin was studied based on environmental isotopes of $\delta^{18}O$, D and T. Pumping wells were located along the main streams, based on the assumption that recharge to groundwater occurs mainly during the floods in the Rillito wash. About 60% of the floods occur during summer time and the rest during winter time.

Water samples which were collected along the Rillito wash during the last decade showed young water with TU value ranging from 9 to 25 and $\delta^{18}O$ ranging from -11‰ to -9‰ with no evaporation effect.

The average $\delta^{18}O$ of the rain water during the winter time is -9.5‰ while in summer time the average value is around -6‰.

The $\delta^{18}O$ value of the groundwater was found to be close to the winter value, with no mixing with rain summer. The meaning is that during summer floods there is no recharge to groundwater. If we eliminate water percolation to groundwater during summer floods, we should eliminate the same process during winter time. That means that the source of the groundwater is not from the Rillito wash.

Based on $\delta^{18}O$ values, the authors suggest that the melting snow cover the Catalina Mountain during winter time percolates along the joints to recharge the groundwater in Tucson basin.

Multi-Component chemistry-based Dead Sea modeling: The role of salt precipitation and double diffusive mixing

Dvorkin Y. [1], Lensky N. [1], Lyahovsky V. [1], Gavrieli I. [1], Gertman I. [2]

1. Geological Survey of Israel, Malkhei Iisrael 30 Jerusalem 95501 Israel
2. Israel Oceanographic and Limnological Research, Tel-Shikmona, Haifa 31080

The Dead Sea is an hypersaline terminal lake located in the lowest part of the Dead Sea Rift Valley. It is a monomictic lake with a Ca-Chloride composition that differs significantly from regular seawater. Halite (NaCl) precipitates from the brine since 1983. Since 1995 the salinity of the DS rises by 0.3 g/Kg/yr and its temperature by 0.3°C/yr.

The main aim of the model is to reproduce the monomictic behavior of the Dead Sea: Development of a stabilizing thermocline and a destabilizing halocline during summer followed by autumn cooling and overturn in late autumn. The model should also reproduce the long term rise of salinity and temperature observed in the DS.

To model this behavior, one has to take into account the unique features of the Dead Sea. These features include salt precipitation, a wide range of salinities and compositions (fresh water through the highly concentrated (above Dead Sea) rejected brine from the chemical industries) and the dependency of evaporation rate on the water activity of the surface brine. This was done by modifying the 1D Princeton Oceanographic Model (POM) to a multi-component chemistry-based (rather than the usual salinity-based) model. This approach enables determination of the degrees of saturation for specific salts and the calculation of the amount of salt that must precipitate to maintain saturation. A new chemically-based equation of state is also included in the model.

The preliminary results of the multi-component chemistry-based model reproduce well the yearly cycle of the DS but show higher sea surface temperature at the time of the autumn cooling. Since the modeled temperature after the overturn is correct, we believe that the reason for the autumnal temperature discrepancy is insufficient mixing in the model. We suggest that the additional mixing mechanism acting in the DS is double diffusive mixing. This double diffusive mixing mechanism will be incorporated into the model in the coming months.

The diamonds and kimberlitic indicative minerals within the context of stratigraphy and source in Shefa Yamim drill SY-15, Pliocene-Pleistocene, Qishon River Valley, Israel

Eskel M., Kalmanovitch E., Roup A

Shefa Yamim (A.T.M.) Ltd. Laboratories: 36 Hata'asia Street, Nesher, Israel

Shefa Yamim study of the sedimentary layers of the borehole SY-15 in the Qishon river valley reveals an enrichment of heavy minerals in the conglomeratic layer. The occurrence of heavy minerals points to different mineralogical associations, thus revealing genetic and/or dynamic correlation to diamond occurrences. Further analysis of the sediments reveals that the highest occurrence and largest size of minerals is correlatable with about half clastic weight percent of the sample and predominantly fairly coarse grain size fraction.

The Shefa Yamim borehole SY-15 was drilled in the Qishon River valley on 15-16 November 2004. This 1-m diameter borehole represents a classical section through the Plio-Pleistocene sedimentary layers of the Qishon River extending from the ground surface to bedrock (depth 59.5m). Fifty-nine sample bags were collected, totaling about 41.4 metric tons. The borehole consists of three distinct horizons: an upper horizon consisting of mostly clayey layers (Upper Horizon), thin black fossiliferous clay layer (Marker Horizon) and a lower horizon consisting of mostly conglomeratic layers (Conglomerate Layer).

The Conglomerate Layer is enriched with heavy minerals (diamonds and kimberlite indicative minerals) by both quantity and diversity, and is the most interest for Shefa Yamim as an exploration company. The heavy minerals have been traced to originate from the Mount Carmel and from the magmatic bodies in the northeastern Qishon watershed.

The heavy and indicative minerals include Garnet (Pyrope), Spinel, Ilmenite, Pyroxene, Olivine, Rutile and Corundum (Ruby and Sapphire). Other minerals include Amphibole, Moissanite, Zircon, Kyanite, Pyrite, Limonite and Barite. Commercially potential minerals are Diamond, Sapphire, Ruby, and Moissanite. Many of these minerals are found in distinct groups or associations; the Garnet-Spinel mineralogical type is the most perspective for finding diamonds. Chemical SEM examination of the Pyrope Garnets shows a significant enrichment of MgO and also a high content of Cr_2O_3 in the Spinels. Both these factors show a strong kimberlite connection. The minerals which are genetically and dynamically associated with diamond are: Garnet, Spinel and Ilmenite; and only dynamically are Corundum, Moissanite, Magnetite, Olivine, Rutile, Zircon and Pyroxene.

Clastic weight percent and clastic grain size were correlated with mineral occurrence, type and size because of the occurrence of coarse grain minerals (>2mm) in the conglomeratic layer. Mineral occurrence is more likely when the clastic weight percent of the sample is between 35-65% and the predominant grain size between 10-25mm, excluding fine and very coarse grain size. Similar results were obtained in two nearby, 1-m diameter boreholes. Hence the mineralogy of SY-15 points to the existence of diamond associated heavy mineral groups, with dynamic control of overall grainsize and clastic fraction of the sample overprinted by geological factors.

Givat Ga'ash, Makhtesh Ramon, is it a Lower Cretaceous volcano?

Eyal M., Yudalevitch Z., Samoilov V.

Ben-Gurion University of the Negev, Department of Geological and Environmental Sciences, P.O.Box 653, Beer-Sheva 84105

Givat Ga'ash is located along the Northern cliff of Makhtesh Ramon in the central Negev, about 5 km east of the main road. Bentor (1952) and Mazor (1961) considered it to be built mainly of olivine basalt flows with pyroclastic rocks around it. Based mainly on the hoof-shaped morphology of the hill, Mazor (1961) describe the structure as a "volcanic eruption which started with an explosion of tuff, followed by the eruption of basaltic lava streams. During the last stage of this eruption the interior pressure was released and the part above the feeding neck sank".

In the framework of the study of the volcanic rocks of Makhtesh Ramon, we reinvestigated Givat Ga'ash. Our main results are: (1), most of the hill is a subvolcanic intrusion. The body is zoned, with basanite in the outer part and basanitic nephelinite and nephelinite toward the center. (2), all of the above rock types occur also as glass-bearing variants (up to 35%). The glassy varieties are distinguished by smaller diameter (<25 cm) and shorter length (<3 m) of the columnar jointing. (3), agglomerates and lapilli tuff surround the hill on the Eastern, Southern and western sides. The total length of pyroclastic exposures from west to east is more than 3 km. All pyroclastic rocks have undergone very strong alteration. (4), small outcrops of weathered vesicular rocks may be relicts of volcanic flows. (5), on the Northern side, sandstone beds with volcanic fragments overlie the subvolcanic rocks with erosive contact. (6), the higher parts of Givat Ga'ash are about 70 m above the lower part of Hatira Formation.

The subvolcanic body has intrusive contacts with the lower part of the Hatira Formation and with the pyroclastic rocks, whereas the upper part of the Hatira Formation unconformably overlies the subvolcanic body. Therefore, the country rock for the upper part of the subvolcanic body should be the volcano itself. Accordingly, the following stages should be distinguished in the evolution of Givat Ga'ash. 1. Construction of an edifice composed mainly of agglomerates and lapilli tuff with some volcanic flows. The diameter of the body was at least 3 km and the height about a few hundred m. 2. Intrusion of the subvolcanic body into the volcano edifice. 3. The glassy bodies intruded after the main body, probably as volcanic domes. 4. Contemporaneous deposition of upper Hatira sandstone with erosion and deposition of the volcanic edifice. 5. The central depression of Givat Ga'ash is probably the result of the less resistant glassy rocks.

Mapping of the underground water flows using TEM FAST method as applied to the Dead Sea sinkhole problem

Ezersky M. [1], Legchenko A. [2], Camerlynk C. [3], Al-Zoubi A. [4]

1. Geophysical Institute of Israel, POB 182, Lod 71100, Israel
2. IRD-LTHE, BP 53, 38041 Grenoble Cedex 09, France
3. UMR 7619 Sisphe, Université Pierre and Marie Curie, 4 place Jussieu, 75252, Paris Cedex 05
4. Al-Balqa Applied University, Engineering Faculty, Salt, 19117 Jordan

Underground water streams are the important factor of the sinkhole formation mechanism at the Dead Sea (DS) area in Israel and Jordan. The most efficient geophysical parameter for the study of water saturated soil salinity is bulk resistivity. In Israel Time Domain Electromagnetic (TDEM) method (named also Transient Electromagnetic - TEM) is for a long time being used for the mapping of the very low resistivity zones in the problem of the delineation of the fresh water aquifers. We have applied TEM method in its FAST mode to map the bulk ground resistivity down to 70-100 m. The "quasi" 3D techniques, as well as monitoring are used for the problem solution. The Combination of resistivity measurements with the water content distribution derived from the Magnetic Resonance Soundings facilitates the localization of aquifers filled with comparably less salty water in comparison with DS water.

TEM FAST method enabled to map the resistivity distribution of the underground in the Ein Gedi and Nahal Hever sites in Israel and Ghor Al-Haditha in Jordan. The lateral resistivity distributions at the salt layer depth are of a most interest. (Salt location is determined using both boreholes and the seismic refraction method). The mapping permits to distinguish between lateral areas with bulk resistivity less than 0.6 ohm-m ("very low resistivity" structures - VLRS) and above ("low resistivity" ones - LRS). In Ein Gedi these structures are extended in the WE direction whereas in the Nahal Hever south area it is NW-SE one. Generally, the sinkhole location area is delineated by the isolines of a very low resistivity (0.6-0.75 ohm-m). However, there are vertical structures with higher resistivities (1ohm-m and beyond) intruded into very low resistive environment and coming in contact with the salt. We associate the LRS structures with the water streams keeping the potential to dissolve the salt. The different aspects of both the TEM FAST method and quantitative inter-relations will be discussed.

Sinkhole hazard assessment in Israel and Jordan using combined geophysical technology

Ezersky M.[1], Legchenko A. [2], Camerlynck C. [3], Al-Zoubi A. [4]

1. Geophysical Institute of Israel, POB 182, Lod 71100, Israel
2. IRD-LTHE, BP 53, 38041 Grenoble Cedex 09, France
3. UMR 7619 Sisphe, Université Pierre and Marie Curie, 4 place Jussieu, 75252, Paris Cedex 05
4. Al-Balqa Applied University, Engineering Faculty, Salt, 19117 Jordan

In framework of NATO Science for Peace Project SfP 981128 a field study has been performed out aimed to study the relationship between groundwater and sinkholes development, and to verify the potential of geophysics applied to detection of subsurface dissolution caves. In the Dead Sea costal area of Israel and Jordan, different geophysical methods have been applied (Seismic Refraction, Magnetic Resonance Sounding (MRS), Transient Electromagnetic (TEM) in its fast sounding mode (TEM FAST), Microgravity, Seismic Diffraction and Continuous Vertical Electrical Sounding (CVES)). Three sites in Israel (Nahal Hever south, Ein Gedi and Newe Zohar) and one site in Jordan (Ghor Al-Haditha) are under investigation. There are two principal geological models explaining sinkhole development: (a) the flashing model and (b) the salt dissolution model. The latter is accepted today as being the main mechanism of sinkhole formation. However, there are also some signs of the flashing as an alternative mechanism (underground water channels, voids, revealed by boreholes etc). The salt dissolution model requires the simultaneous existence of three factors: (1) a salt layer within the uppermost subsurface, (2) unsaturated groundwater in the vicinity of the salt layer, and (3) fractures or faults able to carry unsaturated water into the salt formation and to evacuate the brine from the dissolved cavity. Consequently, for an efficient management of the sinkholes development phenomenon the following problems have to be resolved (1) Delineation of salt formation; (2) Mapping of unsaturated groundwater; (3) Localizing of subsurface dissolution caverns; (4) Localizing of fractured and porous zones in contact with salt. It was shown that some of these problems can be resolved by jointly using different surface geophysical methods. During our field study of the hydrogeological situation three surface geophysical methods were used:

- The 'quasi' 3D salt layer mapping was performed using seismic refraction method,
- The bulk resistivity (linked with water salinity) was mapped using TEM FAST and CVES methods,
- The depth to the water table was estimated using MRS results; MRS also allows reliable identification of subsurface water-filled caverns.

Joint interpretation of geophysical results provides more complete and reliable information related with the sinkholes development phenomenon.

Airborne laser scanning technology for monitoring geomorphic activity

Filin S. [1], Avni Y. [2]

1. Dept. of Civil and Environmental Eng., Technion - Israel Institute of Technology, Haifa, 32000, Israel
2. Geological Survey of Israel, Jerusalem, 95501, Israel

Many of the techniques that are presently employed for monitoring geomorphic activity suffer from both coverage and resolution limitations. The result is a limited understanding and difficulties in quantifying the overall geomorphic activity. This becomes particularly important when rates of spatial and temporal change are considered for fluvial systems. We present the utilization of airborne laser technology for monitoring the evolution of the geomorphic system in areas undergoing active processes of land deterioration. Key features that make Light Detection and Ranging (LiDAR) technology optimal for this task are the dense three-dimensional description that laser systems provide, their high level of accuracy, and the level of detail that can be noticed in range data. It offers a wider coverage than classical geodetic methods, has better resolution than spaceborne Radar, and automatically provides dense surface information in contrast to image based mensuration techniques. Additionally, the direct acquisition of 3D information paves the way to high level of automation in the detection of geomorphic phenomena. These properties are of great value for detailed analysis of wide regions, for monitoring the evolution of existing phenomena, and for detecting the occurrence of new features that may be small in size but significant in their lateral effect.

To demonstrate the great potential of LiDAR data for geomorphologic studies we study their application to documenting the geomorphic system along the Dead Sea coastal plain. We show its capability to detect small objects in the form of embryonic collapse sinkholes, narrow gullies that have been forming in the last decade as a result of lake retreat, paleo-shorelines that document the sea-level on an almost annual basis, and others. Since all this information is provided in the form of 3D coordinates (providing position and height) wealth of morphometric information can be extracted from this data.

In addition to showing the great capability of LiDAR data to characterize geomporphic features on large scale, we also show it ability to provide information in vegetated areas.

Structural map of top Telamim (LC3 marker) of central Israel - a step towards Early Cretaceous structural map of the Levant margin

Fleischer L.[1], Gafsou R.[1], Ben-Gai Y.[1], Steinberg J.[1,2], Dafny E.[2], Gvirtzman H.[2]

1. Geophysical Institute of Israel, POB 182 LOD 71100
2. Institute of Earth Sciences, Hebrew University, Givat Ram, JERUSALEM 91904

The construction of structural skeleton for the Yarqon-Taninim aquifer is currently based on its subdivision to three main units: the lower aquifer from base to top Yagur Formation, the upper aquifer from top Moza Formation to top Judea Group and the middle aquitard of Moza-Bet Meir Formations. Although these chronostratigraphic markers are well recognized in most of the boreholes in the study area, they cannot provide the details required for a structural map. Such information can be retrieved from seismic data and surface mapping.

Unfortunately, seismic coverage is limited over large parts of the aquifer and the areas north of Heletz suffer from poor seismic resolution within the Judea Group. Concurrently, the entire Cretaceous section appears to be structurally calm and so ensures conformity of strata. The tactic we adopted in order to achieve a structural skeleton was to construct a map of a regional marker and work out the other levels based on corresponding isopachs. The most prominent structural marker in the area is top Telamim (LC_3 marker) of Middle Aptian age. Unlike the top Judea marker, LC_3 is much less affected by the major Cenozoic truncations of base Saqiye and base Yafo.

The map is compiled from ten different sources. In the west, the major contribution is from seismic maps of oil exploration and previous studies of Yarqon-Taninim. In the east, maps are based on surface mapping by several authors. These maps, usually for shallower markers, were converted to the LC_3 level by relevant isopachs. This map may form the basis for a detailed Early Cretaceous structural map of the Levant margin.

Paleoenvironments and facies stacking patterns in the Cenomanian and the Turonian of the Galilee

Frank R. [1], Benjamini C. [1], Buchbinder B. [2]

1. Department of Geological and Environmental Sciences, Ben-Gurion University of the Negev, POB 653, 84105 Beer-Sheva
2. Geological Survey of Israel, 30 Malkhe Israel St., Jerusalem 95501

The Cenomanian-Turonian rock section of the Galilee was studied using high-resolution bed-by-bed sampling followed by sedimentary field analysis and microfacies analysis. A variety of distal to proximal carbonate paleoenvironments were detected such as: (1) Laminites, turbidites and debrites in the distal ramp approaching the deep basin; (2) Shoreface and peri-tidal paleoenvironments reflecting a proximal ramp.

Facies units are stacked vertically as meter-scale shallowing- or deepening-upward cycles, classified into six types. Together they compose higher-order cycles or system-tracts up to tens of meters in thickness. Stacking-pattern analysis is a necessary step toward high-resolution sequence stratigraphy model that is relevant to basin analysis of the Northern Levant margin.

Stacking patterns in the Galilee show an evolutionary trend of the carbonate system toward two paleoenvironmental events that result in sequence boundaries: (1) Drowning of a tidally-controlled ramp system in the mid-Cenomanian; (2) Drowning of a wave-controlled ramp system near the Ce-Tu boundary. The latter is the local manifestation of the drowning event at the Ce-Tu transition known from around the Tethys.

Platform configuration and depocenter shift as reflected in the mid-Cretaceous sequences of the Galilee and Northern Levant

Frank R. [1], Benjamini C. [1], Buchbinder B. [2]

1. Department of Geological and Environmental Sciences, Ben-Gurion University of the Negev, POB 653, 84105 Beer-Sheva
2. Geological Survey of Israel, 30 Malkhe Israel St., Jerusalem 95501

The Cenomanian–Turonian succession in the Galilee is divided into three transgressive-regressive sequences: (1) a Lower- to Middle-Cenomanian sequence; (2) a Middle- to Upper Cenomanian sequence and (3) a Turonian sequence. The thickness and facies configuration in each transgressive and regressive system tract show that most of the Galilee was relatively elevated with respect to two depocenters: (1) A Tethyan depocenter west and north of the Galilean-high; (2) a more southerly depocenter toward the Carmel. The latter, after restoration of the lateral shift along the Dead-Sea rift, is possibly a SW extension of the Palmyride basin. Facies transitions in the Galilee and Northern Levant show a major S-N component, in contrast to the E-W, 'hinge-line'-related, facies transitions south of the Galilee. This may possibly reflects a shift in the N-S direction of the Levantine 'hinge-line' south of the Galilee, toward the NE and NNE in the Galilee.

Gravity-controlled subsidence producing inclined deposits in karst and prehistoric caves

Frumkin A.

Department of Geography, The Hebrew University of Jerusalem, msamos@mscc.huji.ac.il

Cave deposits in prehistoric caves are often inclined or deformed. Understanding the deformation process is essential in terms of site-formation processes and interpretation of archaeological finds. In the Qesem Cave, bedrock and sediment deformation can be studied along a road cut (route 5, near Kafr Qasem, Israel) which intersects the entire cave system. This allows for detailed geological study of the system, supported by Th-U dates of speleothems, archaeological finds, speleological exploration and drilled cores.

Qesem Cave, discovered in 2000, has a rich, well-preserved Acheulo-Yabrudian sequence shedding light on the temporal range of the Acheulo-Yabrudian and the end of the Lower Paleolithic.

The cave's ceiling has been removed by natural erosion and recent construction works. Some of the cave deposits have been damaged, but enough are preserved to justify a long-term multidisciplinary project, taking place since the discovery of the cave. The cave was formed in the western foothills of the backbone mountain ridge of Israel. Like other chamber caves in the area it was formed under phreatic conditions, and after later regional uplift it was dewatered, i.e. transferred into the unsaturated zone. It has undergone several stages of natural and human-induced deposition, as well as subsidence and collapse. Natural deposits include calcite speleothems, bedrock collapse debris, and clay fill, possibly originating from the overlying *Terra Rossa* soil.

Large post-depositional dip (up to 55 degrees) is observed in the cave sediments as well as locally in the surrounding bedrock. This evidence, combined with other sites in the region demonstrating short (~20 m) wavelength bedrock deformations associated with karstification, suggests the continuation of deep underground dissolution process after the dewatering of the cave. The overlying sediments, including both bedrock and cave deposits, have subsided into the underlying voids, creating local sinkholes.

Additional reading

Barkai, R., Gopher, A., Lauritzen, S. E. and Frumkin, A., 2003, Uranium series dates from Qesem Cave, Israel, and the end of the Lower Palaeolithic: Nature, v. 423, p. 977-979.

Perchlorate biodegradation in contaminated deep vadose zone

Gal H. [1], Ronen Z.[2], Weisbrod N. [2], Dahan O. [2], Nativ R. [1]

1. Dep. of Soil & Water Sciences, The Hebrew University of Jerusalem, P.O. Box 12, Rehovot 76100
2. Dep. of Environmental Hydrology & Microbiology, Zuckerberg Institute for Water Research, Ben-Gurion University of the Negev, Sede Boqer 84990

Very widespread contamination of perchlorate, a primary ingredient in solid rocket and missile fuel, was found in the vadose zone near a plant that manufactures ammonium perchlorate in the Israeli Military Industry (IMI) in Ramat Hasharon. As part of the IMI's operations, untreated industrial wastewater was disposed of for over 30 years in unlined wastewater ponds and nearby creeks, causing contamination of the unsaturated zone (peak concentration of 2200 mg kg^{-1} sediment under the most contaminated pond) and the groundwater below it (up to 250,000 ppb perchlorate).

In this study, we examined potential perchlorate degradation in the contaminated deep vadose zone profile by native microbial communities. We explored the effect of nitrate concentration on perchlorate reduction and determined what, if any concentrations of perchlorate are toxic to microorganisms.

Perchlorate biodegradation was found in three of the four sediment samples taken from different depths. The sediments taken from 1 m (shallowest) and 35 m (deepest-close to water table) showed the fastest degradation rates, while the sediments taken from 15 m showed the slowest rate. No perchlorate reduction was observed in the sediment taken from 20 m-the depth at which perchlorate concentrations were highest. We found that at high concentrations (10,000-20,000 ppm), there is no perchlorate reduction, even after long periods (toxicity concentrations).

The lag time for perchlorate degradation was found to be inversely correlated to nitrate concentration. We found no perchlorate degradation as long as nitrate was present in the system: perchlorate degradation initiated only after all the nitrate had been reduced. Nitrate-reduction rates were correlated to the initial concentrations of nitrate and no lag period was observed for nitrate reduction (i.e. the lag period was less than 2 days). Nitrite was temporarily accumulated during nitrate degradation and was totally reduced, like nitrate, after 4.3 days. There was a full molar correlation between nitrite accumulation and nitrate reduction.

Under unsaturated aerobic conditions (16% water content), we found no perchlorate degradation for at least 48 days of incubation. Conversely, an over 90% reduction in perchlorate concentration was observed in sediments taken from ground surface, with no addition of external carbon source. This indicates that perchlorate is degradable under suitable conditions (absence of oxygen), even without the addition of electron donors or a carbon source.

Degassation of earth as a possible factor forming of oil/gas reserves

Galant Y.

P.O.Box 164, Yokneam-Moshava, 20600, Israel

In the frame of conception of contribution of deep fluids into sedimentary layers this investigation has been made. This investigation conducting with aim to found out regime, which favorable for forming oil/gas. And at the present investigation is continuation of previous researches. In the previous researches first of all has been shown, that there is a possibility of distribution up to 40-45 km depth and migration hydrocarbons fluids to sedimentary layers. Were brought regime of spreading rifts system as generating reduced gases: CH4, CO, H2. Were shown, that influence of partial melting degree on oil/gas bearing forming of basins defines indirectly and connected with mantle drainage. As well as was formulated hypothesis, that depth of mantle drainage can forming of reduction regime of fluids and this fluids are being migrating give a certain budget for forming oil/gas fields.

It is known oil/gas accumulation, which connected with volcanoes (acting as well as ancient). Sufficiently, to notice gas/oil fields Galiano, Chizina etc. surrounding volcano Etna. In Azerbaijan is known Muradhanli oil field, etc.

This investigation made with an accent on the Magmatic activity in the Rift systems. These rifts are: Red Sea, Ethiopia, Dead Sea, Rein, Baikal, Dneprovo-Doneck, South Caspian, Rio-Grande, West Siberia and lot of other.

Researched regularity between following Characteristics of Rifts: Age, Period of Magmatic Activity, Roof of Mantle, Partial melting degree of Mantle and Intensity of Magmatic Activity.

The investigations show the following results:

1. In the Rifts of the different period of Magmatic activity, approaching to Recent Time the Intensity of Magmatic Activity is increasing.
2. In the Rifts of different age, the Intensity of Magmatic Activity increasing towards youngest age of rifts.
3. Connection between Intensity of Magmatic Activity and roof of Mantle has not been found.
4. According increasing of Partial Melting Degree increasing Intensity of Magmatic Activity.
5. Approaching to Recent Time the period of Magmatic activity decreasing according decreasing the roof of mantle.

Beach deposits of MIS 5e high sea stand and the tectonic stability of the Carmel coast, Northern Israel

Galili E. [1], Zviely D. [2], Ronen A. [3,4], Mienis H.K. [5,6]

1. Israel Antiquities Authority, POB 180, Atlit 30300, Israel.
2. Recanati Institute for Maritime Studies, University of Haifa 31905, Israel.
3. Zinman Institute of Archaeology, University of Haifa 31905, Israel.
4. The Max Stern Academic College of Emeq Yezreel, Emeq Yezreel 19300, Israel.
5. Department of Zoology, Tel-Aviv University 69978, Israel.
6. Department of Evolution, Systematics & Ecology, Hebrew University of Jerusalem 91904, Israel.

Ten beach deposits were observed on the Carmel coast, Northern Israel. Six of them have been reported recently. The morphological and lithological characteristics of the deposits are similar: their inner edge (uppermost) altitude varies from 2 to 10 m above the present sea level. They were deposited in or close to channels of seasonal rivers which cross the Carmel coast kurkar ridge, most of them are still active. The beach deposits are composed mainly of fine Nile-derived quartz sand and shells of marine mollusks, firmly cemented by calcium carbonate. The dominant mollusks belong to the families *Glycymeridídae, Cardiidae*, *Donacidae*. In addition a marine gastropod *Lentigo latus* (formerly known as *Strombus bubonius*) was discovered. This Strombid species is considered an index fossil for the Tyrrhenian stage of the Pleistocene in the Mediterranean sea. According to the lithology and chronostratigraphy of the beach deposits, the presence of *Lentigo latus,* TL and IRCL datings of adjacent kurkar layers, the beach deposits were related to last interglacial maximum about 125 kyr before present. The MIS 5e beach deposits and Holocene archaeological finds are used as identifying markers of palaeo sea levels and coastlines and for detecting vertical tectonic changes along the Carmel coast. By comparing the elevations and characteristics of the beach deposits to similar MIS 5e deposits from other locations, and analyzing the archaeological data, it can be concluded that the Carmel coast has been tectonically stable during the last 125 kyr. The recent finds indicate that since the MIS 5e, the maximum possible vertical displacement of these coasts has been less than 40 mm/kyr. Based on MIS 5e deposits of Yassaf formation previously reported, we propose similar (less than 70 mm/kyr) vertical displacement rates for the Western Galilee coast.

Late Mesozoic-Cenozoic folding, uplift, canyon incision and vast sediment accumulation as revealed by seismic reflection surveys from the Levant basin, offshore Israel

Gardosh M. [1], Druckman Y. [2], Buchbinder B. [2]

1. Geophysical Institute of Israel, P.O.B. 182, Lod, 71100
2. Geological Survey of Israel, 30 Malkhe Israel, Jerusalem, 95501

The subsurface, structure and stratigraphy of the Levant Basin, offshore Israel was studied on a grid of regional, 2D seismic reflection profiles, extending from the Mediterranean coastal area westward, some 200 Km offshore. The seismic data set (~ 12,000 km) was correlated with 40 offshore and onshore wells. Six distinct seismic markers that were identified as major unconformity surfaces and lithostratigraphic boundaries were interpreted and mapped. These were used to establish the Late Cretaceous - Cenozoic depositional history and timing of tectonic activity in the basin and its margin.

The seismic data set reveals the following styles of deformation: (a) Basement-involved, high-amplitude folds, and thrust faults, (b) regional inland uplift and westward tilt of the basin margin, (c) subsidence of the basin floor and (d) low-amplitude folds, in places associated with thin-skinned deformation. Style (a) characterizes the Late Cretaceous to Early Tertiary contractional phase (Syrian Arc 1). Styles (b) and (c) prevailed during the Oligocene to Middle Miocene and resulted in intense canyon incisions along the slope and accumulation of an exceptionally thick sedimentary section within the basin. Style (b) occurred in the northeastern margin of the basin also in the Plio-Pleistocene. Style (d) characterizes Middle to upper Miocene contractional phase (Syrian Arc 2).

The various styles of deformation are the result of the northward motion and collision of the Arabian and Eurasian plates, as well as the continuous updoming and breakup of the Arabian Craton since Late Eocene times.

A multi-component, chemistry-based 1D model to the Dead Sea: Preliminary results of stabilizing the Dead Sea level through increased inflows

Gavrieli I. [1], Dvorkin Y. [1], Lensky N.G. [1], Gertman I. [2], Lyakhovsky V. [1]

1. Geological Survey of Israel, Jerusalem 95501, Israel
2. Israel Oceanographic and Limnological Research Ltd., Haifa 31080, Israel

We present a 1-dimentional (1D) limnological model for the Dead Sea that is capable of modeling the long term impact of mixing freshwater and seawater in the Dead Sea. The 1D-DS-POM is based on the Princeton Oceanographic Model (POM) which has been modified to account for the unique features required for such modeling. The original POM code was changed from a salinity-based to a multi-component chemistry-based model. Thus, the new 1D-DS-POM transports and mixes individual ions rather then bulk salts. A new equation of state (EoS) is included in the code to cover the huge density and compositional ranges associated with the Dead Sea and seawater/freshwater. This EoS is based on the chemical composition and temperature of the brine, making use of the Pitzer approach, modified by Krumgalz for the Dead Sea. The degree of saturation of the brine with respect to halite or gypsum is determined based on the thermodynamic approach of Pitzer and Krumgalz for hypersaline waters. When found to be oversaturated, a time-efficient algorithm "precipitates" salts from the oversaturated brine, bringing it back to saturation. The calculated water level accounts also for these precipitated salts, which "accumulate" at the bottom of the lake. The above described thermodynamically-based procedures rely on the concentration of the chemical constituents given in *molal* units (mole/kg H_2O). However, mass transport equations (turbulent diffusion) are based on salinity units (gr/kg solution). Accordingly, the 1D-DS-POM includes an efficient units transformation module which also verifies that no mass is lost during this process.

Preliminary long-term (50 year) 1D-DS-POM runs (pre-calibrated) indicate that stratification and dilution of the surface water will take place under most scenarios in which the inflows to the lake are increased. In fact, even if the additional water diverted to the Dead Sea would only compensate for the current water deficit and maintain the level at its current (or future) level, stratification would still develop. The model runs further indicate that long-term stratification and decrease in surface salinity and density can occur even while lake level declines, provided that the volume of inflow water is greater than that which evaporates from the surface of the lake. This paradox is explained by the net withdrawal of Dead Sea brine by the chemical industries. Stratification develops under such conditions because the water added to compensate for the brine withdrawal is devoid of the salts that were pumped by the industries, and thus they dilute the surface water.

Mg isotope fractionation in the Ca-Chloride Dead Sea brine system- preliminary results

Gavrieli I., Yoffe O., Halicz L.

Geological Survey of Israel, Jerusalem 95501, Israel

Magnesium has three naturally occurring isotopes: ^{24}Mg (79.0%), ^{25}Mg (10.0%) and ^{26}Mg (11.0%). The use of magnesium isotope fractionation in the study of natural systems has recently gained momentum as instrumentation has become more advanced, enabling precise measurements. In the present study Mg isotope analyses were carried out with a NU multi-collector ICP-MS, using Aridus desolvation system for sample introduction. All samples (including brines, salts and carbonate rocks) were treated in a clean room for the separation of Mg from the matrix. Instrument mass-bias was corrected with the bracketing method using the DSM-3 standard reference material (defined as $\delta^{26}Mg = 0.0‰$). The latter is a Mg metal produced from the Dead Sea brine. Analytical precision is ±0.1‰.

We examined the fractionation of Mg in two processes involving the Ca-chloride brine system of the Dead Sea rift valley; 1) Artificial evaporation of the hypersaline Dead Sea brine to degrees that lead to precipitation of carnallite ($KMgCl_3 \cdot 6H_2O$). 2) Natural dolomitization of limestone through water rock interaction. Preliminary results indicate that Mg fractionation occurs during the precipitation of carnallite ($\delta^{26}Mg = 0.0‰$) from the Dead Sea brine (-0.6‰), whereby the precipitate is enriched with ^{26}Mg, leaving the residual "end brine" isotopically depleted (-0.9‰). It is not surprising that the isotope composition of SRM DSM-3 is similar to that of carnallite, from which it is produced.

The discordant dolomites in the Dead Sea Rift Valley evolved from water-rock interaction between the ancient (late Pliocene - Early Pleistocene) Ca-Chloride Dead Sea Rift Valley brines and the Upper Cretaceous limestones exposed at the Rift's escarpment. These dolomites were found to have Mg isotope composition ($\delta^{26}Mg = -2.2‰$) that is significantly depleted relative to present day Dead Sea brine. The composition of these late epiogenetic dolomites is similar to slightly depleted relative to the syngenetic Upper Cretaceous dolomites (-2.0±0.2‰). This, and the similarity in $\delta^{26}Mg$ composition between seawater (-0.8‰) and Dead Sea brine, which evolved from seawater, may suggest that a) the isotope composition of the Ca-Chloride brines has not changed significantly since their formation, b) seawater composition has not changed significantly since at least the Pliocene. Yet, some of the freshwater sources in the Dead Sea catchment area have Mg isotope composition that is depleted relatively to the brines (e.g. Dan and Banias springs) while so far none was found to be more enriched. It is thus still to be determined if the Ca-Chloride brines maintain their Mg-isotope composition over millions of years through processes such as dolomitization, and to what extent Mg-salt precipitation played a role in the determination of the early composition of these brines.

Investigation of in-situ degradation pathways of petroleum hydrocarbons in gasoline contaminated groundwater

Gelman F. [1], Reshef G. [2], Binstock R. [1]

1. Geological Survey of Israel, 30 Malkhe Israel, Jerusalem, 95501, Israel
2. Israeli Water Commission, Water Quality Department, Hamasger 14, Tel Aviv, 61203, Israel

Soil and groundwater contamination by petroleum hydrocarbons resulted from accidental spills, storage and pipelines leakage is a widespread environmental problem all over the world including Israel. The proper control and managing of such contaminated sites is required to minimize a negative impact of the dangerous organic compounds on the environment. Dilution, sorption, chemical transformation, biodegradation are possible pathways of the contaminant reduction in the environment. However, biodegradation is the only way for irreversible destruction of contaminant in nature. It is, thus, important to distinguish between different environmental processes to predict the contamination spreading. The aim of the current research is the investigation of the natural attenuation processes and biodegradation pathways of the major fuel contaminants (BTEX compounds and MTBE) in groundwater. Chemical quantitative analyses of organic and inorganic compounds in the groundwater, as well as isotope ratio analyses are used for the deduction of degradation mechanisms. A case study of the contaminated groundwater near a gasoline station in Tel-Aviv area situated above the coastal aquifer demonstrates degradation of hydrocarbons under suboxic conditions.

Lithofacies and petrophysical analysis of the Yarkon-Taninim aquifer in an expanded composite log format

Gendler M. [1], Goldberg I. [1], Fleischer L. [1], Ben-Gai Y. [1], Gvirtzman H. [2], Dafni E. [2], Steinberg J. [2]

1. Geophysical Institute of Israel, POB 182 LOD 71100
2. Institute of Earth Sciences, Hebrew University, Givat Ram, JERUSALEM 91904

A large number (several hundreds) of recorded oil, gas and water wells were drilled into the Yarkon-Taninim aquifer since 1954. Geological and geophysical information from these wells is of great importance from the point of view of detail description and definition of the lithological composition, capacity-filtration properties and formation water salinity of groundwater reservoir. Available composite logs mainly contain lithological information based on cuttings, cores and electric logs. At the same time, in a significant number of wells, there are hundreds of meters of missing lithological description due to drilling with no return (LOC intervals). These "blind" intervals are commonly corresponding to the Judea Group formations. A lack of reliable lithological information in these intervals considerably complicates the geological correlations. Presently, the exploration of these formations has yielded an abundance of log data, which can compensate for the missing information and thus replenish data to fill in these gaps and to allow a continuous computation of aquifer's petrophysical properties such as limestone, dolomite and clay content, porosity and water salinity.

We present a new "*Expanded Composite Log*" format of digital well logs, which combines petrophysical well log information with lithological and stratigraphic markers. These logs are used in particular to fill the missing data of the LOC intervals. The accurate porosity and the lithology determination are based on a combination of available acoustic, neutron and density logs. Porosity is calculated taking into account lithological variations (sandstone, limestone, dolomite, shale). The results of lithology-porosity calculations are later on used for formation fluid analysis of the aquifer (water salinity), lithofacies model definition and for regional well correlation. The formation water salinity is usually calculated from well logs using the Rwa method, which is the apparent resistivity of formation water obtained using the Archie equation, assuming a clay-free water-saturated formation. The set of statistical relationships between logs and well test data are established in order to facilitate quantitative interpretation of aquifers. Using all collected geological, geophysical and petrophysical information two litho-stratigraphic cross-sections were prepared for characterization of subsurface geology of the Judea and Kurnub Groups sediments.

Presented cross-sections illustrate the following:

- Ø Subsurface stratigraphy for entire groups and for each particular formation
- Ø Lithofacies characteristic of the carbonaceous-terrigene sediments
- Ø Total formation and net productive thickness and lithology variation
- Ø Correlation of highly porous and possible fracture zones
- Ø Division of Yartan aquifer to two sub-aquifers – Upper an Lower
- Ø Regional aquicludes – En Yorqeam shaley formation sediments
- Ø Well test data

Buried and surface experimental explosions: Seismic source features and scaling

Gitterman, Y., Hofstetter, R.

Geophysical Institute of Israel, Seismological Department, Baal Shem Tov, 6, Lod, 71100

We studied empirical features of seismic energy generation for different explosion seismic sources, and partitioning of this energy between P, S and surface waves, in specific geological conditions and tectonic settings of the Middle East. The observations include buried experimental explosions of special design and surface military detonations, for which Ground Truth information (GT0) and blast design parameters were collected.

We analyzed source features and scaling for single-fired, surface explosions at Sayarim military range near Eilat, observed at near-source 3C portable SP seismometers and regional IMS BB stations. A dataset of combined observations of seismic and infrasound waves at collocated sensors was also collected, with S-waves manifestation at distances of up to 150 km. Ground Truth data for 19 explosions in a broad charge weight range (100-8500 kg), recorded at numerous portable and permanent SP and BB stations, facilitated the analysis of energetic characteristics of seismic signals depending on the yield. Source scaling parameters were determined for regional phases observed at BB station EIL (33-38 km). Obtained estimations and waveform features for the surface seismic sources were compared to nearby Sayarim buried (borehole) experimental explosions conducted by GII in 2004, recorded also at EIL. After correction the data for the distance and type of explosives, the scaling power law parameter for P-waves (0.91) with maximal amplitudes was found similar to that for the buried explosions (0.93).

A series of three Depth-of-Burial (DOB) experimental explosions of near-spherical charges at different depths was planned. During preparation of the experiment large cavities (up to 3 m size) were created at Oron phosphate quarry at significant depths (up to 63 m) using a special technique. A number of fully coupled and partially decoupled explosions in the cavities were conducted. Extensive observations in near-source zone and remote area demonstrated peculiar signal features and energy generation related to these specific seismic sources.

Oron decoupling experiment demonstrated feasibility of the utilized method of seismic source design for construction of near-spherical charges of different size (up to 5-7 tons) and at different depths (up to 70-80 m) and conducting broad-scale, low-cost experimental series: decoupling, DOB, variable charge weight.

Oron DOB explosion experiment

Gitterman Y. [1], Levi I. [2], Hayoun B. [3], Yassur U. [2], Peled U. [1]

1. The Geophysical Institute of Israel, P.O. Box 182, 71100, Lod
2. Rotem Amfert Negev Ltd., Yeroham 80500
3. Tamar Advanced Quarrying Ltd., P.O. Box 25100, Tel Aviv 61250

On January 2, 2007, after long preparations and many efforts the unique Depth-of-Burial (DOB) experiment with original design and configuration was successfully conducted at Oron phosphate quarry (the site coordinates 30.897°N, 34.994°E). The goal of the experiment was to provide data for improvement of nuclear test monitoring within the framework of the CTBT.

The explosion series of three charges of 4200 kg ANFO each one were detonated at different depths:

Ex.1, depth h=26 m, Origin Time 09:31:12.3 GMT, local magnitude M_L=2.7;

Ex.2, h=45 m, O.T. 10:01:13.5, M_L=2.5-2.6;

Ex.3, h=59 m, O.T. 10:30:31.3, M_L=2.5.

The design and configuration of the explosions were different from previous similar experiments and preferable: near-spherical charges, small separation (only 180-220 m), placement of all seismic sources in the same consolidated sediments (marls). A special complicated technology was applied for creation of huge cavities (up to 3.5 m size) at large depths for accommodation of explosives, using boreholes with 6.5" diameter only.

The charges were fully stemmed, the explosions were fully contained.

Numerous good recordings of signals from all shots were obtained at portable near-source accelerometers and close-in 3C seismic stations, permanent local Israel SP and BB stations, and IMS stations EIL and MMAI (240 km). A clear correlation between charge deepening and magnitude/peak-amplitude reducing was observed. Obtained data will contribute to the ability of parameter estimation of nuclear explosions.

The research was sponsored by the AFRL of the US Department of Defense.

On the applicability of relationship between H/V fundamental frequency and sediment thickness: Petah Tikva and its surroundings

Gorstein M., Zaslavsky Y., Ataev G., Aksinenko T., Kalmanovich M., Giller D., Dan I., Perelman N., Giller V., Livshits I., Shvartsburg A.

Seismology Division, Geophysical Institute of Israel, P.O.Box 182, Lod, Israel

Recently, different studies showed that H/V spectral ratio from ambient noise can be used to map sediment thickness. Quantitative relationships between fundamental frequency and sediment thickness were derived and applied for calculating the sedimentary layer thickness in geological conditions with significant impedance contrast between cover and bedrock.

On the basis of 580 ambient noise measurements carried out in the study area including the towns of Petah Tikva, Rosh Ha'ain, Hod Hasharon and surrounding settlements we attempted to apply this approach to estimate thickness of sedimentary cover. Cross-plot of the fundamental frequency vs. depth of the regional reflector - Judea Gr. taken from the structural map yields scatter in thickness values reaching a factor 6 at some frequencies. Detailed analysis of this dependence shows that reasons of error of the reflector depth estimation lay not only in the initial data themselves or local structures like erosion channels unmapped in the structural map or difference in location of mapped anticlines/synclines, but rather in simplification of the velocity model. It is clearly seen while comparing fundamental frequency with sediment thickness derived from modeling of the H/V spectral ratio by SHAKE analytical function. 1-D models were constructed considering both fundamental peak and the other one caused by an intermediate hard layer. In particular, it was revealed that at the Petah Tikva anticline the chalky limestone of the Judea Gr. is not reflector; while the reflector occurs some hundred meters deeper. In the high frequency range, influence of the irregularly distributed Quaternary gravel layer is reflected in variation of sediment thickness more than twice. Thickness of upper soft layer also indirectly but strongly affects the fundamental reflector depth.

Thus, the results have demonstrated that the research method using fundamental frequency-depth dependence to determine sediment thickness is not appropriate for the area under investigation neither for depths taken from the structural map nor for calculated ones.

Future geophysical studies in the central Arctic ocean

Hall J. K. [1], Kristoffersen Y. [2]

1. Geological Survey of Israel (Emeritus), 30 Malchei Israel. Jerusalem 95501
2. Institute of Solid Earth Physics, University of Bergen, Allàgaten 41, Bergen, Norway

Before coming to Israel, I did my PhD on the marine geophysics of the Central Arctic Ocean using data acquired during 1962-1970 from the drifting scientific ice station Fletcher's Ice Island (T-3). T-3 was abandoned in 1974, after spending 5 years over the Alpha Ridge, in the Lincoln Sea north of Ellesmere Island in the Canadian Arctic. The Lincoln Sea is perennially covered by ice in compression, with thicknesses of 4-6 m. It is probably the least accessible part of the Arctic Ocean, one of the reasons that the Alpha Ridge, which together with its Russian counterpart the Mendeleev Ridge, remains one of the most enigmatic geological features on Earth.

Recently interpreted seismic profiles taken over the Alpha Ridge by T-3 in 1971-74, along with newly acquired multi-channel profiles, show evidence that the upper 500 m of sediments have been massively disturbed over an area of 200 by 600 km. Analysis suggests that an asteroid impact could be the only plausible explanation.

To study this area in detail, and to open up large parts of the Arctic to long-term and relatively low-budget exploration, a 13 by 6 m hovercraft is now being built in the UK. Fitted with long range tanks, and capable of traveling over water and ice at speeds to 60 km/hr, this Griffon TD2000 hovercraft is capable of passing over obstacles 73 cm in height. Scientific observations, to be carried out by a crew of two from the University of Bergen, will include gravity, EM ice thickness, sediment coring, CDP seismics, CHIRP, and 12/200 kHz echo-sounding, and placement of autonomous buoys for echo-sounding and seismic profiling. Much emphasis will be put on satellite data transmission, GPS navigation, and logistics management by GPS/Iridium transponders. The hovercraft will likely winter over at the UNIS University in Longyearbyen, Svalbard, and spend the daylight months within the Central Arctic Ocean.

Seismic features in 3C records of quarry explosions and earthquakes from Southern Dead Sea area

Harkavi A. [1], Gitterman Y. [2], Ben-Avraham Z. [1]

1. Department of Geophysics and planetary sciences, Tel-Aviv University, Tel-Aviv 69978, Israel.
2. Geophysical Institute of Israel, P.O.Box 182, Lod 71100, Israel

In this study we try to characterize 3-component seismic records of two classes of seismic events in Arad and Southern Dead Sea areas for future discrimination purposes. Two clusters of low-amplitude seismic events are analyzed: (1) small earthquakes (M_L<4.0) from Southern Dead Sea; (2) quarry blasts from the phosphate quarries near Arad.

For the selected events we collected 3-components seismic records from twelve seismic stations of the Israel seismic network. The existent coordinate system of NS and EW was rotated horizontally (digitally) to a station-event system of radial and transversal components. Afterward we measured the P and S phase's amplitudes of each component for each station, calculated the amplitudes ratio and checked the distribution of the phases' amplitudes for different stations.

It was expected that for explosions the Transversal P-phase energy will be significantly smaller than the Vertical and Radial P-phase energy. The data showed that this feature was not observed. Actually, in most cases the P-phase energy on the Vertical component was somewhat stronger than on the Horizontal components, and there was no clear difference between the Radial and the Transversal energies.

As expected, there are significant differences between the two seismic classes. In the earthquakes class, the S/P energy ratio seems to be much higher than the quarry blasts S/P energy ratio. In records of earthquakes, the maximal S amplitude comes shortly after the first S arrival followed by exponential decay, while as for quarry blasts the S amplitude intensifies slowly and decays slowly, probably mixed with surface waves.

Developing a new method of measuring dissolution rates of minerals using isotope dilution and changes in the isotopic composition of Si

Harpaz L. [1], Bullen T. D. [2], Ganor J. [1]

1. Department of Geological and Environmental Sciences, Ben-Gurion University of the Negev, P. O. Box 653, Beer-Sheva 84105
2. US Geological Survey, Menlo Park, CA, USA

Quantification and understanding of the mechanism of low-temperature silicate dissolution and precipitation reactions have important implications on many environmental questions, such as acid rain, relationship between global climate and silicate weathering over geological timescales, composition of ground water and surface water, and global geochemical cycles.

Numerous laboratory experiments and field-based studies have been conducted to quantify the dissolution rates of silicate minerals. Calculation of dissolution rate of a silicate mineral in a flow-through experiment is usually based on the difference between the Si concentration of the outflow and the inflow solutions. However, under close to equilibrium conditions, this concentration difference is small relative to the high concentration of the inflow solution. Therefore, it is not possible to measure accuratly dissolution rates of silicate under close to natural conditions. In addition there is an inherent problem that the change in solution concentration is affected by both the dissolution of the primary mineral and the precipitation of the secondary mineral.

The aim of the present study is to develop a new method for measuring near equilibrium dissolution rates.The use of isotope dilution and changes in the isotopic composition of a solution enriched with ^{29}Si isotope allows us to notice smaller changes in the outflow solution and even to detect precipitation of secondary phases.

The dissolution rates of the primary silicate mineral (Amelia Albite in our study) will be calculated by measuring Si concentrations and isotopic composition using MC-ICP-MS. The forward dissolution reaction (without the precipitation of a secondary mineral) is determined based on changes in isotopic ratio (e.g., $^{28}Si/^{29}Si$) of a spiked inflow solution. The net change in Si concentration is determined using isotope dilution. From this change in Si concentration it is possible to calculate the difference between the dissolution rate of the primary mineral and the precipitation rate of the secondary mineral. By combining the two methods, it is possible to obtain both the dissolution and the precipitation rate.

High resolution marine geophysical survey in the Northern gulf of Elat/Aqaba (MERC research #M25_004)

Hartman G. [1], Tibor G .[2], Ben-Avraham Z. [1], Niemi T. [4], Al-Zoubi A. [5], Sade R.A. [1], Hall J. K. [3]

1. Department of Geophysics & Planetary Sciences, Tel-Aviv University, Tel-Aviv, Israel
2. Israel Oceanographic and Limnological Research, Haifa, Israel.
3. Geological Survey of Israel, Jerusalem, Israel
4 University of Missouri-Kansas City, U.S.A.
5. Surveying & Geomatics Department, Al-Balqa' Applied University, Al Salt, Jordan

High-resolution marine geophysical survey in the Northern gulf of Eilat/Aqaba region was done during October and November 2006. The survey was held by an international research group (Israel, Jordan and USA) funded by MERC. The overall aim of the research is to provide the municipalities of Aqaba and Eilat a base map of active faults for seismic hazard analyses and earthquake preparedness planning by collection and interpretation of high resolution marine geophysical images of the seafloor and subsurface strata.

The marine geophysical survey lasted for 3 weeks and included 263 seismic lines with a total length of more than 370 km. The survey was done in two phases: deep survey (WD 10-700 m) on board the R/V "Etziona" and a shallow phase (WD < 10 m) on board the "Danny-Boy". The high-resolution geophysical survey included the following equipment: (1) A GeoSparker seismic source with energy range of 100-1000 J and frequency between 200-5000 Hz. The system had 2 hydrophone channels, one parallel to the sparker, and the other with about 50 meters offset giving a seismic penetration of more then 100 meters in the soft sediments. (2) A Simrad EM 1002 multi-beam sonar covered the all area with a spatial resolution of about 1 meter. (3) A G-881 cesium magnetometer from Geometrics was dragged behind the vessel during the deep survey and (4) A E-Sea Scan 800 Side-Scan-Sonar for a very high resolution mapping of the sea floor morphology.

Initial processing of the multi-beam and Sparker data reveals very interesting new features both on the seafloor and in the substrata that were not known before. Among them are deep canyons with slumping activity, and a complex fault system.

During 2007 the seismic data will be processed with Promax (Landmark) software and the interpretation will be done with Seiswork (Landmark) and OpendTect. More in-situ data (e.g. coring, diving, ROV) will be collected in the near future to calibrate and interpreted our findings.

Soft sediment deformation by Kelvin-Helmholtz instability: A case from Dead Sea earthquakes

Heifetz E. [1], Agnon A. [2], Wetzler N. [1], Marco S. [1]

1. Department of Geophysics and Planetary Sciences, Tel Aviv University
2. Institute of Earth Sciences, The Hebrew University, Jerusalem

The standard explanation for soft sediment deformation is associated with overturn of inverted density gradients. However, in many cases observations do not support this interpretation. We suggest an alternative in which stably stratified layers undergo shear instability during relative sliding via the Kelvin-Helmholtz Instability (KHI) mechanism, triggered by earthquake shaking (Heifetz et al., 2005, *EPSL* 236, 497-504). Dead Sea sediments have long stood out as a classical and photogenic example for recumbent folding of soft sediment. These billow-like folds are strikingly similar to KHI structures and have been convincingly tied to earthquakes. Our analysis suggests a threshold for ground acceleration increasing with the thickness of the folded layers. The maximum thickness of folded layers (order of meters) corresponds to ground accelerations of around 1g. Such accelerations occur during large earthquakes, recurring in the Dead Sea in about a millennium. Furthermore, a preliminary analysis of the power spectrum of the Dead Sea sediment deformation shows a power law close to the universal turbulent Kolmogorov Cascade, which is associated with the KHI mechanism.

Young geomorphic features in the puna volcanic field, Catamarca, Argentina

Inbar M.

Department of Geography and Environmental Studies, University of Haifa, Haifa, 31905

The Central Andes are characterized by a variety of volcanic features from different ages, some of them erupted recently or a few thousands years ago.

A large field of yardangs developed on an ignimbrite rock blanket, at a present altitude of 3100m. The ignimbrite is a vitric tuff, welded and rich in pumice particles and plagioclase, biotite and hornblende phenocrysts. The yardangs are of different sizes, the largest about 30m x 18m x 6m. They are aligned along a 340° to 360° azimuth, which is the present prevailing wind direction. The yardangs development is explained by the strong annual winds, the poor vegetation cover, the available sand and coarse volcanic particles acting as abrasive agents, and the lithology and structure of the ignimbrite blanket.

Several monogenetic scoria cones were analyzed in the study of the geomorphological development of the volcanic field. The volcanoes are scattered throughout major north-south tectonic features. The obtained morphometric ratio of the cone height/basal diameter was 0.20 and the slope angles measurements were 25° to 30°, similar to the obtained values for other young scoria volcanoes in the Andes. In addition, the fresh looking lavas without vegetation cover surrounding the cones are an indication of their young age.

The delineation of saline groundwater bodies within the Arava Rift Valley, Israel, using deep geoelectromagnetic measurements

Kafri U. [1], Goldman M. [2], Levi E. [2]

1. Geological Survey of Israel, 30 Malkhei Israel St., Jerusalem, 95501 Israel.
2. Geophysical Institute of Israel, P.O.Box 182, Lod, 71100 Israel.

Thirty deep geoelectromagnetic soundings using a central loop time domain electromagnetic (TDEM) configuration have been carried out along the Arava Rift Valley in Israel between the Dead Sea in the north and the Gulf of Elat in the south. Most of the measurements were conducted using 500 by 500 m transmitter loops with a maximum (estimated) penetration depth varying between 1500 and 2000 m.

The main objective of the TDEM survey was to clarify the groundwater salinisation processes that were unclear due to the scarcity of information regarding deep-seated saline sources or end members. Unfortunately, none of the existing boreholes or the previous geophysical soundings in the study area were deep enough to penetrate or detect those end members. In addition, the survey was aimed to reveal the genetic relationship between the end members and the different base levels and paleo-base levels in the south and north.

The hydrogeological interpretation of the geophysical results indicate that salinization of groundwater is controlled by both present days and ancient base levels, namely by the Dead Sea in the north and by the Gulf of Elat in the south. As a result, a salinity zonation drown from the measured resistivities, is observed along the Arava Valley from north to south. In the Hazeva-Dead Sea basin in the north, fresh to brackish groundwaters overlie concentrated brines in the Northern portion of the basin and diluted brines of a nearly normal seawater salinity in its southern part. In the En Yahav-Zofar basin, the distribution of salinities with depth is similar to that one encountered in the southern part of the Hazeva-Dead Sea basin. In the central Arava structural and hydrological divide, fresh waters are encountered in the entire measured sequence. In the Southern Yotvata basin, fresh to brackish groundwater bodies alternate with some residual Pliocene seawater and shallow "sabkha" type local brines.

The geometry of the resistivity zonation, obtained by TDEM, roughly reflects the reconstructed configurations of interfaces and paleo-interfaces between fresh to brackish waters and underlying intruded seawater or brines (partly diluted) from both base levels. The central Arava structural and hydrological divide seems to escape seawater or brine encroachment at least to the considerable penetration depth of the TDEM measurements.

Ambient noise measurements in the Carmel fault zone

Kalmanovich M., Zaslavsky Y., Giller V., Livshits I., Shvartsburg A.

Seismology Division, Geophysical Institute of Israel, P.O.Box 182, Lod, Israel

The Carmel fault is one of the major structural features in the geology of Israel. The fault, which has been active since the Late Miocene, displays 1000m vertical and 1500m sinistral displacements.

Ambient noise measurements were carried out at a distance of 12 km between Haifa port and Kibbutz Yagur along a number of profiles over the Carmel fault zone. Results of H/V spectral ratio analysis showed that the part of the fault zone under study may be divided into three areas differentiated by geological structure. Their positions may be indicated as follow: first area is from Haifa Port to Nesher Intersection; second area occupies the Nesher Industrial Area and third one is the territory between Nesher Enterprises and Intersection Yagur.

The results of ambient noise measurements show that in the first and third areas sharp shift in the H/V fundamental frequency from 12 Hz down to 0.7 Hz and H/V amplitude in the range 2-10 units occurs at a distance of 100-200 m. This is correlated with linear fault zone. Interpretation of H/V spectral ratios allows suggesting subvertical dip-slip two-step fault with dip of more than 80 degrees.

The second area (Nesher Industrial Zone) differs from the first and third ones by very low H/V over the whole territory. Only at a distance of about 400 m essential effect was obtained.

We believe H/V spectral ratio method can be successfully used for mapping of faults with vertical displacement of about 10% of reflector depth

Dense grid of microtremor measurements over the first area allowed dividing it into four zones stretched parallel to the Carmel fault and characterized by different fundamental frequency and amplitude. Analysis of measurements showed that site effect in each zone is produced by different reflectors. For the first zone located western of the Carmel fault and yielding fundamental frequency of 4-12 Hz and amplitude of 4-10 units the limestone or dolomite of the Judea Gr. is the reflector. Next three zones are located eastern of the faults and may be described as follows: second zone up to 30 m wide with frequency 3-3.5 Hz and the same amplitude has a reflector represented by calcareous sandstone of the Kurkar Gr.; the third zone of 70-150 m wide with frequency of 1.3-2.0 Hz and amplitude of 4-6 units has marl of the Yafo Fm. as a reflector and forth, located within the Kishon Graben and showing fundamental frequency 0.7-1.3 Hz and amplitude 5-6 units has the chalky limestone of the Ziqlag Fm. as a fundamental reflector.

Evaluation of rockfall hazard and risk for Qiryat-Shemona (Northern Israel)

Kanari M. [1], Katz O. [2], Weinberger R. [2], Marco S. [1]

1. Department of Geophysics and Planetary Sciences, Tel Aviv University, Tel Aviv, 69978
2. Geological Survey of Israel, 30 Malkhe Israel St., Jerusalem, 95501

Rockfalls are a typical slope-failure mode in steep hard rock slopes. They range in size from small rocks to gigantic boulders of hundreds of cubic meters. Rockfalls move at speeds of up to tens of meters per second and are hazardous to humans and property in mountainous areas. Rockfalls may be triggered by earthquakes or extreme weather conditions. We study rockfalls near Qiryat-Shemona, a town in Northern Israel that lies right on the Dead Sea fault system, at the foot of the Ramim cliff. In this cliff, outcrops of the 40m-thick Ein El Assad limestone Formation are exposed providing the source material for fallen rock blocks. Aerial photos dating 1951 show rock blocks of volumes $1m^3$ to $150m^3$ situated within the now built town premises. It is likely that these blocks have traveled to their present localities from the Ramim cliff by rockfall mechanism. We aim at evaluating rockfall hazard and risk for Qiryat-Shemona.

Three questions are addressed in this study for complete hazard evaluation: (a) what is the origin of the rockfall blocks?; (b) what is the triggering mechanism for block movement?; (c) which are the feasible downhill trajectories of the blocks?

To answer these questions we analyzed the fracture density at the rock source; we mapped hundreds of rock-blocks both on the field and on aerial photos and analyzed their volume and spatial distributions; we simulated rockfall trajectories using a commercial simulation program (CRSP 4).

Preliminary results show that the distribution of block volume follows an exponential function of the form ax^b with b value variance between -1.23 and -1.34, in agreement with other studies. This volume distribution is used to determine most probable rock-block volumes for hazard evaluation. We used maps of maximal downhill block travel distances combined with slope morphological analysis to suggest possible downhill historical block trajectories. For the program calibration we analyzed these trajectories and determined the needed simulation variables (surface roughness, tangential and normal coefficients of the slope, initial horizontal velocity of blocks). We then used these variables and simulated possible downhill rockfall block trajectories towards the town premises. Rockfall simulations of probable block volumes determined from the volume distribution function yielded risk evaluation for the area of Qiryat-Shemona. Simulated results of block velocity and block bounce height along the slope can be used as parameters for a risk reduction engineering program for Qiryat-Shemona.

Landslide hazard in Northern Israel; A 1:200,000 scale map and a GIS based hazard evaluation computer-code

Katz O., Almog E.

Geological Survey of Israel, 30 Malkhe Israel, Jerusalem 95501

Down-slope mass movements (i.e. landslides) occur worldwide as a consequence of earthquakes or extreme rain-storms. When landslides are triggered close to population-centers, they cause damage in life and property and therefore it is important to map sites of high relative landslide hazard. Currently in Israel, there is no national scale landslide hazard map. The objectives of the current work are to (1) evaluate earthquake and rain-storm induced landslide hazard of entire Israel; (2) to locate and map sites of relative high hazard and risk; (3) to create an interfaces that will enable easy-access for authorities and engineers to the hazard maps, this in turn will enhance hazard reduction for the Israeli-society.

We currently present a 1:200,000 scale earthquake-induced landslide hazard map of Northern-Israel and a GIS based computer-code that enables the calculation of slope-performance scenario in a given area resulted from selected earthquake.

The landslide hazard is presented in two formats: a HAZUS like susceptibility map (relative-hazard, grades I to X with increasing of susceptibility) and a map of the critical-acceleration for slope-instability. The process of producing the maps follows five steps: (1) mapping (creating GIS layers) the amount and direction of slope steepness and the geological-structure; (2) grouping the geological mapping units to five geotechnical units consisting of formations with decreasing rock strength; (3) determining the most probable slope failure-types according to the exposed geotechnical-units and the relation between the topography and structure along each slope (25m×25m GIS grid-cell); (4) hazard mapping; assigning susceptibility-grades, where the grade increases with decreasing rock strength and increasing slope steepness (for slumps or rock-falls) or structural slopes (for rock-slides); (5) assigning a value of critical-acceleration to each of the ten susceptibility-grades; calibration is performed using field-observations slope instability and results of previous critical-acceleration evaluation, done in a detailed scale.

Results draw attention to a few areas of high hazard, e.g. slopes surrounding the Hula valley and the Sea of Galilee; slopes of eastern Bet-Kerem valley; slopes of the Carmel and slopes of the Gilboa.

For creating landslides scenario of selected earthquakes we wrote a GIS based computer-code that performs empirical regional Newmark analysis (following Jibson et al., 2000). This code enables the user to define a target area and a few theoretical earthquakes (defined by moment-magnitude and epicenter site) in order to analyze which earthquakes will induce landslides in the target area. For example, using the code we can predict that a magnitude 6 earthquake in Bet-Shean area will not induce landslides in the city of Tiberias area, while magnitude 7 will. The accuracy of the resulted landslide maps is for 0.5 magnitude unit.

Early Mesozoic facial distribution and tectonic-geophysical setting in Israel

Katz Y. [1], Ben-Avraham Z. [2], Eppelbaum L. [2]

1. Paleontological Museum, Faculty of Life Sciences, Tel Aviv University
2. Dept. of Geophysics and Planetary Sciences, Raymond and Beverly Sackler Faculty of Exact Sciences, Tel Aviv University

The division of the Levant and Eastern Mediterranean into distinct crustal domains was first proposed by Ben-Avraham and Ginzburg (1990). According to this model, Israel earth's crust consists of three terranes: Negev, Judea-Samaria and Galilee-Lebanon. Following investigations (e.g., Ben-Avraham et al., 2006) confirmed this tectonic reconstruction.

The presented investigation is based on application of (1) facial analysis, (2) thicknesses of geological formations, and (3) magnetic and thermal fields examination. For items 1-2, the data from Israeli boreholes (altogether 33 units) with Permian, Triassic and Jurassic deposits as well as from a few outcrops were examined. Item (3) was carried out on the basis of modern magnetic and thermal fields analysis.

The results of the investigation can be summarize as following:

(A) Facial-paleogeographic analysis indicates that the most shallow deposits of Early Mesozoic are developed within the Negev terrane and the Palmyride block, (B) Analysis of thicknesses shows that Galilee-Lebanon terrane is characterized by the highest values of Triassic deposits (more than 2,500 m). Southern part of Palmyride block is classified as Jurassic monocline; thickness of Jurassic deposits decreases from 2,850 m (Rosh Pina) up to 2,170 m (Mount Hermon). Judea-Samaria terrane could be classified as tectonic depression, where the maximum Early Mesozoic thicknesses (more than 5,100 m) correspond to area of Ramallah-1 borehole. The Negev terrane is characterized by inversion structure: the Triassic structural floor is tectonically elevated, and the Jurassic floor is depressed, (C) Sharp changes in the trend and thickness of the Early Mesozoic formations coincide with the terranes boundaries, (D) Zones of intensive magnetic field gradients and gradients of Curie discontinuities are confined to boundaries of the abovementioned terranes;

A series of resulted maps – paleogeographic, thicknesses of Triassic and Jurassic formations of Israel (these maps were constructed taking into consideration the Cenozoic sinistral displacement) as well combined magnetic gradient and Curie map – correspond to the deep structure provinces in the Levant area.

References

Ben-Avraham, Z. and Ginzburg, A. 1990. Displaced terranes and crustal evolution of the Levant and the Eastern Mediterranean. Tectonics, 9, 613-622.

Ben-Avraham, Z., Schattner, U., Lazar, M., Hall, J.K., Ben-Gai, Y., Neev, D. and Reshef, M., 2006. Segmentation of the Levant continental margin, Eastern Mediterranean. Tectonics, 25, TC5002, 17 pp.

Crustal growth and recycling in the Arabian Nubian shield: Oxygen isotope ratios of zircon

Katzir Y. [1], Beeri Y. [1], Valley J.W. [2], Eyal M. [1], Litvinovsky B. A. [1], Zanvilevich A. N. [1], Gal A. [1]

1. Dept. of Geological and Environmental Sciences, Ben Gurion University of the Negev, Be'er Sheva 84105, Israel
2. Dept. of Geology and Geophysics, University of Wisconsin, Madison WI 53706, USA

Zircon (Zrn) preserves the most reliable record of both magmatic oxygen isotope ratio and magmatic age. The mantle is a remarkably homogeneous oxygen isotope reservoir [$\delta^{18}O$(Zrn) = 5.3 ± 0.3‰], thus significant deviations of $\delta^{18}O$(Zrn) from the mantle value indicate magma interaction with supracrustal material. In an entirely juvenile and fast-growing crustal province like the Arabian Nubian Shield (ANS), one would expect increase in $\delta^{18}O$(Zrn) towards younger ages reflecting increasing availability of rocks that have interacted with the hydrosphere at near surface temperatures for subduction, melting and assimilation. However, in the ANS exposures of Southern Israel $\delta^{18}O$(Zrn) decreases as the orogenic cycle moves forward. The earliest island arc plutonism (780–740 Ma) represented by metamorphosed tonalite and quartz diorite intrusions is characterized by the highest $\delta^{18}O$(Zrn) values measured in this study: 8.03 to 8.32‰. The Elat granitic gneiss of the same stage has lower and more scattered $\delta^{18}O$(Zrn) values of 6.67 to 7.23‰. One hundred million years younger calc-alkaline batholithic magmatism is less $^{18}O/^{16}O$ enriched: $\delta^{18}O$(Zrn) values range from 6.15 ‰ for the Roded quartz diorite and Timna porphyritic granite to 6.97‰ for the high-K peraluminous Elat granite. Even lower, mantle-like values characterize the postorogenic within plate magmatism: $\delta^{18}O$(Zrn) values of monzodiorite, alkaline granite and syenite of the Timna alkaline complex range from 5.50 to 5.93‰.

An indication for *intra-crustal recycling* at the early orogenic stage is given by the Elat schist [Rb/Sr age = 800 Ma; $\delta^{18}O$(Qtz) = 13.5‰]. The schists may represent a shallow counterpart of deeper buried sediments presumably melted and mixed with magma that intruded the continental crust resulting in high $\delta^{18}O$ (>8‰) magmatic zircon. Notwithstanding detrital zircon from the Elat schist itself has much lower value of 6.35‰. Considered to derive solely from island arc volcanics (820 Ma), the Elat schist zircon may bear isotope signature of *mantle recycling*, where hydrated oceanic crust and sediments are subducted and returned to the mantle. The strong intra-crustal recycling effect imprinted in magmas produced during the island arc stage is, however, transient. Imtermediate to felsic plutons of the late to post collisional stage [630–600 Ma; $\delta^{18}O$(Zrn) = 6 to 7‰] suggest reduced availability of sediment for melting. Finally, the postorogenic A-type magmas indicate melting of almost pure mantle, suggesting migration of melting to deeper, asthenospheric sources. Rising of mantle-derived magma through continental crust without apparent contamination most likely requires crustal extension and thinning.

Simulations of groundwater flow and saline water circulation during a lake level drop: The Dead Sea case

Kiro Y. [1,2], Yechieli Y. [1], Lyakhovsky V. [1], Shalev E. [1], Starinsky A. [2]

1. Geological survey of Israel, 30 Malkhei Israel St., Jerusalem 95501, Israel
2. Institute of Earth Science, The Hebrew University of Jerusalem, Givat Ram Campus, 91904 Jerusalem, Israel

Lake and sea levels have been known to fluctuate in the past, mainly due to climatic changes. Since the 1960's the Dead Sea level has been dropping due to human influence on its water budget. This fast lake level drop has a major affect on the groundwater system in the lake vicinity. Therefore, it is important to understand the dynamics of groundwater flow and saline water circulation in a dynamic system of a receding lake. For this purpose, simulations were done with the USGS SUTRA code (Voss, 1984) testing the responses of the groundwater level and the transition zone between the fresh and saline water to a lake level drop and to hydrological parameters. In order to analyze the groundwater level response, a typical time (t) was defined as the time interval in which the discharge from the eastern boundary decays by a factor of *e*. An obtained relation between the typical time and the hydrological parameters allows approximating a typical time of a given system with a set of parameters. This relation could also be used to estimate whether the groundwater level is in equilibrium with the lake level.

The response of the transition zone between the fresh and saline water depends on the groundwater level response as well as on the density differences. The horizontal component of the density gradient has the most significant effect on the movement rate. Thus, the transition zone moves slowly when the transition zone slope is small and vice versa.

There are two types of transition zone movement: (1) back and forth movement when the groundwater level responds slowly and the transition zone responds fast, (2) gradual movement toward the lake when the groundwater level responds fast and the transition zone responds slowly.

In the equilibrium, the saline water circulates beneath the transition zone. Following the instantaneous lake level drop, the saline water flow is initially directed only toward the lake and after a certain period of time the circulation returns. The magnitude of the velocity after the lake level drop and the rate of the flow direction change depend on the hydrological parameters and on the response rate of the groundwater system.

A gradual lake level drop causes a gradual increase in the discharge at the boundary until it reaches a constant value. When the discharge attains this new constant value, the groundwater system reaches a new dynamic equilibrium in which there is a groundwater level drop, but the hydraulic gradient remains constant. This process is also evident in the saline water flow direction. While the discharge from the boundary increases, the saline water flow direction tends to be toward the lake. When the system reaches the new dynamic equilibrium, the circulation returns.

Resonant radar pattern over void-models and comparison with radar data over revealed voids that later collapsed forming sinkholes in Ein Gedi, Dead Sea area, Israel

Kofman L. [1], Frumkin A. [2], Ronen A. [3]

1. Technion Research and Development Foundation Ltd., Haifa
2. Geography Department, The Hebrew University of Jerusalem
3. Geotec –Engineering & Environmental Geophysics Ltd., Rishon Lezion

Results are discussed as to the field and laboratory investigations of factors causing resonance phenomena in reflected pattern of subsurface voids. The main objective was to examine the relationship between voids' dimensions and wavelength using different antennas. Most experiments were conducted in the Technion Field System Laboratory, in a deep test trench filled with sand. The sinkhole models (empty fiberglass cylinders with various diameters) were buried vertically. Tests were performed by towing 500, 300 and 100 MHz antennas along a pre-established grid for the various model conditions [1].

The factors causing resonance phenomena in the reflected pattern are the following:

1. The antenna wavelength in the air must be smaller than the diameter of subsurface hole.
2. The vertical size of the void should not be significantly smaller than its horizontal dimension or alternatively considerably bigger than its diameter. The latter is well suitable in locating sinkholes that continue upwards to the surface in a pipe form.
3. The required density of the GPR survey grid must be 1 meter for observing reverberation phenomena above sinkholes with diameters of 1.5 m and smaller.

The 300MHz bistatic antenna (wavelength in air-1m) provided resonant pictures and was optimal for identifying subsurface holes, at least within the diameter range of 0.6-2.4 m. The resonant pictures obtained in the laboratory experiments are similar to the results of field GPR surveys performed with the 300MHz antenna in the En Gedi Caravan Park in 1997/98. Since then, six collapses occurred on the GPR transects within the area (100 m. north/south by 250 m west/east) which coincided well with anomalous places marked on the result map of 97/98 GPR surveys. Besides separate collapses, great subsidence (tens of meters in diameter) in an area of several formerly separate GPR anomalies was formed between inner way and store room. In this study, the original resonant GPR pictures obtained above these collapsed and subsided places are analyzed. According to radar data, the depths to the roofs of revealed voids, which later collapsed, were in 1997 between 1.5 to 5.3 m. Maximum penetration with 300MHz antenna in the surveyed area was 8 m. It is important to stress that at present no collapse occurred outside the contours of the anomalous places in the surveyed spots. In our opinion, observing similar resonant pictures in radar records will serve as clear and reliable indicators of subsurface holes in future field GPR surveys. Review of scientific literature indicates that this is the first study concerning the appearance in radar records of strong resonant oscillations above hollow underground structures.

[1] Kofman, L., Ronen, A. and Frydman, S., 2006. Detection of model voids by identifying reverberation phenomena in GPR records. Journal of Applied Geophysics, 59, 284-299.

Cross-correlation study of the ambient seismic noise in Israel

Kraeva N., Pinsky V.

Geophysical Institute of Israel, P.O. Box 182, Lod, Israel
Seismology Division

Shapiro and Campillo (2004) have shown recently that broadband surface waves can be extracted from ambient seismic noise recorded at pairs of seismic stations and their dispersion characteristics can be measured in a broad range of periods. This non-trivial result is based on the theoretical finding (Snieder, 2004; Wapenaar, 2004) that the cross-correlation process applied to diffused noise recordings at a pair of stations accumulates over time the coherent deterministic components which coincide with an accuracy of frequency dependent scaling factor with a Green function computed at station locations. Because noise data are easily available and are not earthquake dependable, we are witnesses nowadays of the headily emerging new field of seismological research.

The new method was tested and verified on half-year time-series of the broad-band seismic permanent network installed in Israel and Cyprus taking for analysis firstly only days without energetic earthquakes which are the undesirable source of a noise contributing decreasing the SNR. Testing of different kinds of clipping of single-station data have shown that the best resolving capacity of the cross-correlation analysis gives the so-called temporal and spectral normalizations suggested by Bensen et al. (2006) which essentially reduce the effect on the cross-correlations of earthquakes, instrument irregularities and non-stationary or monochromatic noise sources near to stations, and produce a broader-band signal. Temporal and spectral normalizations are data-adaptive procedures allowing automating data processing without using a catalog or data visualization.

The goal of our investigation is to improve the calibration of surface wave propagation in Israel and West Mediterranean. We computed vertical and transverse component broad-band cross-correlations to produce Rayleigh and Love waves Green's functions for all available station to station paths within the network using one- and two-year time-series. The resulted cross-correlations are partially asymmetric and this asymmetry depends on the frequency band that supports an idea about acting here different kinds of directional noise sources most probably generated by the close Red Sea, Mediterranean, Dead Sea and Indian Ocean.

Application of the multiple-filter analysis to the waveforms extracted from the ambient seismic noise gives us a set of broad band surface-waves dispersion curves which are a database for generating of 1D V_s profiles and 2D group velocity maps of the crust and shallow mantle in the study area.

Influence of basement fault zones and basin inversion on salt tectonics - examples from the Mesozoic mid-Polish trough

Krzywiec P.

Polish Geological Institute, Department of Geophysics, ul. Rakowiecka 4, 00-975 Warsaw, Poland

Development of salt structures within intracontinental basins is often triggered by thick-skinned faulting of the sub-salt basement. During basin extension and subsidence salt pillows start to grow above major basement normal fault zones due to combined effect of basement faulting and differential sedimentation of the supra-salt cover. During later stages of continued extension salt diapirs form, that might extrude onto the basin floor forming salt glaciers. Apart from salt structures formed above basement fault zones also peripheral salt-related structures located at significant distance from the basin centre and detached above salt could form due to mechanical decoupling between sub-salt basement and supra-salt cover. Basin inversion, triggered by regional compressional stresses, could also lead to reactivation of salt structures. Compressed salt diapirs enter next phase of growth, their salt wings formed due to salt extrusion could act as detachments and focus development of salt-cored faults.

The Permian to Cretaceous Mid-Polish Trough (MPT) evolved above the Tornquist–Teisseyre Zone (TTZ) – crustal-scale boundary between the Precambrian and the Palaeozoic Europe, and was filled with several kilometers of sediments including thick Zechstein salts at its base. Extension along the TTZ resulted in development of complex system of salt structures, which in Late Triassic culminated in diapirism and salt extrusion onto the basin floor. Within both basin flanks peripheral syn-sedimentary grabens detached above Zechstein salt evolved. Jurassic subsidence was connected to relatively minor salt movements, next major phase of salt movements was caused by the Late Cretaceous inversion. Active growth of salt structures resulted in very complex sedimentary pattern in their immediate vicinity. Delamination and folding of the supra-salt sedimentary cover facilitated development of salt wings. Some of salt structures have been subjected to asymmetric thrusting, possibly enhanced by gravitational gliding.

Damping of pressure waves in a visco-elastic, saturated bubbly magma

Kurzon I. [1,2], Lyakhovsky V. [2], Navon O. [1], Lensky N. G. [2]

1. Inst. of Earth Science, The Hebrew University, Jerusalem, 91904, Israel.
2. The Geological Survey of Israel, 30 Malkhe Israel St., Jerusalem 95501, Israel.

We explore the attenuation of pressure waves propagating through a saturated bubbly magma. This process is examined analytically and numerically, including effects of mass transfer between bubbles and melt, visco-elasticity, bubble number density and melt compressibility. We show that the physics of wave attenuation is mainly controlled by the *Peclet* and *Deborah* numbers. The *Peclet* number is a measure of the relative importance of advection to diffusion. The *Deborah* number describes the importance of elasticity in comparison to the viscous melt deformation. We solved numerically for wave attenuation for various magma properties corresponding to a wide range of *Peclet* and *Deborah* numbers. For high *Peclet* and low *Deborah* numbers volatile transport and elastic melt deformation are negligible leading to an end-member analytical solution. We applied both solutions to a typical magma properties in a magma-filled conduit and show that the analytical solution is a good approximation for frequencies above . For lower frequencies volatile transport should be accounted for, leading to higher attenuation with respect to the analytical solution. For high frequencies (above), the *Deborah* number is increased and the elastic deformation and melt compressibility should be considered, leading to lower attenuation with respect to the analytical solution. Therefore, including the effect of melt compressibility on the attenuation of pressure waves leads to a significant improvement of the resonating qualities of a magma-filled conduit and widens the depth and frequency ranges where pressure waves will propagate efficiently through the conduit.

Character and preservation potential of coarse-grained flood event deposits of braided channels in the Arava and the Dead Sea margin - do dryland deposits of large floods have a unique nature?

Laronne J., Shlomi Y., Cohen H.

Ben Gurion University of the Negev, Department of Geography & Environmental Development, P.O. Box 653, Beer Sheva 84105

The character of fluvial conglomerates has been described in many environments, but little is known of the dynamics of their formation. These are important for the understanding of the characteristics of conglomerate deposition (e.g., gold and uranium-bearing rich deposits), of the character of river beds during large floods and their ability to transport bedload. Observations are lacking due to the energetic turbulent character of floods, making it difficult to monitor flow conditions, allowing no direct observation or measurement of the bed where deposition takes place. This is pronounced in gravelly environments.

A multi-year study was undertaken with the objective to monitor floods, the dynamic character of river beds as well as to characterize event deposits. Wadis Hemar, Zin and Neqarot were chosen for monitoring because they undergo fast sedimentation above reservoirs and the minor Wadi Samar upstream of dunes deposited along its path. The braided research sections were located close to and also further upstream of these reservoirs and dunes. Monitoring was undertaken on 3-5 floods in each river, including a rare, large flood. Identification of flood event deposits and of river-bed dynamics was facilitated by the deployment and re-location of scour chains to depths exceeding 1 m.

Event deposits are sub-parallel with almost no foresets, in sympathy with Miall's proximal braided Donjek facies. Confluence scour deposits are lacking. The texture of event deposits coarsens as does bar texture. Grading is poorly developed; infrequent inverse grading occurs in the steep and coarse-grained Hemar. Grain-supported and matrix filled packing is most prevalent. Openwork occurs as thin lenses, rarely at the bottom of an event deposit. Scour occurs also when net channels aggrade, but fill>scour. The preservation potential of event deposits increases as the magnitude of the flood increases. Deposits of small as well as large events are partially to totally eroded by successive floods. Hence, the preservation of event deposits increases as their thickness increases, disconformities typifying the entire sedimentary record.

A rare rainfall event (29.10.2004) in the Northern Arava generated large floods in the Lower Zin below the Wadi Peres confluence (ca. 1,100 m^3/sec) and in the Hemar. The scour chains enabled a first-ever documentation of event stratification (0.6-1.6 fill) of a large flood. The extent of armouring in large floods is relevant to their bedload discharge potential. Hitherto all rivers have been maintained to be armoured during large floods. This is based on evidence that bedload discharge increases with unit power in all environments; data (including from the hyper-arid Wadi Qana'im) converge to a single curve at high power. Nonetheless, the 29.10.04 deposits in the Zin and Hemar were unequivocally unarmoured. We conclude that coarse-grained dryland channels are unarmoured during large floods, as are their humid counterparts.

The Dead Sea's surface temperature: Observations from satellites and a buoy

Lensky N. G. [1], Nehorai R. [1,2], Shif S. [2], Lensky I. M. [2], Gertman I. [3], Gavrieli I. [1]

1. Geological Survey of Israel
2. Bar-Ilan University
3. Israel Oceanographic & Limnological Research

We characterize the sea surface temperature (SST) of the Dead Sea using satellite images of different spatial and temporal resolution, and concurrently collect data form a meteorological buoy. The satellite images derive from polar satellites with spatial resolution of about 1 km which overpass about 4 times a day (MODIS, AVHRR), and from a geostationary satellite (MSG) with lower spatial resolution (3 km at nadir) but higher temporal resolution - an image every 15 minutes. There is a good correlation between the images of the different satellites. We use the measured surface temperature from the buoy (measured every 20 minutes) to calibrate the coefficients of the satellite measured SST. The time series of SST measured from the buoy is very similar to that observed from MSG (every 15 minutes), with a typical sinusoidal diurnal behavior. We analyzed the satellite images in the context of the meteorological parameters, for example we examined the time series of the degree of variation in SST at every image (standard deviation of all pixels from the average SST) and found that it is in correlation with the solar radiation (with a little shift) and inversely correlated to the wind speed. The annual variations are also presented. These correlations and the spatial SST are used to calibrate a 3D model of the Dead Sea.

Deformation and seismicity associated with Cenozoic rifts crossing the Levant continental margin. II. The model

Lyakhovsky V., Segev A., Schattner U., Weinberger R.

Geological Survey of Israel, 30 Malkhe Israel St., Jerusalem 95501

Results of a 3-D mechanical model which describes the evolving faults and seismicity pattern associated with the initiation and propagation of the Azraq-Sirhan rift system are presented. The initial 3-D model structure consisting of a weak sedimentary layer over a crystalline crust and an upper mantle represents the reconstructed lithosphere to the end of the Eocene times. The total strain in each layer is the sum of (1) elastic strain, (2) damage-related inelastic strain, and (3) ductile strain. We use a visco-elastic damage rheology model to calculate the elastic strain coupled with evolving material damage and damage-related inelastic strain accumulation. The ductile strain in the sedimentary layer is governed by a Newtonian viscosity, while temperature-dependent power-law rheology is used for the ductile strain in the lower crust and upper mantle. The parameters controlling the kinetics of the damage evolution are constrained by results of laboratory analyses of stress-strain relations, acoustic emission and frictional data, as well as by scaling relations between seismic moments and rupture areas. The material constants for a creep law of a diabase are used to control the ductile flow of the lower crust, and the constants for the ductile flow of a wet olivine are adopted for the upper mantle below the Moho interface. The depth-dependent temperature distribution in the simulated volume is prescribed according to a given geothermal gradient corresponding to the measured regional heat flux. The boundary conditions correspond to the NW propagation of the Azraq-Sirhan rift system. The results of the modeling demonstrate how depth to the Moho interface affects the geometry of the propagating rift system and its associated strain field as well as its seismicity pattern. In the case of a homogeneous lithosphere with a flat layered structure, the rift system bisects the area modeled in a direction corresponding to the remote loading. With the same boundary conditions and physical properties of rocks, the rift terminates at the continental margin and a new NE-trending fault system is created. These results demonstrate that the local lithosphere structure is one of the major factors controlling the geometry of the evolving rift system, faults and seismicity pattern.

Fluorescent dyes as conservative tracers for highly saline groundwater

Magal E. [1,2], Weisbrod N. [1], Yechieli Y. [2], Yakirevich A.[1]

1. Dep. of Environmental Hydrology & Microbiology, Ben Gurion Univ. of the Negev. Sede Boker 84990
2. Geological Survey of Israel, 30 Malkhe Israel St., Jerusalem 95501

Fluorescent dyes are commonly used artificial tracers in groundwater studies due to their easy and precise measurement at low concentrations. Yet, as all other tracers, fluorescent dyes suffer from some adsorption to the aquifer minerals. At highly saline groundwater, such as the Dead Sea water (DSW), dyes sorption might be a major concern. Sorption of dyes onto different types of sediments was tested in previous studies, though the impact of high salinities on dye sorption was never examined before. Therefore, we have investigated the ability of five fluorescent dyes to serve as conservative tracers in high salinity environments.

Batch experiments were conducted for characterizing sorption of Uranine, Eosin, Naphthionate, Sulfo-Rhodamine B and Pyranine on pure minerals (calcite, quartz, dolomite, kaolinite, montmorillonite) and sediments from the Dead Sea area at different salinities. The impact of dye concentration and the ratio of solution to sediment were also tested.

The dyes Naphthionate and Pyranine were found to be most resistant to sorption at all salinities. In DSW their sorption to carbonates and quartz was low (0-30%). Yet, sorption on Kaolinite clay was highly affected by salinity, where 100% was lost to sorption at DSW in comparison to 28 and 39% at 1% DSW (Pyranine and Naphthionate respectively). Sorption on natural sediment samples was found to be particularly affected by the clay content of the sediment. The background noise of Naphthionate was high and therefore the minimum concentration to be used was over 10ppb. Pyranine fluorescence intensity is dependent on solution salinity and pH. Therefore in order to calibrate dye concentration, solution with similar composition as the groundwater on field should be used. Uranine, commonly used dye in groundwater tracing, was found to be practically unsuitable for saline environments. Its sorption to natural sediment is highly influenced by salinity, where 77-100% was adsorbed at DSW, while at 1% DSW sorption was close to zero. Sulfo-Rhodamine B was found to be highly adsorptive on all sediments and minerals and at all salinities. Sorption of Eosin on natural sediment is influenced by the solution salinities, where at 1% DSW the adsorption % was 57-91, at 50% DSW 85-100% and at DSW the dye completely adsorbed. Therefore, Sulfo-Rhodamine B and Eosin are not recommended for use in the Dead Sea area.

Slip- and rupture-partitioning at the tip of Elat transform basin

Makovsky Y. [1], Agnon A. [2]

1. Interuniversity Institute at Elat, Elat 88103, Israel.
2. The Institute of Earth Sciences, Hebrew University of Jerusalem, Jerusalem 91904, Israel.

Detailed analysis of high resolution sub-bottom profiles demonstrate the presence of an active strike slip fault that crosses the shelf offshore Elat and the eastern side of Elat hotels district. About 20 m offset of a fossil reef that evolved approximately 10-15 Ka imply an average Holocene slip rate of about 2 mm/y on this fault. Our observations imply that the major strike slip fault splays at the Northern tip of Elat basin, and traverses the basin internally away from the western longitudinal fault. Thus slip is partitioned at the basin tip between the major strike slip fault and a system of primarily normal basin-bounding faults. Enigmatically large dip-slip per rupture event are observed along the western shoulder of the Elat basin, of the order of half the horizontal slip per event estimated on the DSFS farther to the north. The apparently anomalous dip-slip per event may be consistent with of M~8 earthquakes with a ~ 10 Kyr recurrence interval. Alternatively the recurrence interval of normal slip earthquakes may be several times larger than that of the strike slip earthquakes. Either model has considerable implications regarding the faulting mechanism and earthquake hazard assessment around the Elat basin and in other transform basins around the world.

The tectonics of the Levant: The structural patterns of a fading ocean

Mart Y.

Recanati Institute for Marine Studies, Haifa University, Haifa 31905

Centrifuge structural scaled experiments of subduction showed diverse patterns of deformation when the contacts between the experiment slabs, representing the continental and the oceanic lithospheres were lubricated differentially. Experiments showed that little lubrication between the slabs led to the collapse of the edge of the modeled continental slab, so that the brittle lithosphere was extended on top of the oceanic slab due to faulting and rifting, while the ductile lithosphere was stretched thin, and the rate of lithospheric overlap was considerable. As the collapsed continent drove the subduction zone seawards, back-arc basin developed behind the island arc concurrently, exposing the modeled upper mantle. Where no lubrication was applied, the friction led to bending of the continental lithosphere, and the rate of lithospheric overlap was small. These observations led us to presume that seismic friction controls the configuration of the wide range of subduction processes, so that the difference between subduction-related mountain-range and subduction-derived back-arc basin is based primarily on the rate of seismic friction between oceanic and continental slabs. Consequently the simultaneous tectonic evolution of the Aegean-Cypriot domain to the west and the Zagros-Makran province to the east could be the products of the convergence of Arabia towards central Eurasia, where continental collision along Bitlis Zone just started while high-friction and low friction subduction took place east and west of the collision zone, respectively. The consequential anticlockwise rotation of Arabia caused the approaching Carlsberg Ridge to rotate westwards to form the Gulf of Aden and the East African rifts from the late Oligocene, and then swerve northwestwards to develop the Red Sea. Thus the Zagros-Bitlis mountain range, the Aegean and the Cilician back-arc basins, the Gulf of Aden, the Red Sea and their offshoots are all by-products of the closure of the Tethys and the collision of Arabia with Eurasia.

Accretion of ophiolites

Mart Y.

Recanati Institute for Marine Studies, Haifa University, Haifa 31905

Ophiolites are blocks of oceanic crust that accreted along marine volcanic ridges. They are built of basaltic pillow lavas and sheeted dikes, gabbro and peridotites, that overlie metamorphic series and underlie black shales and abyssal chert. Though formed at the depths of marine basins, ophiolites were eventually emplaced and exposed within uplifted collisional segments of the continental crust. Due to hydrothermal circulation in the marine volcanic ridge, ophiolites are commonly altered to serpentinites and chlorites, with abundant epidotization which turn the original hard peridotite into a pliable rocky mélange. Ophiolites are enigmatic rock suites. Their lithology suggests that they represent the oceanic crust but their average silica content of ~55% associate them with forearc lithological series. However the association of ophiolites with subduction is also far from obvious because occasionally it contains volcanic rocks of MORB composition. Furthermore, the occurrence of ophiolites in subduction zones is not omnipresent, and they are conspicuously absent in many prominent subduction zones, consequently they were commonly presumed to belong to a process to which there is no modern analog.

A series of analog experiments of the initiation of subduction that used centrifugal enhanced gravity as the only source of deformational force, shed new light on the origin of ophiolites. We encountered indications that the development of back-arc basins and the seawards rollback of subduction zones is associated with the collapse of the edge of the continental slab. While the ductile continental lithosphere stretches in the collapse process, the brittle lithosphere breaks up to extensively expose the upper mantle. Volcanism extracted from the down-going oceanic slab generates magma chambers, sheeted dikes and pillow basalts that were accreted directly on the exposed upper mantle to generate the typical ophiolites lithology. We also found out that seismic friction between the convergent slabs determines the configuration of the subduction zones, its rate of rollback, its continental collapse and the opening of the back-arc basin, therefore we presume that the rate of fore-arc serpentinization determines the characteristics the accretion of ophiolites at the seafloor, or regarding their absence. Subsequent mountain building processes would emplace the merged system of ophiolites and metamorphics at mountain tops.

Radon as a proxy of subtle geodynamic activity in the volcanic context - Tenerife (Canary Islands)

Martín C. [1], Steinitz G. [2], Gazit-Yaari N. [3], de la Nuez J. [1], Quesada M. [1], Fernandez C. [4], Casillas R. [1]

1. Department of Geology and Soil Science, University of La Laguna, Tenerife, Canary Islands, Spain
2. Geological Survey of Israel, Jerusalem, Israel,
3. Soreq Nuclear Research Center, Yavne, Israel
4. Dept. of Geology, University of Huelva, Huelva, Spain

A radon monitoring array is installed at the volcanic edifice of Tenerife for studying the radon flux as an indicator of geodynamic activity. The steep topography of Tenerife and the existence of a dense network of underground galleries has enabled setting up a 3D network of monitoring stations (located from 400 to 5,000 m horizontal distance and from 1 to 800 meter depth), covering the overall structure of the island at a scale of several tens of kilometers.

Systematic radon signals are found at different stations, located in the subsurface of Tenerife. Large-scale Multi Day (MD) variations, lasting 2-20 days, are the major variation type. Daily Radon (DR) signals occur locally, superimposed on the MD signal.

Radon variation is temporally correlated over edifice scale distances, with systematic time lags. Radon signals (MD) are temporally correlated over distances from 1 km to around 40 km, i.e. at the scale of the volcanic edifice itself. The synchronicity of the temporal variation in the radon level in the deep subsurface of the volcanic edifice of Tenerife, indicates that the radon flux is operating to a large scale as one system within the volcanic edifice. Small temperature variations of the geogas are also observed, co-related over large distances, with a systematic time lag. The temperature rise must be due to warmer air from a lower level, indicating a large scale geogas flow operating within the volcanic edifice. It is suggested that this is a manifestation of subtle volcanic activity. This indicates an active system of large spatial extent. Radon must be carried by the flowing geogas from a source which is probably at a larger distance than the source of higher temperature. This co-relation indicates in turn that the radon flux, showing large signals, is also reflecting subtle volcanic activity.

It is supposed that mechanical processes – stress and strain - govern the increased release of radon from the source rock located within a limited distance. The spatial correlation suggests that the timing of mechanical release is communal over large distances. Such synchronized release (and detection) of radon implies that the operative mechanical process is a regional one. It is suggested that it is of an active geodynamic nature.

The established monitoring array provides a geochemical data set incomparably superior to that obtainable by grab sampling of soil gas or underground water, and provides an image of high time resolution spatial (3D) changes in the radon flux. The subsurface array is of importance for long term radon monitoring, as it seems to be sensitive to the volcanic activity, and thus could serve as a natural laboratory and test bed for establishing radon phenomena as a proxy of subtle volcanic activity.

Deformation and coluvium lithification associated with normal fault stepping, Upper Galilee, Northern Israel

Matmon A.[1], Katz O.[2], Agnon A.[1], Ron H.[1]

1. Institute of Earth Sciences, Hebrew university, Jerusalem 91904
2. Geological Survey of Israel, 30 Malkhe Israel, Jerusalem 95501

A sequence of six distinguishable coluvial wedges is exposed at the base of the Zurim Escarpment west of Majd-El-Kurum, Upper Galilee. The wedges are composed of carbonate clasts embedded in a carbonate matrix. The wedges rest at angles progressively decreasing from 67° at the bottom to 30° at the top. The lower four wedges are well-lithified and tilted at angles greater than the angle of repose suggesting significant tilting during and after calcification. The fifth, and thickest wedge is moderately lithified, and the coluvial layer at the surface is unconsolidated. We suggest that the increasing angle of the wedges is the result of a growing flexure developing over a left step between two normal faults (relay ramp). Previous mapping, measured dips and air-photo analysis support this explanation. A similar setting is exposed along the Zurim Escarpment in another location.

Paleomagnetic measurements show strong magnetization carried by a cubic ferromagnetic phase, probably maghemite, associated with the calcification of the wedges, implying CRM which was acquired over a long time. All samples show northerly declinations and positive inclinations that range between 33°-56°. Mean inclinations of wedges (1), (2) and (4) are similar (40.1°±6.4° to 42.4°±5.2). The expected GAD inclination is 50°.

Samples from wedge (1) show secondary magnetization with opposite direction which was most probably acquired during the reversed geomagnetic field at the end of the Matoyama chron (0.99-0.78 Ma) after the normal Jaramillo subchron (1.07-0.99 Ma). All other samples (except one from wedge 2) show single component vectors that most likely were acquired during the Brhuns geomagnetic normal period.

Our working hypothesis is that each sample records the amount of tilting that occurred since magnetization stabilized. For example, if magnetization was acquired during deposition at the repose angle of 30° and tilting of 35° has occurred since, the measured inclination should be 15°. Inclination data suggests that: 1) magnetization did not occur immediately after deposition, 2) magnetization was acquired initially at nucleation centers and progressed outwards, and 3) some areas in each wedge acquired their magnetization after tilting was completed. Since magnetization was controlled by the calcification process, paleomagnetic results do not testify to the relation between tilting and seismic activity but they bear on the pedogenetic process. Nevertheless, the age constraints indicated by the paleomagnetic declinations suggest that most of the tectonic tilting could have occurred between 1.1-0.7 Ma and that since then this part of the Zurim Escarpment has been relatively quiet. This is in contrast to the inferred activity on the Nahef fault, several km eastward, where an exposed fault scarp reveals substantial seismic activity during the late Pleistocene and Holocene. This implies long term and independent activity of fault segments along the Zurim Escarpment.

The dynamic coast of the Dead Sea - going back to the landscape that prevailed 10.000 y ago? Or even more!

Mazor E.

Weizmann Institute of Science, Rehovot

Published observations: (1) Collapse sinkholes evolved along the N-W shore of the Dead Sea since 1992; (2) this coincided with the drop of the lake to -410 m below sea level, 20 m deeper than the level till the 1950th; (3) river beds were deepened, (4) drillings at the shore revealed at a depth of around 20 m the presence of a halite bed, 7 to 11 m thick; (5) the halite age is around 10.000 a.; (6) springs and drillings revealed that the base of drainage of the regional groundwater (recharged at the Jerusalem Mountains) was to the surface of the Dead Sea; and following the drop of the lake surface the groundwater level dropped around 20 m.

A general note: The groundwater level at coastal planes is as a rule slightly tilted seaward, and the base of drainage is the sea surface, as in the case of the rivers. The shallow cycling groundwater is recent, whereas groundwater encountered at below sea level depths is old, i.e. it is fossil and statically entrapped in rock compartments.

Conclusions based on the listed observations: (1) The base flow of the shallow groundwater was limited within the upper part of the coastal sediments, (2) the deeper groundwater, at a depth that included the buried halite bed, was static and fossil; (3) the shallow groundwater level dropped in response to the lowering of the base of drainage; (4) as the dropping groundwater base flow reached the buried halite bed, it started to dissolve it intensively, forming subterranean galleries into which the overlying coastal sediments began to collapse.

The events at the Dead Sea some 10.000 years ago: (1) The Dead Sea was lower and saltier and the named halite bed was precipitated; (2) soon after this stage the Dead Sea level raised, and the young halite bed got covered by fluvial sediments, (3) the former shallow groundwater level responded and raised above the salt bed and the latter got sheltered.

Discussion regarding future developments: If the Dead Sea level remains low, the advancing formation of collapse sinkholes and intensive erosion by the rivers will eventually lower a substantial part of the respective shore to the level of the base of the halite bed, i.e. the shore will be lowered by around 20 m - as it was 10.000 years ago.

Implied research: (1) Niches of the shore with no buried salt bed have to be located by drill holes, and these locations may be preferred for the construction of needed buildings and other installations; (2) deeper boreholes have to be drilled in order to find out whether additional salt beds are buried deeper – this is essential to examine what will happen if the Dead Sea level will drop deeper; (3) channeled ocean water will fill the holes, forming a dangerous landscape!

Initial results from the GEO-DESIRE project across the Southern Dead Sea basin

Mechie J. [1], Stiller M. [1], Meiler M. [2], Petrunin A. [1], Sobolev S.V. [1], Weber M. [1], Abu-Ayyash K. [1], Ben-Avraham Z. [2], El-Kelani R. [3], Qabbani I. [4], DESIRE Group [1]

1. GeoForschungsZentrum Potsdam (GFZ), Telegrafenberg, 14473 Potsdam, Germany
2. Department of Geophysics and Planetary Sciences, Tel-Aviv University, Tel-Aviv 69978, Israel
3. An-Najah National University, P.O. Box 707, Nablus, Palestine Territories
4. Natural Resources Authority, P.O. Box 7, Amman 11118, Jordan

The GEO-DESIRE (GEOscientific DEad Sea Integrated REsearch) project is a multinational and interdisciplinary study of the Dead Sea Transform (DST) in the region of the Southern Dead Sea basin. The DST with a total of about 105 km multi-stage left-lateral shear since about 18 Ma ago, accommodates the movement between the Arabian and African plates. It connects the spreading centre in the Red Sea with the Taurus collision zone in Turkey over a length of about 1100 km. With a sedimentary infill of about 10 km in places, the Southern Dead Sea basin is the largest pull-apart basin along the DST and one of the largest pull-apart basins on Earth. The project is divided into five themes - plate movement, crustal structure, aero-gravimetry, earthquakes and radon, and geodynamic modeling. Field experiments within the first four themes have either been completed or are being carried out or are planned. Calculations within the geodynamic modeling theme are also progressing. Within the crustal structure theme, seismic wide-angle reflection / refraction (WRR) and near-vertical incidence reflection measurements and magnetotelluric measurements were completed in 2006 along a profile crossing the DST in the region of the Southern Dead Sea basin. The WRR measurements comprised 11 shots recorded by 200 three-component and 400 one-component instruments spaced 300 m to 1.2 km apart along the whole length of the E-W trending 240 km long profile. First models of the P-wave velocity structure derived from the WRR data show that the Southern Dead Sea basin is filled with salt-rich sediments about 8 km thick beneath the profile. In contrast, the interfaces below about 20 km depth, including the top of the lower crust and the Moho, show less than 3 km variation in depth beneath the profile as it crosses the Southern Dead Sea basin. Thus it seems that the pull-apart basin beneath the Southern Dead Sea is mainly confined to the upper crust. Thermo-mechanical modeling within the geodynamic modeling theme supports such a scenario and indicates that, in order for the Southern Dead Sea pull-apart basin to form, the surface heat-flow in the region must be greater than 50 mW/m^2.

Microbialites of the Saharonim Fm, middle Triassic, Makhtesh Ramon, Israel

Meilijson A., Benjamini C.

Department of Geological and Environmental Sciences, Ben Gurion University of the Negev, P.O.B. 653, Beer Sheva, Israel 84105
meilijso@bgu.ac.il; chaim@bgu.ac.il

Microbialitic sediments are mainly laminated biogenic accumulations attributed to trapping, binding and chemical actions of non-skeletal, chiefly cyanophycean algae. Microbialitic stromatolites occur in the Ladinian through Carnian Saharonim and Mohilla fms of Makhtesh Ramon. Druckman (1974) considered them to be near-subtidal or shallower depositional facies. In the present study, we assume that peri-evaporite stromatolites are well known, so we are here concentrating on microbialites which appear to occur on subtidal shelf settings.

We have discovered diverse energetic, ecological and sedimentological settings in which the non-peri-evaporitic Saharonim microbialites may occur. Substrates range from fossiliferous limestone to coarse conglomerate, possibly composed of storm rip-ups, and terminating beds can be from massive molluscan accumulations, crinoid bearing beds, or clay and marl. These diverse, often open marine shelf settings, point to microbialite proliferation either in distinctive environmental conditions (e.g., elevated salinity in deeper subtidal settings), default growth in the absence of framework builders, or a combination of these.

The large-scale configuration of each bed, the macro- and mesostructure (hand specimen and polished slabs) and microstructure were recorded in the field and laboratory. Microbialitic morphotypes exhibit planar, columnar, pseudocolumnar, cumulate, bulbous or hemispherical domed macromorphologies. The usually domed fascicles size ranges from a few to a hundred and forty cm in diameter and five to forty cm in height, except for the uppermost microbial bed, of 'paper' stromatolite buildups one hundred and thirty cm thick and up to 150 cm in diameter. One novel approach we are adopting is a Matlab-based morphometric analysis to the classification issue. The program uses statistical (principal components) and image analysis (mainly using Gabor filters used in applications such as texture segmentation, target detection, fractal dimension management, edge detection, retina identification, image coding and more) to define morphotypes.

Microbialite classification is today in flux. There is no consensus on correlation between morphology at macro- or microscales and environmental or ecological settings. Our ultimate goal is to contribute to a morphometric-based classification that correlates with sediment-based environmental parameters.

Attenuation of ground motion in Israel region

Meirov T.[1], Hofstetter R.[2], Ben-Avraham Z. [1], Steinberg D. [1]

1. The Tel-Aviv University, P.O. Box 39040, Tel Aviv 69978
2. The Geophysical Institute of Israel, P.O. Box 182, 71100, Lod

The main goal of our work is a generation of frequency dependent attenuation model for the Israel region based on regional data. For this purpose we use regression technique that was proposed by Yazd (1993), Herrmann (1999), Raoof et al. (1999) and Malagnini et al. (1999). The introduced regional ground motion scaling relationship can be used in seismic hazard analysis and for design other applications. For the analysis we use 4786 waveforms recorded by 30 stations of the Israel Seismic Network from 2000 to 2005. We restricted our analysis to events recorded at 5 or more stations, resulting in 330 appropriate earthquakes, with a magnitude range between 0.8 and 5.2. We derive the empirical excitation, site, and attenuation terms by regressing the peak amplitudes of shear-waves and peak rms Fourier spectra measured from the band pass filtered waveforms.

The regional attenuation functional is empirically determined with its uncertainty calculated by using Jackknife statistics. Theoretical modeling is performed by Band Limited White Noise Random Vibration Theory (Boore, 1983). The method assumes a point source model with a single corner frequency (Brune, 1970, 1971) and energy distributed randomly over duration of slip.

The logarithm of peak velocity was scaled in terms of crustal parameter Q, geometrical spreading, coefficient of shallow attenuation, regional site effect, stress drop etc. Our estimate of quality parameter ($Q = 270*f$ **0.7) differ and somewhat higher than previous estimates. The geometrical spreading rate is r**(-0.95), where r is hypocentral distance. The new attenuation has a significant impact on predicted ground motions. Our analysis demonstrates that attenuation in the Israel region is slower than previously believed. Possible reasons for this difference in values that our estimates of Q value tend to average the regional attenuation effects and may be caused by the differences in the seismotectonic zones taking in account. It should be noted that the attenuation model was not constrained by data within 15 km of the earthquake source. The attenuation behavior inside 15 km is not known, and this is a possible source for significant uncertainty in our modeling and scaling.

Neoproterozoic carbonate-slate sequences of the Tambien Group, Tigre, N. Ethiopia - chemostratigraphy of cryogenian metasediments

Miller N. R. [1], Avigad D. [2], Beyth M. [3], Stern R.J. [1], Schilman B. [3]

1. Geosciences Department, University of Texas at Dallas, Box 830688, Richardson, TX 75083-0688, USA
2. Institute of Earth Sciences, Hebrew University of Jerusalem, Jerusalem 91904, Israel
3. Geological Survey of Israel, Jerusalem, Jerusalem 95501, Israel

The Arabian-Nubian Shield (ANS) records the Neoproterozoic conversion of the Mozambique Ocean into the East African Orogen (EAO), in association with major fragmentation of the Rodinian supercontinent and Gondwana amalgamation. This timing paralleled the development of Cryogenian Earth systems. New radiometric age constraints from the Southern ANS in N. Ethiopia demonstrate that ANS-EAO evolution involved two discrete magmatic phases with peaks near *c.* 780 Ma and *c.* 630 Ma, respectively related to episodes of arc crust formation (*c.* 850-740 Ma) and orogenic thickening/ differentiation (*c.* 660-580). The diamictite-bearing Tambien Group of N. Ethiopia (Tigre) is a largely marine slate-to-carbonate sequence that was deposited during the ANS-EAO intra-magmatic lull, and as such it records the history of plate tectonic, climatic, and biotic events that characterized the Mozambique Ocean realm during this time.

Litho- and chemostratigraphic variations of the Tambien Group, compiled from investigations of four areas of Tigre, demonstrate that $\delta^{13}C_{carb}$ and $^{87}Sr/^{86}Sr$ stratigraphies provide an effective basis for regional correlation and the construction of a composite reference section. The composite record reveals two consecutive positive-to-negative carbon isotope excursions, the first associated with an abrupt transition to carbonates with cap carbonate-like features and the second associated with the transition from relatively organic-rich black limestone to diamictite. Sr isotope compositions rise ballistically from values less than 0.7055 near the base of the carbonate sequence to a plateau near 0.7068 in upper limestones, before declining to 0.7064 (or lower) in the transition to diamictite deposition. Sr contents of limestones increase (10x) systematically above the lower negative $\delta^{13}C_{carb}$ interval. These principal variations show coherent agreement with other pre-"Sturtian" glaciomarine reference sequences and suggest that they are intrinsic features of Cryogenian seawater. Radiometric age constraints within the crustal evolution of the ANS-EAO suggest that the Tambien Group was mainly deposited between 775 and 685 Ma. This framework appears to provide an important new temporal perspective on the pre-"Sturtian" evolution of seawater $\delta^{13}C_{carb}$ and $^{87}Sr/^{86}Sr$. Correlation of the lower negative $\delta^{13}C_{carb}$ excursion above the *c.* 754 Ma Kaigas glacial, as opposed to the *c.* 815 Ma age inferred for the Bitter Springs anomaly, represents a critical new correlation that is compatible with constraining ages for other pre-"Sturtian" reference sequences.

The 780-630 Ma intramagmatic lull derived for the ANS-EAO, thus seems to naturally subdivide the Cryogenian system in the ANS.

Timna copper ore as an example for prospecting and production according to the mining ordinance

Mimran Y.

Ministry of National Infrastructures, P.O.Box 36148, Jerusalem, 91360

In mineral prospecting, according to the Mining Ordinance, four stages are defined by which one should proceed in zooming into the target site and getting a discovery certificate after proving economic feasibility of production.

Prospecting starts usually with surface sampling and remote sensing survey over large areas, followed by drilling, and integration of all data available. The professional work plan is subject to the Mining Commissioner's approval and usually executed according to defined milestones. The professional material is kept in confidentiality as long as the prospecting right is still in power.

Arava Mines Company (AMC) is a daughter company of the Mexican AHMSA Co. which has been operating a few large mines for generations. AMC purchased all the professional material held by Timna Mines which terminated the mining activity some 20 years ago. After adding a few tens of drillholes, the geologists of AMC prepared an integrated model of the copper ore, and proved a feasible economic production. A discovery certificate was granted to the company and it is now eligible for a Production License as soon as a pilot plant starts operating and producing pure copper by heapleaching and electrolysis within a few months.

Needless to say that all operations in the area are subject to an approved detailed plan which will relate to the various environmental aspects.

GIS applications in the interpreting of economic geology data, Mishor Rotem oil Shale deposit

Minster T.

Geological Survey of Israel, 30 Malkhei Yisrael St., 95501 Jerusalem

The Mishor Rotem Oil Shale Deposit (ROSD) is the most thoroughly investigated of the Israel oil shale occurrences. Hundreds of boreholes and many thousands of analyses were carried in an attempt to develop adequate technologies for energy utilization. The processed data was the basis for building mining models in earlier stages of prospecting which led to the development of the Havarbar open pit mine from which raw material for the existing power-station is supplied.

A renewed interest in the potential utilization of oil shale has resulted from the recent increase in the price of energy resources. This, in addition to domestic planning conflicts on future land use, requires an updated presentation of geo-technical aspects the ROSD. The main parameter applied herein for data processing was the EOM (Easily Oxidised Material), which was obtained for some 20,000 samples. For most processing targets, a cut-off value of 10% EOM was adopted, and this together with the borehole locations, the top and thickness of the ("economic") oil shale units, were used to calculate average grades of ore.

Data was processed and presented using the ArcGIS9 package. Lateral calculations were made by kriging, and the results were restricted to the ROSD polygon (~23-25 km^2) based on the known continuous extension of the oil shale. The resulting maps present computerized solutions regarding the topography of the top of the oil shale unit (taking into account the DEM database), lateral changes in oil shale thickness, average grade, overburden thickness, and overburden to oil shale thickness ratio. They demonstrate the difference between the Northern, low overburden area and the southern area in which both overburden and oil shale are generally thicker. Of special interest is the overburden ratio in the Northern part of the ROSD which reveals possible sites for future open-pit mining. A map showing the organic matter "weight" (arbitrary parameter = oil shale thickness x average grade in each borehole) allows an interpretation of the location of original centers of deposition (Depo-centers). Some of these localities differ significantly from the present-day synclinal axis.

Sinkholes development over natural tunneling in the past and today

Motzan Z.[1], Arkin Y.[2], Avni. Y.[2]

1. Ministry of Science and technology, Dep. of Science Literacy, POB 49100, Jerusalem 91490
2. Geological Survey of Israel, 30 Malkhe Israel St. Jerusalem 95501

Natural tunneling with seepage flows have occurred in recent years in mud sediments on the shores of the Dead Sea. These seepages of water of ranging salinity flow out on beach terraces near the shore line. Above the subsurface path of these natural tunnels sinkholes of various sizes have developed. The sinkholes express the collapse of the roof of the tunnel at various locations along its path. Today this phenomena occurs near the shore where the interface between the Dead Sea water and groundwater migrates eastwards as the Dead Sea retreats. At present most of the tunnels are exposed along the active shore exposing the local water table. In the past these features were well developed in along the entire costal plain to the western border fault of the Dead Sea in the sediments of the Lisan Formation and alluvial fans.

The mechanism of development of these features is different from that proposed previously in that they occur above the regional water table and are not connected with deeper seated salt layer below the water table or necessarily connected to tectonic lineaments as previously proposed.

We propose that the wide range of collapse structures developed in the Dead Sea costal plain is generated by an integration of several physical mechanisms such as salt dissolution and subsurface flow erosion. However, the end result of these different physical mechanisms is almost identical resulting from the similar geotechnical characteristics of the lithological sequence exposed in the Dead Sea costal plain.

Quantifying thermal convection within surface-exposed fractures

Nachshon U. [1], Weisbrod N. [1], Dragila I. M. [2]

1. Department of Environmental Hydrology & Microbiology, Zuckerberg Institute for Water Research, Blaustein Institutes for Desert Research, Ben-Gurion University of the Negev, Israel.
2. Department of Crop & Soil Sciences, 3017 Agriculture and Life Sciences Building, Oregon State University, Corvallis, OR, USA.

Fractures in the vadose zone, especially within low permeability rocks in arid regions, have a major role in the hydrological cycle. Fractures may serve as the major or even the only conduits for recharge from land surface to underlying aquifers. Recent studies have found that fractures serve another important hydrological function; water evaporates from the fracture surfaces, resulting capillary flow of solutes from the surrounding matrix towards the fracture walls. As water evaporates, the dissolved salts are deposited on the fracture surfaces and a salty crust develops. During flow events, these salts might be dissolved and migrate downward toward the water table. This could be a significant groundwater salinization mechanism.

It was found, both experimentally and theoretically, that the evaporation and the salt deposition rates are a few orders of magnitude higher than the rates expected from diffusive flux of water vapor. The suggested mechanism for the high evaporation rates was that water vapors are being released from the fracture by thermal convection of the air. Convection could be developed as a result of thermal gradient (and the resulting density differences) between the air inside the fracture and the ambient atmospheric air above it, which is much colder during the nights. This hypothesis was proven in a series of laboratory experiments.

This research explores the development of convection cells under natural field conditions inside fractures and quantifies the convective velocities and pattern generated under different thermal gradients. Hele Shaw laboratory experiments and *in situ* field measurements were obtained in order to observe and characterize the convection cell flows.

We have found that the convection cells are being developed as theory predicts, above a critical Rayleigh number. The thermal gradient and the aperture size affect: (1) convection cell shapes and dimensions; and (2) convection flow velocities. In general, as the fracture aperture and/or the thermal gradient increases, the convection velocities increase, and the ratio between the convection cell height to width increases as well. *In situ* thermal measurements in a natural fracture at Secher wash have shown thermal evidences for the development of the convection cells. As expected, these conditions developed during the nights, when the atmospheric air is cold and the air inside the fracture is warmer.

This research proved, for the first time directly, the existence of convection flows inside natural fractures. The convection cells were quantified and it was found that the mass transfer rates due to convection are more than 80 times higher than the mass transfer rates due to diffusion. It was also clear that the convective cells pattern is very sensitive to both the thermal gradient and the fracture aperture.

Sulfur isotopic variations within the evaporites of the Danakil Depression, Southern Red Sea rift system

Nielsen H. [1], Wakshal E. [2], Holwerda J. G. [3], Hutchinson R. W. [4]

1. Geochemical Institute, Goettingen University, P.O. Box 1142, D-37116, Bovenden, Germany
2. The Leo Picard Groundwater Research Center, The Hebrew University of Jerusalem, Israel
3. The Ralph M. Parsons Co., Pymble, N.S.W., Australia
4. Geology Department, University of Western Ontario, London, Canada

The Danakil Depression has accumulated during its formation in the Quaternary a sequence of more than 1,000 m of relatively undisturbed evaporate strata. The depositional period was accompanied by active volcanism and mafic intrusions. Sulfur isotope measurements of the sulfate sulfur (anhydrite, kieserite, etc.) within these strata of Musley area, Ethiopia, have been undertaken in order to gain additional information about the mode of their deposition.

Our results point to a marine composition of the sulfate sulfur within the potash-bearing Houston Formation, accidentally succeeded by sulfur contributions from other sources (volcanic?, eolian?, meteoric?).

The larger part of the measured samples originate from the cores of drillhole Ht 10A, sampled by two of us (J.G.H. and R.W.H.). Anhydrite of the basal analyzed section has a $\delta^{34}S(SO_4)$ of 22.4‰, which correlates well with the sulfate sulfur of inflowing seawater of the early Quaternary. This agrees with an isotope fractionation between the dissolved and precipitated phases of about 1 to 2‰. Due to this preferential extraction of the heavy isotopes, the overlaying sulfates became lighter, as is documented by the final δ value of 19.3‰. This observed range of fractionation has been verified also in the course of evaporation and sedimentation of Red Sea water, now happening in natural pools along the Ras Muhamad coastline of Sinai, close to Ofira-Sharm-a-Sheich (23.3‰).

Experimental study of manganese adsorption on coastal plain aquifer sediments - Quantifying the model of Manganese mobilization in the Shafdan reclamation plant

Oren O. [1,2], Gavrieli I. [1], Burg A. [1], Lazar B. [2]

1. Geological Survey of Israel, 30 Malkhe Israel St., Jerusalem 95501, Israel
2. The Institute of Earth Sciences, The Hebrew University of Jerusalem, Jerusalem 91904, Israel

Manganese retardation due to adsorption on aquifer sediments was suggested to be the main mechanism responsible for the delay in appearance of high Mn concentrations in the production wells of the SAT (soil aquifer treatment) system of the Shafdan plant (Oren et al., 2007). In order to quantify this process we conducted Mn adsorption experiments with columns filled with undisturbed clayey sand sediments from the Shafdan area. During each experiment, solution similar in composition to that of the SAT system but with variable Mn content was pumped through the column. In order to prevent oxidation of the soluble reduced Mn and to simulate the suboxic conditions prevailing in the aquifer, nitrogen gas was continuously bubbled to the input solution container. Water samples were collected throughout the experiments before and after the column. The column sediments were analyzed by sequential extraction for different Mn fractions prior and at the end of each experiment. The water samples were analyzed for Mn, Na, K, Ca, Mg and SO_4.

The results show significant adsorption of dissolved Mn(II) (up to 25 mg Mn/kg sediments) on Shafdan sediments within the column. The Mn(II) breakthrough curves explain the long retardation time in the Shafdan aquifer sediments. The adsorption behavior was dependent on the dissolved Mn(II) concentration enabling the calculation of the Mn(II) distribution coefficient (between Shafdan aquifer sediments and 100% effluents-type groundwater). These experiments corroborated our model for Mn mobilization within the Shafdan SAT aquifer system comprising of the following steps: reduction of sedimentary Mn-oxides, adsorption and retardation of the dissolved Mn(II), attainment of equilibrium between the cation exchange sites and the Mn-rich water, enabling Mn mobilization.

2D Diffraction as a method for a cavity detection applied for the Dead Sea sinkhole problem

Pelman D., Ezersky M., Keydar S.

The Gephysical Institute of Israel

One of the main aspects of the Dead Sea sinkhole problem is the subsurface cavity detection. We consider the sinkhole development as multi-step process including (1) dissolution cave formation within the salt layer at the 30-70m deep (latent stage), (2) gradual ascent (raising) of the cave from salt top up to surface (second stage) and (3) the sinkhole formation at the final stage. The process develops with a time and gives the possibility to detect its signs before the collapse of the surface will take place. Different structural models describe the subsurface at the different stages of sinkhole formation. If at the first stage cave would be considered as the water filled isolated cavity within the layered media, at the second stage the shallow subsurface above the salt dissolution cavity is presented by the scattered medium damaged by the fractured, water channels etc. Different geophysical techniques should be applied at different stages of the sinkhole development.

We propose to use the method based on stacking diffractions in 2D. The wave fields arising in the media that include local inhomogeneous, such as karsts, cavities, voids, etc., are usually characterized by the presence of diffracted waves. Diffracted waves contain valuable information regarding both the structure and the composition of seismic media. Our approach suggests that every point is a possible location of a point diffractor, and its imaging is performed by stacking seismic energy along diffraction curve. This approach does not require information on velocities

We present the diffraction images constructed for the Nahal Hever south and Newe Zohar sites using the data that was acquired at the stage when first sinkholes appeared at the surface.

Development of pc-based software for approximation of H/V spectral ratio by 1D shake model using stochastic optimization algorithm

Perelman N., Mikenberg M., Zaslavsky Y.

Seismology Division, Geophysical Institute of Israel, P.O. Box 182, Lod 71100

A spectral ratio from ambient noise we use normally to estimate a first mode of the transfer function for the vertical incident S-waves. This function is computed using SHAKE program for a specified 1D subsurface model. Such a model is characterized by a matrix of parameters (thickness, density, S-wave velocity and damping factor) of multilayer system.

To approximate the spectral ratio by analytical function in the best way, considering the resonance frequency, its associated amplitude level and the shape of the curve new stochastic optimization algorithm is used. This algorithm is based on The Differential Evolution, which is a simple and efficient adaptive scheme for global optimization over continues spaces.

The main program was written using the MATLAB Graphical User Interface (GUI) technique to facilitate user interaction with the program. The calling external program module, which executes the fitting by method stochastic optimization, was written using the FORTRAN90.

This software realizes the following interactive possibilities: visualizing, editing and printing input data; computing 1-D analytical transfer function; fitting analytical transfer function to H/V spectral ratio; drawing, editing, printing and saving all results as graphical and ASCII files. An option for direct computation of a site response function for a given subsurface model separately is also included.

Investigation of network beamforming for the real-time earthquake location in Israel and Japan

Pinsky V. [1], Horiuchi S. [2], Hofstetter A. [1]

1. Seismology Division, Geophysical Institute of Israel, P.O.Box 182, Lod, Israel
2. National Research Institute for Earth Science and Disaster Prevention (NIED) 3-1 Tennodai Tsukuba, Ibaraki-ken 305-0006, Japan

The problem of reliable and accurate seismic event location is a key issue in seismic events monitoring for early warning systems. This issue is determined by how we manage to fight various detrimental factors such as sporadic seismic noise, poor network configuration, heterogeneity of Earth, wrong phase association or multiple event manifestation with minimum given number of phase readings.

For this purpose we developed a robust sparse network location technique, based on array location principles: Network Beamforming (NB), which processes bulletin phase arrival time data via the use of complex exponents in a grid-search for the maximum semblance in hypocenter space. The use of the robust semblance statistic provides reliable and fast phase association and location results for 1D and 3D Earth in local, regional and teleseismic distance ranges, effectively separates double events and associates depth phases. The method is working in combination with several automatic picking approaches and effectively resists to false readings even when other methods fail.

The method was verified using a data-base of P phase picks for well constrained earthquakes and explosions from the world-wide network of stations and national seismic networks of Japan and Israel.

Relief evolution of the upper Revivim valley

Plakht J.[1], Zilberman E.[2], Avni Y.[2], Porat N.[2]

1. Ramon Science Center, Blaustein Institute for Desert Research, Ben-Gurion University
2. Geological Survey of Israel, 30 Malkhe Israel St., Jerusalem, 95501

The Neogene to Late Pleistocene landscape evolution of the drainage basin of upper Revivim valley was reconstructed using morphostratigraphic and sedimentological analyses.

The drainage basin of Nahal Revivim occupies some 50 km^2 in the southWestern part of the Yeroham syncline located between the Hatira and the Yeroham anticlines. Nahal Revivim crosses the Yeroham anticline in a narrow transversal valley, and therefore its long-term rate of denudation is controlled by the incision rate of outlet canyon.

The morphological history of the Revivim drainage basin is represented by well preserved series of fluvial terraces: four upper rock-cut terraces (VIII-V) mantled by alluvial pebble-sandy sediments, which range in age from the early Miocene to Pleistocene, and four (IV-I) Late Pleistocene to Middle Holocene terraces, consisting mainly of re-deposited loess.

Morphostratigraphic analysis coupled with lithological investigations and OSL data permits the following conclusions:

During the early Miocene the upper basin of Nahal Revivim was separated from the Avedat Plateau by a local water divide. Therefore, the Base Conglomerate of the Hazeva Formation does not contain alluvial materials deriver from the Eocene Avedat Group. Since the removal of the regional thick cover of the Hazeva Formation from the Negev, and re-exposure of the Early Miocene relief, the basin was separated from the neighboring Boqer syncline by the present local water divide. Alluvial sediments of the Miocene and Early Pleistocene terraces were deposited under high energy fluvial regime, probably of perennial streams. The Late Pleistocene is dominated by episodic loess accumulation in the stream valleys, while erosion regime prevailed in the Holocene. Calcic paleosols dominate the loess sequence, indicating stable periods with very slow loess accumulation under climatic regime wetter than the present. The terrace morphostratigraphic sequence in the upper reaches of Nahal Revivim and the makhteshim is similar, suggesting a remarkable control of climatic fluctuations on surface processes in the central and Northern Negev, rather than tectonics.

New Israel seismic network acquisition system - NISNAS

Polozov A., Pinsky V., Kadosh D., Avirav V., Karmon Y., Hofstetter A.

Seismology Division, Geophysical Institute of Israel, P.O. Box 182, Lod, Israel

Last years essential development of seismic acquisition and processing tools is observed all over the world in response to the rapid progress of the internet and satellite technologies. The national networks are being rebuilt and the new-born international networks are constructed on the bases of the modern broad-band and short period stations, connected to the data centers via seismic intranet. These principles, which allow fast and reliable data processing and exchange, are employed, for example by such new networks as Earth Scope (US) or VBSN (Europe) created by linking local networks.

For updated seismic monitoring and preparedness of Israel to future large earthquakes as well as for improved waveform data exchange with other world seismic systems and the progressive seismological research Geophysical Institute of Israel (GII) now carries out modernization of Israel Seismic Network (ISN) and creation of the New ISN Acquisition System (NISNAS) in the frame of the contract between the GII and Nanometrics Co. The NISNAS is based on satellite and radio real-time communication and close-to-real time automatic waveform analysis. The project consists of four stages:

1) Transformation of the trigger-based acquisition to the continuous waveform recording;
2) Replacement of the part of the existing stations to the new ones;
3) Changing of the seismic network configuration;
4) Modernization of the existing software for processing the continuous data.

The NISNAS structure comprises four networks:

1) Site network (between data loggers and satellite transmitter);
2) Network between the stations and the data center hub;
3) Data center acquisition network, including communication between the hub and the servers and connection between the main and the backup center;
4) Analysis network – internal GII network.

The NISNAS includes several types of acquisition: radio-link, new satellite, broad-band frame relay communications based on the SeedLink and Naqs servers.

The NISNAS system includes new algorithms of real-time detection, picking and location as a part of the JSTAR analysis system, developed in GII.

The planning of a modern copper production plant in Timna

Rahamimof A.

Rahamimoff Architects and Urbanists, 34 Mei Naftoah, Jerusalem 95863

The Detailed Master Plan for the new copper production plant in Timna is under preparation at present. The essence of the project emerges from a unique geological situation.

1. Timna is one of the oldest copper mines in the world, with evidence of mining dating back more than 6,000 years, from the Khalkolitic, Egyptian, Roman and Early Islamic periods.
2. Since 1955 the State of Israel has renewed production of copper cement in the modern copper mines of Timna.
3. Production took place by extracting ore from open pits and underground mining.
4. The volume of the open pits and is more than 40 million m^3. Depth and height of the open pits is approximately 70 meters.
5. The total length of the underground mining in tunnels is about 37 km.
6. The copper ore in Timna is located at a depth of 70-300 meters. The thickness of the ore layer is about 10 meters.
7. The ore is extracted by conveyors, trucks and vertical shaft.
8. Due to lack of sufficient technology and reduction of copper prices in world markets the State of Israel decided in 1985 to close the copper mines of Timna.
9. More than 1500 workers were employed on a continuous basis in Timna during 30 years of operation.
10. In 2004 the Mexican company AHMSA, through its Israeli subsidiary Arava Mines received from the State of Israel exploration rights and subsequently the rights to mine copper ore and produce copper. The surface area of the site is about 20,000 dunams (2000 Hectares).
11. Copper is produced through the following stages: mining, crushing, heap leaching, solvent extraction, electrowinning.
12. The plant is planned to produce 20,000 tons of pure copper (99.99%) per year. All the production will be for export. Estimated investment is US $ 180 million.
13. An environmental impact assessment is being prepared at present in coordination with the Ministry of Environment.
14. A large team of professionals is participating in the preparation of the plan –AHMSA is supplying the know-how in geology, mining and the design of the process of production of copper, and specialists in hydrology, soil surveys, structures, infrastructures, traffic, ecological expertise, etc.
15. Several months ago a small quantity of copper was produced and at present a pilot project is under construction.
16. Construction is scheduled to start in 2008 and the full production will start within approximately 2.5 years. The plant will employ 400 workers directly and about 1200 indirectly.

The local committee has already approved the plan and the district committee will discuss it in the near future.

The lack of the bazalt aggregate resources to the Israeli infrastructure development

Ravina A. [1], Nsichi S. [2], Boidek Z. [1]

1. Geokom LTD - Civil engineering & Geology
2. PWD - The National Roads Authority

The increasing demand for a good quality Basalt-aggregate relays on the recognition of the engineering community about the contribution of these aggregate to improve the skid resistance of the asphalt layers. These conclusions were first published during the 80's, by the PWD (Maatz). The research has pointed out the advantage of the Basalt aggregate owing to it's soundness, significance contribution to the skid resistance and availability.

After some modifications the Basalt mixtures were emmbeded into the PWD & the general specifications. An average Basalt mixture contained 45% basalt and 55% dolomitic sand. At the late 90's the PWD has introduced the advance asphalt mixtures such as "S shape" & SMA. These mixtures use more Basalt, ranging from 55% (S Mixtures) to 80% (SMA). The PWD has also announced his new policy to use Basalt aggregate along the main roads and HWYs.

The production of Basalt aggregate requires the usage of crushers and sieves with special alloys due to the rock soundness. While marketing the required Basalt products, a lot of crushed materials remain in the quarries as a non marketable by-products.

The annual consumption for Asphalt-Basalt-aggregate is around 800,000 tons. To produce the good quality Asphalt-Basalt-aggregate the total production should be 3 to 4 time that figure. Accordint to "TAMA14" there are only a few basalt quarries. Only one quarry produces a good quality aggregate but it has run out of reserves.

Most of the good quality aggregate is being supplied by the Bteha Pit, which is not a part of the TAMA. The total annul production capacity of this quarry is evaluated as 2,500,000 tons, which is not enough for the current consumption. This leads to an un-controlable increase in the prices of the Basalt aggregate.

An action should be implemented in the various disciplines; The PWD is developing new methods to restrain the consumption; such as new methods for aggregtae mixture design and carful usage of recycled asphalt layers. The geological community should devote resources to prospect for new sources for good quality Basalt aggregate. The authorities should devote economical resources for the prospection works.

The conduit and the benefit

Raz E.

Dead Sea Institute for Rsearch and Development, Ministry of Science.

Versions for stabilizing the Dead Sea (D.S.) level were examined and abandoned occasionally. Today, RSDSC (Red Sea Dead Sea Conveyer) is marketed by Jordan, supported by Israeli personalities, as "Peace Conduit", while other alternatives were ranked much higher. Jordan desires to desalinate 840 Mm^3/y by a flowage of ~ 2 Bm^3/y from the Gulf of Aqaba and to stabilize the Dead Sea level by the brines. Experts warn that the current in the narrow edge of the gulf might damage the delicate ecosystem of the coral reefs and the tourism based on it, and that various negative effects on the limnology, microbiology and the chemical industry are expected by mixing the water of the two seas.

A desalination project in Ashkelon, already supplies 100 Mm^3/y, more projects will increase the capacity up to 320 Mm^3/y within four years, according to governmental decision. Desalination projects on the Mediterranean shore, in front of inland consumption centers, has an advantage over desalination by the seas canals, due to lower cost per production capacity and the product cost, shorter times of construction, lower environmental risks and simpler and safer integrating with the water supply system.

Producing desalinated water beyond meeting the increase in demands may replace, in a relatively short period of time, the pumping of ~ 400 Mm^3/y from the Kinneret, in order to release them to recover the Jordan River (J.R.) and minimize the drop in the level of the D.S. Directing seas canals to the D.S. will determine the mythological J.R. as a sewage canal, will bury it's potential comeback as a most desired pilgrimage site, and will introduce > 60 M tones dissolved salts of strange chemical composition.

Directing desalinated sea water from Hadera to the Jordan valley (Ben-Meir 1996), can meet the Jordanian's expectations from RSDSC + 200 Mm^3/y additional support for the Jordan River system at a shorter, quicker and lower, both economical and environmental cost, without including the threats that are mentioned above.

Kinneret-J.R.-D.S. should be regarded as one system, stabilizing the D.S. level by the recovery of the J.R. is the closest to the original situation and hence the most proper one.

Replacing the pumping from the Kinneret by desalinating sea water, and turning it to a binational reservoir fed by the Ben-Meir alignment (in the route of the national conveyer but the opposite direction) with easily manageable stable water balance, is a feasible and rational option, carrying a real message of peace and cooperation, that suits the motivation of the international financiers.

This option deserves feasibility study not less, if not more than the RSDSC.

The kinetics of gypsum precipitation as a result of mixing Red Sea water with Dead Sea water

Reznik I. [1,2], Ganor J. [1], Gavrieli I. [2]

1. Department of Geological and Environmental Sciences, Ben-Gurion University of the Negev, P. O. Box 653, Beer-Sheva 84105
2. Geological Survey of Israel, 30 Malkhe Israel, Jerusalem, 95501

In recent decades, the Dead Sea level has receded dramatically. In order to stabilize the lake's water level, it has been proposed to build a pipeline connecting the Gulf of Eilat and the Dead Sea (The "Peace Conduit"). However, before carrying out this project, there is a need to examine the impact of mixing seawater in the Dead Sea on the lake's physicochemical properties. One of the results of such mixing is gypsum precipitation, which may influence the general appearance of the Dead Sea and its physical parameters (such as evaporation rate). The aim of the current study is to quantify, by combining laboratory experiments and theoretical geochemical models, the different parameters affecting gypsum nucleation and precipitation rates.

In order to examine the kinetics of gypsum precipitation in Dead Sea brine and in mixtures of Dead Sea brine and Red Sea water, mixed-flow-through experiments were conducted. Precipitation rates were calculated based on SO_4 balance. The degree of super-saturation in the reaction cell was manipulated by changing the flow rate, the amount of seeding, and the Dead Sea / Red Sea ratio. The degree of saturation was calculated using a computerized code based on Pitzer's equations.

Spontaneous nucleation of gypsum was not observed in experiments with pure Dead Sea brine. This is in accordance with field observations indicating that the Dead Sea retains a high degree of super-saturation with respect to gypsum. However, after introducing gypsum crystallization seeds into the Dead Sea brine, gypsum precipitation takes place. The precipitation rate depends on the degree of saturation and the amount of gypsum crystals at steady-state.

Red Sea – Dead Sea mixtures (1:1 ratio) exhibit a lower super-saturation degree with respect to gypsum than pure Dead Sea brine. However, unlike in pure Dead Sea brine, spontaneous nucleation of gypsum occurs within the mixtures. Moreover, the precipitation rate is faster in the mixtures than in pure Dead Sea. We suggest that one (or more) of the ions in the Dead Sea brine inhibits nucleation and slows down the crystal growth rate. By mixing Dead Sea brine with Red Sea water the concentration of the inhibitor(s) is reduced, thereby enabling nucleation and faster crystal growth rate to occur.

Precipitation rate of gypsum from Red Sea – Dead Sea mixtures (1:1 ratio) was found to be first-order with respect to the amount of gypsum. However, beyond some threshold (1 gram in our experimental setup) the dependence changes to zero order. We suggest that when enough gypsum crystals are present (i.e. increased surface area), the reaction rate is limited by the degree of super-saturation, and it becomes a pseudo zero order reaction.

Groundwater reservoir mapping and characterization in the Negev using stratigraphy, seismic and rock physics

Reznikov M. [1], Weinberger G. [2], Aksinenko T. [3], Grossowicz Y. [1], Sobolevsky L. [3]

1. Ecolog Eng. Ltd., Oppenheimer 5, Rehovot
2. Israel Hydrological Service, Yaffa 234, Jerusalem
3. Geophysical Institute of Israel, POB 182, Lod

The Lower Cretaceous aquifer underlies the central Sinai, Negev and Arava areas. The productive horizon is buried at a depth of 0.2 - 1.5 km and comprises of the sandy-carbonaceous Kurnub Group.

A quantitative methodology for identifying groundwater reservoir and mapping its storage properties (porosity) was developed and tested in the northWestern part of the Negev area. The method is based on the integrated interpretation of data from wells and seismic reflection data.

Our approach is based on the combination of geophysics, rock physics, and stratigraphy. Advanced technologies, developed for the petroleum industry, have been applied to identify and characterize the groundwater reservoir. The main principle is that the elastic properties of the sandy-carbonaceous Kurnub Group differ from the overlying Upper Cretaceous limestone and dolomite rocks and underlying Jurassic dolomite and marly shale. Thence, seismic reflection can be used to identify the geometry of the groundwater reservoir. Because the thickness of the reservoir is significant (on the order of more then 300 m) it was possible to resolve the reservoir seismically, i.e., estimate its elastic P- and S-wave properties, such as the impedance and Poisson's ratio. Interpretation of well log data and the construction of petrophysical model reveal that these elastic properties are directly linked to porosity, lithology and diagenetic type (cement). Seismic inversion techniques and obtained relationships allow prediction of high-porosity zones within the reservoir.

The current project includes a lithostratigraphic correlation of Lower Cretaceous units that have been assembled from wells and tied to seismic data. Processing and interpretation of all subsurface data enabled a reliable and well established regional mapping of the main units and sub-units in the area. The combined interpretation of various geophysical data provided estimation of the reservoir properties. These parameters have a major significance in the planning and management of aquifers in the Negev specifically and in other regions of Israel.

The impact of land use on quantity and quality of groundwater recharge into the Coastal Plain Aquifer

Rimon Y. [1], Dahan O. [2], Nativ R. [1], Adin A. [1]

1. Soil and Water Sciences, The Hebrew University of Jerusalem, P.O. Box 12, Rehovot 76100
2. Zuckerberg Institute for Water Research (ZIWR), Ben-Gurion University of the Negev, Sede Boker Campus 84990, Israel

A study on the impact of land use on the quantity and quality of groundwater recharge is being carried out in the city of Ashdod, where urbanization has probably been the fastest in Israel. Infiltration processes under different urban land setups are being compared to those beneath nearby cultivated areas and the undeveloped sand dunes.

Temporal variations in water content at various depths were measured for two entire years at five research sites. These measurements were conducted using a monitoring system that includes flexible time domain reflectometry sensors (FTDRs) installed in slanted boreholes throughout the entire vadose zone. The system enabled quantification of wetting front propagation velocities, variation in the vadose zone water storage and direct calculation of the infiltration fluxes.

In addition to the FTDR system, the dune site was recently instrumented by a new monitoring system that allows continuous measurements of the water potential and frequent sampling of the sediment pore-water. The new monitoring system is comprised of vadose-zone sampling ports (VSPs) and FTDR sensors which are installed in slanted boreholes.

Preliminary results show a response in pore-water pressure to the infiltration process generated by a rain event. Vadose-zone pore-water were frequently sampled by a second VSP system and analyzed for chemical and isotopic compositions.

In addition to the measurements and water samples taken from the vadose zone, the groundwater at each site is monitored using a multilevel compartmental sampler which was specially developed to differentiate the recharged water and the aquifer's ambient water.

Structural and tectonic problems in the Western part of the Ramon anticline

Ronen O. [1], Avni Y. [2], Eyal Y. [1]

1. Department of Geological and Environmental Sciences, Ben Gurion University of the Negev, Beer Sheva 84105, Israel
2. Geological Survey of Israel, 30 Malkhe Israel St, Jerusalem 95501, Israel

The Ramon structure, the largest in the central Negev comprises two main sub-structures: the Ramon anticline and the Ramon fault or Ramon line. The relationships between these two have been disputed over the past forty years. Two main approaches have been suggested: A genetic relationship between the anticline and the fault was argued by Garfunkel (1964) whereas independent formation and activation was suggested by Bartov (1974). The study area of this work, west to Arod Pass, can contribute to solve this discussion.

The structures found in this area are: 1. The WSW–ENE trending Ramon anticline and Har Lotz syncline, sharing a flexure located on their common limb. 2. A series of N–S trending folds: Shkedim and Esh'harim synclines, and Har-Harif and Central anticlines, located west of the Makhtesh Ramon erosional cirque. 3. A main fault system trending E-W, and transects these folds and the Ramon anticline. these faults are mostly normal and dipping to the south. Along some faults evidence for dextral movement was found. 5. A secondary fault system trending NNW along one of them evidence for sinistral movement was found.

The Ramon fault, in the area between the Arod pass area and the Lutzan graben next to the Egyptian border, does not exist as a single fault. Instead, there is a complex splay of faults, domes and flexures collectively regarded as the Ramon line. There is a clear geographical relationship between the Ramon anticline axis and flexure and the Ramon line.

The Nahal Lotz Dome (Avni 1989) whose axis is trending 225° is located along the Ramon line and parallel to it. This dome is crossed by many faults, of which the important ones are an "S" shaped fault that is parallel to the dome's axis, and an E–W trending reversed fault.

Close to the Arod pass, the Ramon fault splits into several segments, of which the main one, called "Har Ramon fault" (Avni, 1989), trends E-W. The geometric relations between Ramon fault and the two fault systems described above resemble the pattern of a right-lateral tip damage zone (e.g. Kim et al, 2004). The pattern of the main fault system in this area seems to be a "horsetail splay" of the Ramon fault. The pattern of the secondary fault system may be of "antithetic fault" type (Kim et al, 2004).

Two stress regimes are manifested in the area: 1. A NNW–SSE compression which is compatible with the folding of the Ramon anticline, the Nahal Lotz dome, and the dip-slip movement along the Ramon fault. 2. An E–W compression which is compatible with the lateral movement along the Ramon fault, the E–W trending main fault system and the N-S trending folds.

A high sea stand in Eastern Plesehet

Ronen A. [1, 2]

1. Zinman Institute of Archaeology, University of Haifa, Haifa 31905.
2. Max Stern Academic College of Emeq Yezreel, Emeq Yezreel 19300

Remains of a sea stand 160-168 m amsl are found in N. Sad west of Tel Nagila. The remains consist of a small abrasion platform on the Eocene bedrock covered by a calcareous sandstone 10-20 cm thick with small, mostly flint river pebbles. Some 300 m to the east there is a bed of pebbles ca. 1 m thick, covered by loess ca. 1 m thick. The basal 20 cm consist of relatively well sorted pebbles up to 15 cm in diameter. The main part of the bed is made of very well sorted small pebbles, mostly of flint. In a random sample of 381 pebbles, 98% are below 32 mm wide. The pebbles are very thin: 88% have a sphericity index (Ψ_p=) lower than 0.61 and in 56%, the sphericity index is below 0.54. This is significantly below the dividing line between river vs. beach pebbles, 0.65-0.66. Hence the N. Sad pebbles seem to have been subjected to a marine abrasion. No other concentration of similar pebbles is known to us on the Israeli coastal plain. The pebbles and the near-by abraded platform may belong to the same sea stand. The location and elevation of the N. Sad sea stand suggest a Pliocene age.

Molybdenum isotope variation in iron mineralization along the Northern Negev monoclines

Ryb U. [1], Matthews A. [1], Erel Y. [1], Gordon G. [2], Anbar A.[2], Avni Y. [3], Ilani S. [3]

1. The Institute of Earth Sciences, Hebrew University, Jerusalem 91904
2. School of Earth and Space Exploration, Arizona State University, Tempe, AZ 85287-1404 USA
3. Geological Survey of Israel, 30 Malkhe Israel, Jerusalem, 95501

Molybdenum stable isotopes ($^{97}Mo/^{95}Mo$) are becoming recognized as important paleoredox proxy in the marine sediments, where an approximately -2‰ fractionation occurs between Mo adsorbed on ferromanganese nodules and anoxic sediments. Less is known, however, about the Mo isotope variation in continental settings where igneous and clastic sediment lithologies show a relatively narrow range of $\delta^{97/95}Mo$ values (0.0±.25‰, relative to the Johnson-Mathey ICP Mo standard). In the present study we measured $\delta^{97/95}Mo$ values of molybdenum in iron oxide mineralization occurring in veins along the Northern Negev monoclines. Previous studies have shown that these veins have unusually high concentrations of elements usually transported as anion complexes: Mo, V and U. Potential source rocks for the Mo anomaly were also measured for $\delta^{97/95}Mo$, including a local igneous rock from a borehole and Cretaceous organic matter-rich shales and phosphorites. The range of the $\delta^{97/95}Mo$ results for the iron oxide veins was 2.6‰ (-0.4 ± 0.2 to 2.2 ±.07‰); this range is larger than any other lithology measured to date and contrasts strongly with the narrow range of Mo-isotope compositions found for igneous rocks. The $\delta^{97/95}Mo$ values of the iron oxides show a general positive correlation with Mo/Fe ratios. These variations can be interpreted as mixing trends between three isotopic end-members: (1) $\delta^{97/95}Mo$ (~ 0‰); (2) $\delta^{97/95}Mo$ ~ 0.9‰; (3) a Mo-enriched end-member with $\delta^{97/95}Mo$ ≥2.2‰. Two of these end-members can be explained by solutions containing Mo derived by congruent (i.e, non-fractionating) leaching of the isotopically-light igneous intrusion with a $\delta^{97/95}Mo$ value of 0.12±.06‰, and the Ghareb Formation oil shales with $\delta^{97/95}Mo$ = 0.85-±.15‰. The highest $\delta^{97/95}Mo$ values (1.1 - 2.2‰) are obtained from Mo-enriched iron oxides in the Kidod and Zohar monoclines. Such high $\delta^{97/95}Mo$ values require an isotopic fractionation mechanism because they are higher than any known natural source rock. The general regional trend is for Mo/Fe ratios and $\delta^{97/95}Mo$ values to increase in the northeast of the study area, adjacent to the Dead Sea. This spatial trend suggests that the isotopically heavy Mo end-member was located in the Dead Sea Rift. Molybdenum transport with hydrocarbons from oil shales buried in the Dead Sea Rift by infiltrating Sedom lagoon brines (Gvirtzman and Stanislavsky, 2000) and isotopic fractionation of Mo as thiosulphide complexes became oxidized to form molybdate anions (MoO_4^{2-}) could possibly account for the high Mo-contents and $\delta^{97/95}Mo$ values.

Preliminary results of a high-resolution aeromagnetic survey in the Southern Dead Sea area

Rybakov M. [1], Gardosh M. [1], Berger Z. [2], Tannenbaum E. [3]

1. Geophysical Institute of Israel, Lod, 71100, Israel
2. Image Interpretation Technologies (IITech), Calgary, Canada
3. Ginko Oil Exploration Ltd. Ramat-Gan

This study shows results of a high-resolution aeromagnetic (HRAM) survey that was carried out in the western flank of the Southern Dead Sea basin. The survey was conducted in June 2006 by Aeroquest (Canada) on behalf of Ginko Oil Exploration. High-resolution magnetic data were collected using the Heli-Mag magnetic gradiometer aboard a helicopter over an area of 70km (N-S) on 15km (E-W). The E-W lines spacing was 600m and the nominal magnetic sensor terrain clearance about 50m. Helicopter speed ~100 km/hr. A total of ~1,500,000 magnetic measurements were collected along 2,089 kilometers of survey lines.

The data were incorporated into a GIS together with geology, elevation, and gravity maps to facilitate interpretation.

The main findings of the magnetic survey are as follow:

- N-S oriented magnetic zone consisting of five elongated magnetic anomalies was identified. A good correlation was found between these local magnetic anomalies and the steep (up to 10mGal/km) gravity gradient that corresponds to the western master fault of the Dead Sea graben. The Northernmost and southernmost anomalies, which were previously identified in regional magnetic surveys, probably represent subsurface magmatic intrusions.

- The presence of rift-parallel magnetic lineaments interpreted as faults. The lineament system extends NNE as the continuous trace over all the study area. The lineaments correspond to the active trace of the Dead Sea Fault and at a few locations they coincide with geologically mapped faults.

The Northernmost magnetic anomaly appears to be the eastern edge of the large Hebron magnetic anomaly. That was formerly interpreted as caused by a Jurassic volcanic body similar in age to the Asher volcanics of Northern Israel. To study the possible source of the anomaly we measured the magnetic susceptibility of the rocks at the bottom of the Emunah 1 drill hole, located inside the anomaly. The well penetrated a highly magnetized ($2\text{-}5*10^{-3}$ SI units) magmatic rocks in the interval 2724-2847m. This depth corresponds to the calculated depth of the Hebron magnetic body and therefore is a most likely source of the anomaly.

We thank Ginko Oil Exploration Ltd. for the opportune to present the new magnetic observations.

Levant: Sources of the magnetic anomalies

Rybakov M. [1], Goldshmidt V. [1], Hall J. [2], Ben Avraham Z. [3]

1. Geophysical Institute of Israel, Lod, 71100, Israel
2. Geological Survey of Israel, 30 Malkhe Israel St. Jerusalem, 95501
3. Department of geophysics & planetary sciences of Tel Aviv University

The magmatic events of the Levant were investigated using the recompiled regional scale magnetic map, the renewed petrophysical and gravity data bases and the reviewed previous interpretations. In the area of study the Earth's magnetic field vector has the low inclination and the total magnetic intensity map is difficult to interpret for location and strike of magnetic bodies. Therefore we compiled pole-reduced magnetic map. That provided excellent view of the distribution of the magmatic events. The integrated interpretation of the magnetic and local gravity anomalies allowed estimating of the depth and size of the magmatic bodies and at the some cases to identify theirs composition. Reliability and accuracy of the results was estimated by forward modeling and by comparison with seismic reflection data and drill-holes.

The study region was divided into five areas of consistent regional scale magnetic pattern with more or less distinct boundaries. Such zonation of the magnetic bodies was based not only on the formal magnetic pattern recognition but using the correlation with known (or expected) geology. The coinciding strong magnetic and positive gravity anomalies correspond most probably to the ophiolite massifs in the Northern part of the study region or basic magmatic intrusions in the southern part; strong magnetic anomalies, what are not supported by the positive gravity anomalies, correspond most probably to the Mesozoic and Cenozoic volcanics located mainly in the central part of the region; absence of the magnetic anomalies in the some area suggests reliably what there is no the basic magmatic bodies (volcanics or plutonic) but nothing about the acid magmatics (granite etc.).

Seafloor acoustic backscatter at 95 khz off Northern Israel

Sade A. [1,4], Hall J. K. [1], Golan A.[2], Amit, G.[2], Gur-Arieh L.[3], Tibor G. [2], Ben-Avraham Z. [4], Ben-Dor E. [4], Fonseca L. [5], Calder B. R. [5], Mayer L. A. [5], de Moustier C. P. [5]

1. Geological Survey of Israel, 30 Malchei Israel, Jerusalem 95501, Israel
2. Israel Oceanographic & Limnological Research Ltd., Tel Shikmona, Haifa 31080, Israel
3. Survey of Israel, 1 Lincoln Street, Tel Aviv 65220, Israel
4. Tel Aviv University, Tel Aviv 69978, Israel
5. Center for Coastal & Ocean Mapping, University of New Hampshire, Durham, NH, USA

A new poster shows the acoustic backscatter as determined by innovative analysis of the returns from high resolution multibeam mapping of the Mediterranean continental shelf and slope off Northern Israel. On each swath, the National Bathymetric Survey's Simrad EM1002 measures around 4,000 samples of the backscattered acoustic energy returning from the 111 2° beams impinging on the seafloor. Thus the 840 million soundings in the Northern Israel bathymetric survey represent about 7.5 million swaths, with over 40 billion backscatter samples.

The recorded backscatter was reanalyzed using the new Geocoder software developed at the Center for Coastal and Ocean Mapping (CCOM) at the University of New Hampshire in the USA. Geocoder corrects the original backscatter time series registered by the sonar for angle, varying gains, and beam pattern. It filters out speckle and corrects for slant range. Every backscatter sample is geocoded using several algorithms, which apply anti-aliasing, mosaicking, and blending between swaths. The final mosaic exhibits low noise, few artifacts, reduced seams between parallel acquisition lines and reduced clutter in the near-nadir region, while still preserving regional data continuity and local seafloor features. The mosaic resolution here is 5 m, tied to the underlying bathymetric grid.

The poster is at scale 1:50,000 on the Universal Transverse Mercator (UTM) Projection (Zone 36), on the WGS-84 datum. The Survey of Israel's 1:50,000 scale topocadastral map sheets are reproduced on land in Hebrew. They are texturized with the Survey's 4 m digital terrain model (DTM) using Global Mapper software with the sun in the northwest (N315°E) at 45° altitude and a vertical exaggeration of 2.

This laminated poster, which appears on the backside of the laminated poster showing the bathymetric results, will be distributed at the IGS meeting.

Latest multibeam results from the Med, Red, and Dead Sea

Sade R. [1,4], Hall J. K. [1], Al-Zoubi A. S. [5], Tibor G. [2], Amit G. [2], Golan A. [2], Gur-Arie L. [3], Ben-Avraham Z. [4]

1. Geological Survey of Israel, 30 Malchei Israel, Jerusalem 95501, Israel
2. Israel Oceanographic & Limnological Research Ltd., Tel Shikmona, Haifa 31080, Israel
3. Survey of Israel, 1 Lincoln Street, Tel Aviv 65220, Israel
4. Tel Aviv University, Tel Aviv 69978, Israel
5. Al Balqa' Applied University, Al Salt 19117, Jordan

The bathymetry of Northern Israel, presented in two posters to be distributed at this meeting, represents only a small fraction of what has been mapped since 2001 by the National Bathymetric Survey (NBS). This lecture will highlight the results of new findings on the Mediterranean continental shelf and slope, as well as the cooperative work with Jordan in October and November 2006 in the Northern Gulf of Elat/Aqaba, and the ongoing survey of the R/V Tuglit in the Dead Sea.

Multibeam bathymetry of the seafloor off Northern Israel

Sade R. [1,4], Hall J. K. [1], Golan A. [2], Amit G. [2], Gur-Arie L. [3], Tibor G. [2], Ben-Avraham Z. [4], Hübscher C. [5], Ben-Dor E. [4]

1. Geological Survey of Israel, 30 Malchei Israel, Jerusalem 95501, Israel
2. Israel Oceanographic & Limnological Research Ltd., Tel Shikmona, Haifa 31080, Israel
3. Survey of Israel, 1 Lincoln Street, Tel Aviv 65220, Israel
4. Tel Aviv University, Tel Aviv 69978, Israel
5. Institut für Geophysik, Universität Hamburg, Germany

This new hypsometrically colored shaded relief image of Northern Israel is based upon the highest resolution bathymetric datasets currently available. The offshore is based upon over 850 million soundings from multibeam sonars. Water depths from about 8 m to over 900 m were mapped by the Israel National Bathymetric Survey (NBS). The survey was carried out between 2001 and 2006 by the IOLR's 53' vessel R/V Etziona using a Kongsberg Simrad EM1002 multibeam sonar. The EM1002 has 111 2° beams operating at 95 kHz spread over an arc of up to 150°, giving maximum swath coverage of up to 7.4 times the water depth. The survey involved some 4,218 km of track, acquired during 55 days at sea. Farther offshore F.S. Meteor Cruise 52/2 in 2002 obtained partial coverage in deeper waters with an Atlas Hydrosweep system projecting 60 beams at 12 kHz over a 90° arc. This coverage was obtained under rough sea conditions, so that numerous artifacts are present. This data is hypsometrically colored using a different palette, which accentuates the physiography at these greater depths.

On land the Survey of Israel's 1 m orthophoto of Israel has been shaded using their 4 m Digital Terrain Model (DTM) using Global Mapper® software with the sun in the northwest (N315°E) at 45° altitude and a vertical exaggeration of 2. The image is at scale 1:50,000 on the Universal Transverse Mercator (UTM) Projection (Zone 36), on the WGS-84 datum.

This laminated poster, which appears on the backside of the laminated poster showing the acoustic backscatter from the same area, will be distributed at the IGS meeting. The legend of the poster points out many of the interesting features revealed in the image.

Tsunami hazard evaluation of the Eastern Mediterranean: Historical analysis and selected modeling

Salamon A. [1], Rockwell T. [2], Ward S. N. [3], Guidoboni E. [4], Comastri A. [4]

1. Geological Survey of Israel, 30 Malkhe Israel St., Jerusalem, 95501, Israel
2. San Diego State University, San Diego, CA, USA
3. University of California, Santa Cruz, CA, USA
4. Storia Geofisica Ambiente, Bologna, Italy

We constructed a catalogue of tsunamis that occurred since about the middle of the 2nd century BCE along the Eastern Mediterranean coast, along with the significant earthquakes originating from the Dead Sea Transform (DST) system. We identified 22 sea waves that struck the Levant coast, from Alexandria to Iskenderun Bay and Cyprus, with an average frequency of about once in a century. These tsunamis varied in size, from barely noticeable in local ports to greatly damaging along several coasts.

Ten of the tsunamis were triggered by earthquakes that originated in the DST system. We estimate that the threshold of tsunamigenic DST earthquakes is likely to be in the range of M6-6.5. Thus about a seventh (14%) of the moderate and between one-fourth to a third (29%) of the large DST earthquakes were probably tsunamigenic.

Another ten tsunamis were associated with remote and non-DST sources in the Eastern Mediterranean, including the Cypriot and the Hellenic Arcs and as far away as Italy. The source of the remaining two tsunamis is as yet unidentified. Most of the DST originated tsunamis are clearly associated with on-land earthquakes, and were associated with a significant retreat of the sea. This suggests that the waves resulted from seismic triggering of offshore submarine landslides.

We recognize three characteristic tsunamigenic mechanisms: convergent arc earthquakes focused in the sea; seismically-induced submarine slumps; and on-land active faults that cross into the sea. We modeled each of these mechanisms and, due to the great concern generated by the Sumatra giant-tsunami, we focused on the worst case scenarios.

Earthquake scenarios produced run-ups ranging from 1 to 3 m and the landslide scenario produced a run-up of 4-6 meters. Tsunami travel time between start and arrival of the waves to Northern Israel ranges from several minutes for near offshore landslides to about half an hour for tsunamis originating in the Cypriot Arc.

Zones of required investigation for liquefaction hazard in the Western Zevulun Plain, Israel

Salamon A. [1], Na'aman I. [1,2], Zviely D. [3], Bitton R. [1,2]

1. Geological Survey of Israel, 30 Malkhe Israel St., Jerusalem, 95501, Israel
2. Institute of Earth sciences, The Hebrew University, Jerusalem, Israel
3. Recanati Institute for Maritime Studies, University of Haifa, Haifa, 31905, Israel.

Holocene coastal and shallow marine Nile-derived sand covered by dunes and recent clays, and artificially filled areas are found in the Western Zevulun Plain, Northern Israel. The groundwater table is shallow and high seismic accelerations are expected; thus, all the necessary conditions for liquefaction seem to exist. We screened the sensitive areas in the region according to the geological, hydrological and seismological conditions and delineated the zones that require specific geotechnical investigation for liquefaction hazard.

We first examined the lithology of the surface and the shallow subsurface, the depositional environment and age of the sediments, and also identified areas that were originally marine and artificially dried. Next we evaluated the level of the groundwater table and its fluctuation with time. Finally we looked at the expected seismic accelerations in regard to the critical threshold for the occurrence of liquefaction. Putting everything together, we defined three vulnerable environments where a potential for liquefaction exists: 1. artificially filled sea areas; 2. sand dunes and sand exposed on the surface; and 3. sand covered by clay. The areal extent of these environments is displayed on a summarizing map. A potential for lateral spreading may exist in areas with a free face along natural stream banks, dredged channel banks, sloping ground and sloping contact between liquefiable layers and underlying materials.

This map is an essential layer of qualitative data that could be used for environmental and municipal planning, emergency response planning and lifeline and utility vulnerability studies, especially in a metropolitan area where dense residential neighborhoods are very close to heavy petrochemical industries. The map can also assist in conducting site-specific geotechnical examinations necessary for liquefaction-resistant engineering planning.

Possible primary volcanogenic copper accumulations in the Timna-Elat area

Segev A. [1], Rybakov M. [2]

1. Geological Survey of Israel, 30 Malkhe Israel St., Jerusalem 95501
2. Geophysical Institute of Israel, P.O. Box 182, Lod, 71100

Copper and manganese deposits occur in the Middle Cambrian Timna Fm., Timna Valley, southern Israel, ~25 km north of Elat. The main late (since Tertiary) epigenetic copper mineral assemblages, which only include oxidized minerals, occur within the sandy residual sandstones (after dissolution of the dolomites) and in the shaly lithofacies of the upper Sasgon Mbr., Timna Fm. The dolomitic lithofacies of the same member consists of early diagenetic assemblages that include copper sulfides and their hydroxide products. Most of the studies suggested that the source for the copper was in the erosion of adjacent Precambrian rocks, but up to present times this was not substantiated.

High copper ore concentrations were found also mainly within the sandstones of the Early Cretaceous Avrona Fm. This copper probably derived from Cambrian dolomite dissolution during Early Cretaceous magmatism and was mobilized upward in the sedimentary sequence. This copper was extracted during the Chalcolitic, early Bronze, Roman and Nabatean periods.

About 10 km south of the Timna Valley, in the southern Har Amram region, a few deposits hosted by the Amir and Avrona formations were exploited in the past. In this area there are no significant copper ore concentrations within the underlying Cambrian rocks, therefore it is suggested that a buried primary volcanogenic copper deposit may have been the source for the copper accumulations hosted by these Early Cretaceous sandstones in the Amram region. The following sequence of Late Precambrian-Early Cambrian magmatic rock units and events have been suggested for the Amram region: 1) emplacement of hypabyssal alkali granites; 2) rhyolitic volcanism; 3) intrusion of sub-volcanic monzonite; 4) intrusion of sub-volcanic quartz-monzonite. All these rocks are intruded by mafic and felsic dikes. These magmatic rocks belong to the final stage in the evolution of the Arabian Nubian Shield. Interpretation of available gravity and magnetic data from the Har Amram region indicates the presence of a shallow basic magmatic body (maybe of Early Cretaceous age) below the Northern part of the Amram region and slightly dense and non-magnetic bodies near and below Amudei Amram. It is possible that a shallow Early Cretaceous magmatism (such as at Timna) cause hydrothermal activity which remobilized some of the suggested primary volcanogenic copper that later accumulated within the Amir and Avrona formations.

Geochemistry of Cambrian carbonates in southern Israel and southwestern Jordan

Segev A. [1], Sass E. [2], Yoffe O. [1], Halicz L. [1], Starinsky A. [2]

1. Geological Survey of Israel, 30 Malkhe Israel St., Jerusalem 95501
2. The Institute of Earth Sciences, The Hebrew University, Jerusalem 91904

The Cambrian limestones and dolomites in southern Israel and southWestern Jordan contain a wide range of siliciclastic constituents. The geochemical analyses of such rocks commonly display various degrees of contamination, and consequently provide limited insight into their origin. In the present study we developed a special digestion method, which minimizes the analytical artifacts, and provides significant and reliable results for most of the limestones, and for some of the dolomites as well. The analytical data (elemental – Ca, Mg, Mn, Sr, Na, K, and isotopic – $\delta^{18}O$, $\delta^{13}C$, $^{87}Sr/^{86}Sr$) provide indications to the composition of the Cambrian seawater, and to the role of early diagenetic pore water modifications. The evidence for anaerobic conditions during early diagenesis is of particular interest, since it accounts for the accumulation of Mn and Cu in the carbonate muds and rocks, which were later modified, mobilized and enriched.

Limestones - The geochemical data point to the presence of a primary manganese oxide (kryptomelane) as a minor constituent, and to the incorporation of Mn in the calcite lattice in some of the limestones. These occurrences formed in response to reducing microenvironments, which affected also other ionic ratios (Sr/Ca, Mg/Ca, Na/Ca) and $\delta^{13}C$. This interpretation allows us to recognize a range of modified porewater, which lies between an open system and a (partly) closed one. The open system end member represents closely the Cambrian seawater.

Dolomites - Most of the dolomites are rich in siliciclastic constituents, and the chemical analyses of some of them are masked in part by analytical artifacts. The dolomite samples that demonstrate low contamination have a significant content (up to 10 mol %) of incorporated Mn in their lattice, and display clear trends between $^{87}Sr/^{86}Sr$, $\delta^{18}O$ and $\delta^{13}C$. These trends seem to reflect varying degrees of a closed system, which were controlled by fluctuations in salinity and temperature.

Following the analysis of the limestones and dolomites data, it is suggested that the early Middle Cambrian seawater was characterized by $^{87}Sr/^{86}Sr$ of 0.7089, $\delta^{18}O$ of ~ -6.5‰ PDB, and $\delta^{13}C$ of ~ +1‰ PDB. Interestingly, some of the $^{87}Sr/^{86}Sr$ readings in both limestones and dolomites are lower than the aforementioned estimate of the Cambrian seawater, contrary to the findings in other studies. This observation seems to reflect the effect of pore water modification by siliciclastic grains, whose igneous source rocks were still young during the Cambrian, and therefore having low (unevolved) $^{87}Sr/^{86}Sr$ ratio. This conclusion is consistent with the view that the carbonate rocks largely retain their primary composition, and were not altered despite their long age and prolonged contact with circulating water, some of them of thermal origin.

Deformation and seismicity associated with Cenozoic rifts crossing the Levant continental margin. I. Geologic setting

Segev A., Schattner U., Weinberger R., Lyakhovsky V.

Geological Survey of Israel, 30 Malkhe Israel St., Jerusalem 95501

The mechanics of faulting associated with major Cenozoic rifting was studied respecting two rifts: the Azraq-Sirhan rift and its continuation in Israel, and the Suez rift in Egypt are two major NW-trending fault systems activated during the Tertiary, most likely before the initiation of the Dead Sea Transform. The former rift system propagated from the Arabian continental part, with Moho depth exceeding 35 km, toward the southEastern Mediterranean Sea, with Moho depth less than 25 km. The rift reached the Levant continental margin, where its propagation was terminated. The Carmel-Gilboa fault in Israel is the major bounding fault of the Azraq-Sirhan rift system in Jordan. Several options of its seaward extension were suggested over the years. To perform mathematical modeling of a propagating rift system we prepared a 3-D lithosphere structure for a study area that includes central Israel, central Lebanon, NW Jordan, SW Syria and the Levant marine basin. The lithosphere examined consists of the continental crust (Arabian plate), continental margin and oceanic? crust of the southEastern Mediterranean basin (Sinai plate). The 3-D structure was established using four interfaces: the elevation; the top of the crystalline basement; the depth of the Moho; and the lithosphere-asthenosphere boundary. According to the above geological scenario we constructed the 3-D lithosphere structure to the end of the Eocene times, and restored the ~100 km sinistral motion along the Dead Sea Transform. The relative motion between the Arabian plate and the African (Sinai) plate during the opening of the rift systems is based on the inferred Early Miocene Euler pole. This plate kinematics is consistent with the intraplate stress field inferred from jointing of Eocene rocks in central Israel.

Submarine groundwater discharge in Dor bay, Carmel coast, as determined by time series of ^{222}Rn and by seepage meters

Shalem Y. [1], Weinstein Y. [1], Yechieli Y. [2], Swarzenski P. [3], Burnett W.C. [4], Herut B. [5]

1. Bar-Ilan University, Ramat-Gan 52900, Israel
2. Geological Survey of Israel, 30 Malkhei Israel St., Jerusalem 95501, Israel
3. U.S. Geological Survey, St. Petersburg, FL 33701 USA
4. Department of Oceanography, Florida State University, Tallahassee, FL 32306 USA
5. Israel Oceanographic and Limnological Research, P.O. Box 8030, Haifa, 31080, Israel

Due to its interdisciplinary nature and to technical problems, assessment of Submarine Groundwater Discharge (SGD) was usually restricted to water balance calculations and to hydrological modeling. Field measurements were hardly done before the mid 90's. In the last few years, radon monitoring has become a major tool in SGD measurements. This is because radon is highly enriched in groundwater compared with seawater. We present here the results of three campaigns of continuous radon measurements that were conducted in Dor Bay, southern Carmel coast, during 2006 (March, May and July). The water in the bay was usually somewhat less saline than the open sea (by up to 1 ppt), and accordingly it showed high and very variable radon activities (1-13 dpm/l, compared with 0.5 in seawater). The radon varies with a tidal pattern, showing negative correlation with bay water level.

The changes in radon inventory in the bay were converted to radon fluxes after making allowance for tidal influx and outflux, losses of radon to the atmosphere, and mixing with offshore water. SGD advection rates were derived from the radon fluxes, using a weighted average activity of 235 dpm/l for the groundwater end-member. This value includes a fresh water component with 370 dpm/l and a radon-poor recycled seawater. Average advection rates in all three campaigns were 8.3 cm/d, of which 5.4 cm/d was of the fresh water component. Considering the 100 m width of the bay, the flux of fresh water to the sea is estimated by 5.4 m^3/d (or 1970 m^3/yr) per one meter of shoreline. A similar value (7 m^3/d) was derived from the differences between low and high tide resistivity profiles in the bay sediments.

Direct discharge measurements by four seepage meters, showed similar advection rates in May (mean values of 7-13 cm/day). However, there is no correlation between rates and bay water level. In March, rates (measured by two meters) were much higher (mean values of 20 and 50 cm/day), probably due to prior rain events, while in July rates were significantly lower (2.1-6.8 cm/d) than the Rn-calculated values. Both the high and the low values suggest that discharge is not uniform in the bay, and specifically that discharge in sand-covered areas of the bay is different than where Kurkar is exposed.

Geodynamic signals in confined aquifers along the Dead Sea

Shalev E. [1], Steinitz G. [1], Malik U. [1], Piatibratov O. [1], Woith O. [2]

1. Geological Survey of Israel, 30 Malkhe Israel, Jerusalem, 95501, Israel
2. GeoForschungsZentrum, Potsdam, Germany

High sensitivity water pressure sensors were installed at the wellhead of two artesian wells in the Dead Region: a) Borehole T-30 located in Nahal Hemar, in the western border fault zone of the Dead Sea rift, fed from the Hevyon Fm. (Cenomanian) at a depth of 200-300 meter; and b) Borehole EZ-10 located in the Enot Zuqim nature reserve, fed from a local aquifer in the unconsolidated fill, at a depth of 30-34 meters. Sampling rates are 1-minute at T-30 and 10 seconds at EZ-10. Several features indicate that non-hydrologic processes are also influencing the temporal variation of the water pressure: a) Solid earth tide periodic constituents are observed; b) a rise in the water pressure at EZ-10 is observed in August-September 2006, which is incompatible with the dry season and the regional recession of the Dead Sea and groundwater levels, and c) abrupt changes in water pressure at EZ-10 which coincide with 3 earthquakes (ML = 3, 4.4, 4) that occurred at this time interval, some 30 km to the north.

These non-hydrologic responses are considered as preliminary indications for response to geodynamic processes in these systems. These observations, especially in the shallow unconsolidated rift fill aquifer open a new potential for monitoring of active geodynamics of the DSR system.

Furthermore, the data allow calculation of aquifer hydrological and elastic properties from the response of the groundwater level to tidal and barometric forcing.

Detection of Submarine Groundwater Discharge (SGD) in the northern inner shelf of Israel and an assessment of the capability of remote sensing and shallow geophysical methods combination to locate the springs

Shapira S. [1], Tibor G. [2], Ben-Avraham Z. [1]

1. Department of Geophysics and Planetary Sciences, Tel Aviv University
2. Israel Oceanographic and Limnological Research

In the current research, an effort was made to locate Submarine Groundwater Discharge (SGD) in the Northern continental shelf of Israel utilizing a combination of remote sensing geophysics methods and geochemical samples of the water. During the survey, images from the thermal band of Landsat ETM7 satellite (bands 6a, 6b) were processed and analyzed, producing maps describing the Sea Surface Temperature (SST). The maps were integrated with the Geographic Information System (GIS), which included layers of relevant data for locating springs, such as faults, geology and geomorphology. In some areas along the shelf local anomalies in the water temperature were identified, which may be a result of fresh water springs. From these areas, three sites were chosen: a crater in the sea bottom near Bustan Hagalil, another crater near Shiqmona adjacent to the Carmel Fault and a cluster of craters near the Carmel Fault's continuance to the sea. In these three sites, there is high reasonability of existence of fresh water springs because all had previously identified thermal anomalies, all were located adjacent to faults, all contained craters (which may have been created by water or gas flow), and in all of them a decrease in electrical conductivity was measured.

In the chosen sites, a shallow geophysical survey was conducted, which included a seismic survey with a shallow seismic system of chirp type and a morphological mapping with side scan sonar. The aim of this survey was to identify underground structures, such as faults, fractures or layers that enable the flow of groundwater from the aquifer to the sea. The survey's results did not provide a clear view of the underground, because the seismic system did not penetrate the hard kurkar layer. The water column and the sediments in the craters were sampled and chemical measurements were conducted which indicated that the waters in the craters are normal sea water and do not contain fresh water.

Despite the results of the current research, the possibility of the existence of fresh water submarine springs in the research area can not be rejected, since it is possible that these springs are not stable, but exist for short periods after the increase of groundwater levels. Alternatively, they may exist durably, but their flow is relatively weak. In addition, it seems that the water flows through wide seepage area and not through specific springs.

It is possible that using remote airborne sensing, which permit better spatial resolution and better identification of small temperature changes, will permit identification of weak or seasonal springs. In addition, using a high penetration geophysics survey (such Sparker) will allow the possibility to estimate the flow paths of the groundwater from the aquifer to the sea.

Using FT-IR spectroscopy for identification of the thermal phases in calcinied calcareous oil shales

Shoval S. [1], Harari D. [1], Yofe O. [2], Nathan Y. [2]

1. Geology Group, Department of Natural Sciences, The Open University of Israel, The Dorothy de Rothschild Campus, 108 Ravutski Street, Raanana, Israel.
2. The Geological Survey of Israel, 30, Malkhei Israel St., 95501 Jerusalem, Israel

FT-IR spectroscopy was used for identification of the thermal phases in calcinied calcareous oil shales. Vibrational spectroscopy enables identification of changes in the amorphous and crystalline material, whereas X-ray diffraction is limited to examination of crystallized materials. However, the former method has received less attention in oil shale combustion. The different thermal phases were identified according to their indicative bands in the infrared spectra and by applying curve-fitting technique. Spectra of minerals typical for such calcination were served as standards for the identification. The results were correlated with those observed by XRD.

The calcinied samples include organic-rich calcareous oil shales collected from the Maastrichtian Ghareb Formation of the Ein-Bokek section. For comparison, calcinied samples of organic-free marls collected from the Ghareb Formation of the Arad Section were examined. The samples were heated in an electric kiln to temperatures between 400-1000°C for 6 hours. This heating time is reasonable for completion of the indicative thermal reactions at each temperature.

The thermal products of the organic-rich calcareous oil shales differ significantly from these observed in the organic-free marls. In oil shales rich in sulfur the main thermal products are free lime (CaO), anhydrite ($CaSO_4$), hydroxylellestadite [$Ca_{10}(SO_4,SiO_4)_6(OH)_2$] and gehlenite ($Ca_2Al_2SiO_7$). The decomposition of the organic material and the dehydroxylation of the clay simulate early decarbonation of the microcrystalline calcite and at about 600°C free lime is formed. The sulfur releases from the organic material brings to thermal sulphatization and the formation of anhydrite. At higher temperature, with the presence of apatite, hydroxylellestadite is crystallized. An early formation of gehlenite is observed at 700°C due to the reaction of the free lime with the decomposition products of the clay. The excess of the decarbonated calcite appear as free lime and portlandite. On the other hand, the main thermal phases of the organic-free marls are meta-clay and amorphous phases of Ca-silicates and Ca-Al-silicates. Formation of gehlenite and bredigite (Ca_2SiO_4) is observed at about 800°C.

FT-IR spectroscopy technique seems to be a useful method for the materials analysis in the oil shales combustion industry. XRD is not sensitive to the meta-clay and the amorphous phases of the Ca-silicates and Ca-Al-silicates observed by the FT-IR spectroscopy technique.

Morphometric and geomorphic approaches for assessment of tectonic activity, Northern Dead Sea Rift (Israel)

Shtober Zisu N. [1], Greenbaum N. [2], Porat N. [3], Inbar M. [2], Flexer A. [4]

1. Department of Israel Studies, University of Haifa, Haifa, 31905, Israel
2. Department of Geography and Environmental Studies, University of Haifa, Haifa, 31905, Israel
3. The Geological Survey of Israel, Malkhei Israel 30, Jerusalem, Israel
4. Department of Geophysics and Planetary Sciences, Tel Aviv University, Israel

A series of 31 short, parallel, steep channels, mostly of first or second order, are developed at distances of 300-500 m, along 16 km of the western margin of the Northern Dead Sea rift. The analysis of the tectonic and geometric activity along the marginal faults between the various segments is based on various morphometric parameters, such as sinuosity of the mountain front, channel gradients, drainage basin elongation ratio, planimetric ratio, facet area, hypsometric curves, and integrals. Longitudinal profiles of the channels were studied in relation to the underlying lithology and the presence of marginal faults. Despite the large differences in climatic and geomorphologic settings, comparison with other studies worldwide showed morphometric values similar to other tectonically active regions.

Southward of the Qiryat Shemona area, the escarpment faces the deep Hula depression, indicating enhanced geomorphic and tectonic activity. The Kefar Giladi area proved dissimilar to the others and is explained by its different tectonic setting.

To calibrate rates of tectonic activity, six sedimentary units were dated. The fans are composed of polymictic conglomerates and were deposited along the mountain piedmont at the channel mouths. The units were dated by OSL, K-Ar, and archaeology to <1.1 Ma (Q_1 and Q_{1-1}), < 0.56 Ma (unit Q_2), ~ 120 ka (unit Q_3), and <10 ka (units Q_4 and Q_5). The morphology and structure of the sedimentary units indicate pulses of depositional activity followed by periods of quiescence and calcic-soil development. No major faulting occurred along the Naftali escarpment during the late Pleistocene, despite the high tectonic morphometric values obtained for the study area. The marginal faults displaced unit Q_2 during the Mid-Pleistocene, and since then the tectonic activity has migrated from the western marginal faults eastward to younger faults deeply buried in the center of the Hula graben. The field data calibrate the morphometric analysis: carbonate (limestone and dolomite) hillslopes developed under the Mediterranean climate have maintained "active class" morphology since the last major faulting events during the Mid–Pleistocene.

The age of the ancient, tectonically stable Paran Plains, southern Negev, and its sedimentological and pedological characteristics

Simhai O. [1,2], Matmon A. [1], Amit R. [2], Enzel Y. [1], McDonald E. [3], Porat N. [2], Finkel R. C. [4]

1. Institute of Earth Sciences, Hebrew University, Jerusalem 91904
2. Geological Survey of Israel, 30 Malkhe Israel St., Jerusalem 95501
3. Desert Research Institute, 2215 Raggio Parkway, Reno, NV 89512
4. Lawrence Livermore National Laboratory, 7000 East Avenue, Livermore, CA 94550

The alluvial surfaces that comprise the Paran Plains in the southern Negev, ~35 km west of the Dead Sea Transform, are tectonically stable but were subjected to minimal long-wavelength folding during the early Pleistocene. The current hyperaridity of the area (<50 mm/yr) adds to the preservation of these surfaces. These conditions allowed the continuous development of cumulative-welded soils that preserve pedogenic features since the abandonment of the surfaces. These features can be used as indicators for paleoclimate. We reconstruct several stages in the development of the Paran Plains since the Pliocene by investigating morphological, pedological, geochronological and climatological aspects. Ages are based on a high-resolution sampling for optically-stimulated luminescence and ^{10}Be concentration.

The current flat Paran Plains are covered by desert pavement and patches of shallow dry playas are distributed over these plains. The studied profiles revealed calcic soils at ~ 1 m depth developed within alluvial or colluvial sediments overlain by a less gravelly gypsic-salic soil with a thick Av horizon and a well-developed desert pavement at the top. Most of the soil profiles in the playas developed in fine grain sediments, do not contain gravel above the calcic horizons and are not covered by a desert pavement.

The ^{10}Be concentrations indicate that the alluvium at ~2 m below the surface was deposited at ~3.2 Ma and the surfaces were apparently abandoned at ~1.8 Ma. The complex soil profile started to develop sometime after 3.2 Ma with a calcic soil developing during the early stages, probably during the late Pliocene and earliest Pleistocene. The calcic horizons developed under climatic conditions wetter than those of the rest of the Pleistocene and/or the Holocene that produced salic-gypsic soil horizons; this transition in soil properties indicates increasingly arid conditions in the region with extremely arid conditions prevailing since at least the middle Pleistocene. The OSL ages indicate that most of the eolian input to the top soil horizons occurred during the past 300ky.

Oxygen isotopes in pore fluid sulfate

Sivan O. [1], Turchyn A. V. [2], Schrag D. P. [3]

1. Ben Gurion University, Dept. of Geological and Environmental Sciences, Beer Sheva, 84105, Israel
2. U.C. Berkeley, Dept. of Earth and Planetary Sciences, McCone Hall, Berkeley CA 94720
3. Harvard University, Dept. of Earth and Planetary Science, 20 Oxford St Cambridge, MA 02138

We present new data of oxygen isotopes in marine sulfate ($\delta^{18}O_{SO4}$) in pore fluid profiles through organic-rich deep-sea sediments from eleven ODP sites around the world. In almost all sites studied sulfate is depleted with depth, through both organic matter oxidation (OMO) and anaerobic methane oxidation (AMO). The $\delta^{18}O_{SO4}$ increases rapidly near the top of the sediments, from seawater values of 9‰ to maxima between 22 and 25‰, and remains isotopically heavy and constant at these values with depth. The $\delta^{18}O_{SO4}$ in these pore fluid profiles is decoupled from variations in sulfur isotopes measured on the same sulfate samples ($\delta^{34}S_{SO4}$); the $\delta^{34}S_{SO4}$ increases monotonically with depth and exhibits a shallower isotopic increase. This isotopic decoupling between the $\delta^{34}S_{SO4}$ and the $\delta^{18}O_{SO4}$ is hard to reconcile with the traditional understanding of bacterial sulfate reduction in sediments. Our data support the idea that some sulfur intermediate and water isotopically exchange during sulfate reduction and that some of the isotopically altered sulfur pool returns to the environment. We calculate that the rapid increase in the $\delta^{18}O_{SO4}$ in the upper part of these sediments requires rates of this oxygen isotope exchange that are several orders of magnitude higher than the rates of net sulfate reduction calculated from the sulfate concentration profiles and the $\delta^{34}S_{SO4}$. We suggest several mechanisms by which this may occur, including "net-zero" sulfur cycling, as well as further experiments through which we can test and resolve these processes.

The continual radon monitoring at soil and rock environment in Slovakia

Smetanová I. [1], Holý K. [2], Müllerová M. [2], Polášková A. [2], Túnyi I. [1]

1. Geophysical Institute, Slovak Academy of Sciences, Dubravska cesta 9, 845 28 Bratislava, Slovakia
2. Department of Nuclear Physics and Biophysics, Faculty of Mathematics, Physics and Informatics, Comenius University, Mlynska dolina, 842 48 Bratislava, Slovakia

The continual monitoring of ^{222}Rn activity concentration in soil and rock environment has been performed at the three different stations in Slovakia: Bratislava, Modra and Vyhne.

The ^{222}Rn activity concentration in soil air has been continuously monitored at Bratislava since 1994. The measurements have been performed by scintillation cell of Lucas type, the soil air has been sucked from the depth of 0.8m. The soil type at measuring site is middle gas permeable. The measurements of the ^{222}Rn concentrations do not show the distinct changes during the day. The amplitude of the average daily courses varies for different months from 1 to 5%. The seasonal variations are observable with the minimum during the summer months. The dependence of the ^{222}Rn activity concentration on the precipitation was observed.

Radon monitoring at Astronomical and Geophysical observatory of Comenius University at Modra (Little Carpathians, 30km NE Bratislava) have been performed since August 2003. Alpha detectors are placed in boreholes V-3 (10m), V-2 (40m) in the Lower Triassic quartzite folded in the Modra granodiorite massif. Meteorological parameters (atmospheric temperature and pressure, rainfall, snowfall) were obtained locally and the variations of radon activities in the boreholes have been correlated with them. The hourly and daily mean values of ^{222}Rn activity concentration were calculated. The daily, short term and seasonal variations of ^{222}Rn activity concentration were observed. The daily variations were caused by changes of atmospheric temperature during the day. Short term (2-5 days) variations were mainly influenced by the difference between external atmospheric temperature and temperature inside the borehole. The changes of temperature during the year also gave rise to seasonal variations of ^{222}Rn activity concentration with minimum at spring and summer months. Water samples from boreholes (including V-1; 10 m) were analyzed for ^{222}Rn activity and the water level was measured. The water level and the radon concentration were strongly affected by rainfall and melting of snow. Usually since the end of summer until the winter there is no water in V-1 and V-3 borehole.

Radon monitoring at the gallery of St. Anthony of Padua near Vyhne (Central Slovakia) commenced in October 2005. This gallery, located in Variscian age granites, is used as the tidal station of the Geophysical Institute of Slovak Academy of Sciences. In the gallery the daily and seasonal variation of ^{222}Rn concentration was observed, their amplitudes were significantly lower like in boreholes at Modra station.

The geological map of Israel 1:50,000 sheet 2-IV: Rosh Pinna

Sneh A., Weinberger R.

Geological Survey of Israel, 30 Malkhe Israel St., Jerusalem

A new geological map of the Rosh Pinna quadrangle was completed as part of the 1:50,000 map series of the Geological Survey of Israel. The major sources are Glikson (1966) who mapped the southern part of the Naftali Mountains and Mor (1987) who mapped the volcanic fields of the Golan Heights. During the course of the present mapping, the Judea, Mount Scopus and the Avedat groups were divided into their individual formations.

Further geochronological studies were carried out in the volcanic units. In addition to sites previously examined by Mor (1987), Heimann (1990) and Weinstein (1998), some twenty additional selected locations were examined in cooperation with Y. Harlavan. Based on these results an enhanced subdivision of the basaltic rocks was achieved. The course of the Dead Sea Fault in this region was delineated along the Jordan gorge and at the base of Plio-Pleistocene flexures observed in the Yarda/Ruman Basalt and the Gadot Chalk. Vertical displacement of the volcanic units on both sides of the fault has not been proven.

So, what is the age of the Sedom lagoon?

Stein M. [1], Agnon A. [2]

1. Geological Survey of Israel, Jerusalem, Israel
2. Institute of Earth Sciences, The Hebrew University, Jerusalem, Israel

A long standing question in the geological history of Israel concerns the timing of the Mediterranean seawater invasion into the Dead Sea rift valley that led to the formation of the Sedom lagoon and the deposition of the thick sequence of evaporites comprising the Sedom Formation. Several years ago we tried to address this question by analyzing $^{87}Sr/^{86}Sr$ isotope ratios in Sedom Fm. salts and dolomites. The idea was to compare the $^{87}Sr/^{86}Sr$ ratios in the Sedom salts with the seawater $^{87}Sr/^{86}Sr$ curve, which is used as a global chronometer for marine primary deposits. Yet, it was found that the $^{87}Sr/^{86}Sr$ in the salts and thus in the lagoon were modified by interaction of the marine water with the Cretaceous limestone during dolomitization of the carbonates. This interaction caused the production of Ca-Chloride brine that returned to the lagoon and modified its primary chemical composition and $^{87}Sr/^{86}Sr$ ratio (Stein et al., 2000).

Here, we used Pb isotope data obtained on epigenetic dolomites and their surrounding "host" Cretaceous limestone (the Nezer Fm.) to provide new constraints on the age of the Sedom lagoon. It turned out that the dolomitization process was accompanied by extensive fractionation of the trace elements and production of large range in the $m=^{238}U/^{204}Pb$ ratios (up to 11,000!). The epigenetic dolomites as well as the Cretaceous limestones lie on linear trends in the U-Pb isochron diagram yielding ages of 3.2 Ma and ~ 90 Ma, respectively. Thus, we conclude that the invasion of the Sedom lagoon occurred in the upper Pliocene ca. 3 Ma ago. Based on geological and geochemical considerations Zak (1967) suggested that the lagoon could exist for ~1Ma. This suggestion will be examined by analyses of other epidolomite bodies located in various stratigraphic horizons in the Judea Mt. Cretaceous sedimentary section.

Statistical characteristics of Radon time series in Israel

Steinitz G. [1], Piatibratov O. [1], Barbosa S. [2], Woith H. [3]

1. Geological Survey of Israel, Jerusalem, Israel
2. Dept. of Applied Mathematics, Porto University, Porto, Portugal
3. GeoForschungsZentrum, Potsdam, Germany

High time resolution radon time series in geogas display different components of variation in the Measured Signal (MS) – primarily periodic Daily Radon (DR), non-periodic Multi Day (MD) and periodic Seasonal Radon (SR) signals. Signals of such types are directly observable in the radon time series recorded in geogas from Elat, the Bloch Geophysical Observatory (BGO) at Har Amram, and at monitoring sites at Enot Zuqim (EZ) along the NW Dead Sea. DR and MD signals are also observed in radon time series from the hot spring of Hamei-Tveria (HT; Tiberias). The time series were investigated in the time domain applying Cross-Correlation (CC) of the signal and difference time series among adjacent sites and in the frequency domain (FFT).

Time offsets occur among time series of the MS in the Elat Granite and were investigated also for the MD and DR components, using consecutive 20-day intervals spanning +900 days. The resulting time series show that systematic time offsets occur, whereby the radon signal always occurs first at the easternmost site. The MD shows a gradually varying lag of 0-12 hours, and the DR a stable 1-3 hour lag.

Spectral analysis shows that diurnal (24-hour) and semidiurnal (12-hour) periodic constituents characterize the DR at Elat, BGO, EZ and HT. The amplitudes of these constituents exhibit regular temporal variation having a seasonal pattern. The ratios of co-occurring amplitudes of these constituents define a linear pattern indicating a fundamental statistical property in the frequency domain of the radon time series. Periodic constituents typical for tidal effects in the diurnal band (mainly M2) are absent from the spectra. Predominance of the 24-hour and 12-hour periodic constituents suggests a relation with the rotation of the earth.

These statistical characteristics are distinctive for the radon time series and as far as known are do not occur in other geophysical time series – e.g. in atmospheric and tidal parameters. The results indicate that unrecognized dynamic processes are driving the radon signal in the subsurface regime, presenting new prospects for radon phenomena in the frame of interacting geodynamic (tectonic?) and earth-sun system related geophysical processes.

The radon flux at IUI, Elat, Israel - geophysical implications

Steinitz G., Zafrir H., Malik U., Piatibratov O.

Geological Survey of Israel, Jerusalem, Israel

Radon is monitored at a 15-minute resolution at four locations in the Inter University Institute (IUI) in Elat, using gamma detectors: a) at depths of around 1 and 2 meters below seawater in a hole dug in the shore gravel, about 15 meters from the shoreline; b) 3 meters under sea level at the far end of the pier; c) Beyond the pier at a water depth of 30 meters; d) in the air at the end of the pier some 4 meters above seawater and 70 meters from the shore.

Very high levels and large temporal variations of radon are encountered in the shore gravel. The Measured Signal (MS) is composed of very strong periodic Daily Radon (DR), non-periodic Multi Day (MD) and periodic Seasonal Radon (SR) signals. Small variations reflecting MD and DR signals occur in the seawater about 1 meter above sea bottom, at a depth of 3 meters at the pier and at a depth of 30 meters. Similar MD and DR signals are recorded above sea, in the atmosphere around IUI. Collimation tests using Pb shielding indicate that the signal originates to a large extent from the shore sector.

Spectral analysis (FFT) of the MS from all locations shows that the diurnal band is dominated diurnal constituents indicative of tidal influence. The primary indicator is the M2 constituent around 1.93 cycles/day. At his stage it is not known whether the diurnal tidal signature observed in the radon is due to the effect of sea tide or local solid earth tide. A tidal signature cannot be generated in radon in the air. Therefore its occurrence in the air around IUI indicates that a large flux of radon is flowing out from the ground into the atmosphere.

These observations are the first of radon signals in the marine environment. The implications of the occurrence at IUI are: a) A large radon flux probably exists along further sectors of the major western active boundary fault of the Elat deep; b) Defining the DR signal as reflecting solid earth tide will imply that the radon flux along the fault might also be sensitive to geodynamic transients (MD signals); c) It is suggest to test and try to develop this radon system as a new and sensitive proxy and monitoring parameter relevant to the seismic risk of Elat, located on the fault several km to the north and for the southern Arava.

Evolution of iron mineralization and dolomitization along the Paran fault in the Haspas-Beroka area

Stern D.[1], Erel Y.[1], Matthews A.[1], Avni Y.[2]

1. Institute of Earth Sciences, Hebrew University of Jerusalem, Givat Ram, Jerusalem, 91904
2. Geological Survey of Israel, 30 Malkhe Israel St., Jerusalem, 95501

The fluid sources for iron mineralization and dolomitization in Cretaceous sedimentary rocks of the Negev shear zone have been studied since the 1950's. Three major fluid sources have been suggested: hydrothermal fluids associated with Tertiary volcanism in the Negev and Sinai (1); fossil formation water driven up the faults as the result of the 'piston effect' of Pleistocene recharge in Sinai (2); mixing between topographically-driven groundwater that leached subsurface igneous rocks and clastic sediments and Mg-rich Dead Sea Rift-type brines. These conclusions were largely based on studies of the Menuha Ridge area of the Paran Fault. The present study focuses on the isotope geochemistry of mineralization in the western part of the Paran fault, in the structural half domes of the Haspas – Beruqa ridge, located 80 km from the Dead Sea Rift and close to Sinai.

High $^{87}Sr/^{86}Sr$ values (0.7085-0.7116) are found in the iron-oxide (goethite) lenses. Such high values were not found along the Menuha Ridge and suggest a metallic component derived from the leaching of Precambrian basement rocks or their detrital fragments. Sr-isotope values in the epigenetic dolomites near the fault (0.70813-0.70822) are significantly higher than those expected for Upper Cretaceous limestones (~0.7075) and point to Mg-rich dolomitization fluids containing a high $^{87}Sr/^{86}Sr$ component. This could be the igneous basement component suggested by the iron oxides and/or a brine/subsurface evaporite source similar to the Rift-brine source suggested for Menuha Ridge.

$^{207}Pb/^{204}Pb$ vs. $^{206}Pb/^{204}Pb$ ratios of Fe-oxides, dolomites and host-rock limestones plot along a straight line relationship. Tamar Formation limestones are the most radiogenic, whereas the Ora-Shales rocks plot close to the non-radiogenic end of the line and Grofit Formation limestones are in the middle. An age of 80±20 Ma calculated from the $^{238}U/^{204}Pb$ – $^{206}Pb/^{204}Pb$ ratios of the limestones is consistent with their Upper Cretaceous formation. Most epigenetic dolomites and all the Fe-oxides are enriched in lead, but $^{207}Pb/^{204}Pb$ and $^{206}Pb/^{204}Pb$ ratios of dolomites are lower (i.e. contain a greater non-radiogenic Pb-isotope component) than the limestone of the same formation. This suggests that the Pb-isotope variations can be interpreted in terms of two end-members: the limestone host rock and a metalliferous fluid derived from the leaching of basement igneous rocks and clastic Nubian sediments.

Field relations between the mineralization and the structures in the fault zone along the Haspas – Beruqa ridge suggest that the iron mineralization and dolomitization commenced prior to the tectonic activity that formed the half domes in the Oligocene, but was complete before the Late Miocene-Early Pliocene arching of the Negev.

References:

(1) Shraga, M., *Isr. J. Earth Sci.* 20, 51-88 (1971). (2) Ilani, S., Ph.D. thesis, University of Tel Aviv (1989).

Geochemical, hydrological and paleo-hydrological characteristics of En-Qedem springs

Stern O. [1,2], Yechieli Y. [1], Stein M. [1], Gavrieli I. [1], Lazar B. [2]

1. Geological Survey of Israel, 30 Malkhe Israel St., Jerusalem, 95501
2. Institute of Earth Sciences, Hebrew University of Jerusalem, Givat Ram, Jerusalem, 91904

The rapid retreat (currently ~1m·y^{-1}) of the Dead Sea during the past decades exposes the Holocene sedimentary sections (e.g. Ze'elim gullies) and is accompanied by seaward migration of the springs system at En Qedem shore. The Qedem springs are saline thermal springs (42-45°C) that discharge along the western shores of the Dead Sea, between En-Gedi in the south and Mineral Beach in the north, mainly to the south of Wadi Qedem. The total discharge of the springs is 13x10^{6}m^{3}·y^{-1} (measured by the Hydrological Service), showing a diversity in time of ±20%. Most of the springs are located very close to the shoreline and follow the decline in the Dead Sea level. The springs and the Dead Sea share a unique Ca-chloride composition. However, the salinity of the springs is about half that of the Dead Sea (190g·L^{-1}) while their sulfate concentration is significantly higher. Most of the springs have a "Qedem" composition (125gCl·L^{-1}, Na/Cl=0.34) but some, mostly the southern springs, are less saline, indicating mixtures with fresher water probably discharging from the En Gedi system. Along the shore there are also some springs with higher salinities, representing a mixture with the Dead Sea brine.

The late Holocene sedimentary section at the En Qedem area contains sequences of thick gypsum layers and abundant aragonite crusts that interfinger to the north and south with the typical sediments of the Holocene Dead Sea (laminated aragonite, gypsum and detritus that comprise the Ze'elim Fm). Their deposition age is older than 2000 years BP (radiocarbon date of a Roman anchor discovered in a layer above the gypsum). The unique appearance of the gypsum sequences and their proximity to the modern En-Qedem springs may indicate a genetic connection between them. Yet, currently only native sulfur is being deposited in the vicinity of the springs, most likely through sulfide oxidation by chemo-autotrophic organisms.

The late Holocene En Qedem gypsum appears as massive layers containing large and sharp crystals all pointing upward (a typical precipitate of shallow evaporate ponds) or as laminated thin layers. Both the massive and the laminated gypsum have a mean $\delta^{34}S_{SO4}$ value of 16.4‰±0.1, slightly heavier than the mean Holocene $\delta^{34}S_{SO4}$ value of 15‰±0.7 (gypsum laminae recovered from the En-Gedi core, A. Torfstein p. comm.). The heavier values of the gypsum exposed at the Qedem shore may represent a mixture between the Holocene Dead Sea brine with En-Qedem brines having a heavier $\delta^{34}S_{SO4}$ values of 22.5‰.

Geochemical, chronological and hydrological characterization of the Qedem springs and sediments, could shed light on the past spring activity and the sedimentological- limnological conditions at the Qedem shore during the Holocene.

Dynamics of floodwater infiltration and groundwater recharge underneath ephemeral channels in arid regions

Tatarsky B. [1], Dahan O. [1], Enzel Y. [2]

1. Zuckerberg Institute for Water Research, Ben-Gurion University of the Negev
2. Institute of Earth Sciences, Hebrew University of Jerusalem

Shallow alluvial aquifers underneath ephemeral streams are often the only reliable source of water that can sustain human habitation in arid environments (e.g. Arava Valley, Israel; Rio Andarax, Spain; Kuiseb River, Namibia). The main source of replenishment of these alluvial aquifers is by recharge from floodwater infiltration. Accordingly, effective management of surface water and groundwater in arid regions requires improved understanding of the processes controlling floodwater infiltration and recharge of alluvial aquifers. This study focuses on understanding the dynamic process of floodwater infiltration from ephemeral channels while implementing innovative methods specifically designed to quantify the recharge fluxes.

The monitoring system provides real time continuous measurements of the hydraulic conditions in all three domains involved in the recharge process: (a) the flood (b) water content variations along the unsaturated profile (c) the groundwater response to the recharge event. Water content variations along the unsaturated profile were monitored using Flexible TDR (FTDR) probes installed in slanted boreholes underneath the stream channel. Water levels and salinity of both the flood and the groundwater were measured simultaneously.

Two study sites were selected for this work: the Buffels River, South Africa and the Kuiseb River, Namibia. The monitoring stations installed at those sites recorded several flood events during 2005/2006. Data collected during this period revealed the dynamic process in which floodwater percolates through the vadose zone and recharges the groundwater.

Each flood initiated an infiltration event expressed by a wetting process of the vadose zone and a water table rise. The sequential wetting of the vadose zone allowed direct calculations of the wetting front propagation velocities and percolation fluxes from land surface down to groundwater. With the arrival of the wetting front to the water table, groundwater started to rise indicating an increase in ground water storage in response to the recharge event.

Water fluxes were calculated using several independent methods: (a) Combining the calculated wetting front propagation velocity with the change in moisture profile, (b) the rate at which the water table rises as an indication to the percolation rate and (c) the final increase in groundwater storage through the measured change in groundwater levels. Interestingly the calculation made for all floods yield corresponding flux values of approximately 1 cm/h. Aquifer dimensions as well as total recharge estimations were also derived from the data. Salt transport dynamics at each site and the influence of the flood events on groundwater quality were revealed from the EC measurements.

Brine exchange between Dead Sea rift lakes and surrounding rocks: Evidence from sulfur mass balance and isotopic compositions in lake sediments

Torfstein A. [1,2], Gavrieli I. [2], Katz A. [1], Kolodny Y. [1], Stein M. [2]

1. Institute of Earth Sciences, The Hebrew University, Jerusalem, Israel
2. Geological Survey of Israel, Jerusalem, Israel

The mass balance and isotopic composition of sulfur was studied in the deposits of the three major water bodies that occupied the Dead Sea basin during the late Quaternary (lakes Amora (~700-130 ka BP), Lisan (70-14 ka BP) and the Holocene Dead Sea) and used to estimate the sources and evolution of subsurface, sulfate-rich brines in surrounding sediments.

The Amora and Lisan sediments display a similar distribution of sulfur isotopic compositions (primary gypsum layers: $\delta^{34}S$=14-28‰; native sulfur, disseminated and thin laminae of gypsum: $\delta^{34}S$ = (-26)-15‰), while the isotopic compositions of primary and disseminated gypsum in the Ze'elim Fm. are uniform at $\delta^{34}S$=15 ±0.7‰, and similar to those of the present day Dead Sea.

The thickness of primary gypsum deposits in the Amora and Lisan Formations reaches up to several tens of centimeters, approximately an order of magnitude higher than those observed in the Ze'elim deposits (~1 mm).

The precipitation of primary gypsum is explained by the continuous import of sulfate to the lake from freshwater sources and its accumulation in the lake water. This process continues until gypsum saturation is reached and gypsum starts to precipitate. This can occur after several thousand years of continuous sulfate build up in the lake or due to evaporation and water column overturn. In the former case, minor quantities of gypsum sink in a continuous flux to the lake's anoxic lower layer where they are susceptible to dissolution and subsequent sulfate reduction. In the latter case, gypsum precipitates during discrete events and forms massive gypsum layers. However, the thickness of these layers is constrained by the sulfate concentration in the water column, which is limited by the Ca^{+2} concentration, ionic strength, and gypsum solubility constant (K_{sp}). Considering these limitations, the observed thickness of primary gypsum layers in the Lisan Formation requires a temporal increase in the sulfate flux to the lake during events of primary gypsum precipitation. The source of this additional sulfate was sulfate-rich lake water that penetrated the sediments during the preceding period of lake high stand. When the lake receded, these solutions were gravity-driven out of the sediments and back into the lake.

During the low stand periods of the Holocene Dead Sea, when level changes and freshwater inputs were rather limited, only small amounts of gypsum accumulated in the section. Thus, although the Dead Sea lacustrine system is often perceived as a contemporary analogous to Lake Lisan, the sulfur system in the latter exhibits a more complex path of evolution, which involves subsurface, short term (several ka) subsurface cycling of lake-derived solutions.

The implications of these findings on the limnological history of Lake Amora will be reviewed.

Depth imaging of the levant basin, offshore Israel using 2D, seismic reflection data

Trachtman P., Gardosh M., Ariely R.

Geophysical Institute of Israel, Lod, Israel

High-quality, regional seismic reflection lines were recently acquired in the Eastern Mediterranean, offshore Israel. This project was aimed to create depth images from these seismic lines, previously processed in time domain.

Four seismic lines, totaling 650 km, were selected for reprocessing. In an initial step a full, standard CMP-processing flow was applied. This flow included pre-stack time migration procedure (Kirchhoff algorithm) that was used to create fully migrated but not imaged data.

In a second step we applied a pre-stack depth migration technique. PSDM is essential to seismic reflection imaging in areas of steeply dipping structures or extreme lateral velocity variations (salt layers). Both conditions are found in the subsurface of the Levant Basin, offshore. A 3D velocity model was built first, guided by existing seismic lines and well information. While these methods provide a sufficient velocity model to produce a preliminary image, a horizon velocity analysis, performed in several iterations was applied to improve the model and to produce the final depth images.

The resulted pre-stack depth migrated profiles provide more accurate images of the subsurface and can be directly used for the construction of geological and structural sections.

Beer-Sheva waste belt

Voznesensky V., Bornstein Y.

Department of Geological and Environmental Sciences, Ben-Gurion University of the Negev 84105

The problem of Beer-Sheva's disposal sites is very acute. We can see a dramatic ecological situation that is determined by urban disposal sites. Disposal sites take up a disproportionate share of the city's area, - about 10%. Adding adjacent polluted fields the disposal sites occupy almost 20% of the area. The disposal sites form a near-circular continuous strip encompassed Beer-Sheva. Its length is about 20 km, and average width is 0.5 km. This is Beer-Sheva Waste Belt that, to regret, is one of the principal components of Beer-Sheva's landscape. It has unfavorable effect upon the moral atmosphere and outer appearance of the city, makes the city unpleasant for living, makes sharply worse sanitary conditions of Beer-Sheva, and prevents the development of tourism. The Beer-Sheva waste belt is, in essence, new ecological technogenic domain that has fundamentally transformed the city outskirts landscape. Disposal sites, big and small, represent visual violation of the citizens' rights to have pleasing surroundings.

The existence of the Belt has a direct influence on key issues of metropolitan planning and development of the infrastructure of Beer-Sheva. The belt includes 14 big disposal sites and many small ones. The basis of the disposal sites is generally a sequence of redeposited loess. Some systems of faults and joints (WNW-, NNW-, NE-, and ENE- directions) cross the loess and underlying rocks. They produce instability of the basis. The most dangerous disposal sites are located at the southeast part of the city. Poisonous substances flow from there to Beer-Sheva stream and may extend along the numerous joints in north-north-west direction to the central part of the city.

Beer Sheva waste belt includes temporary pseudo-disposal sites (rocks and soil extracted from the building excavation).

Distinctive characteristic of Beer-Sheva's disposal sites is the predominance of concrete in the waste. About 100,000 cubic meters of concrete (200,000 tons) are situated in Beer-Sheva's Waste Belt.

The planning of the reconstruction of Beer-Sheva's Waste Belt requires a long-term action coordinated with the Municipality of Beer-Sheva. It is important to include the findings of this work in the overall plane of Beer-Sheva 2020 (from 08.1998), so that there will be a suitable solution for Beer-Sheva's waste belt problem.

Estimating location and size of historical earthquakes by geo-archaeological study of Um-el-Kanatir, Dead Sea Fault

Wechsler N. [1]*, Katz O. [2], Marco S. [1]

1. Department of Geophysics and Planetary Sciences, Tel Aviv University
2. Geological Survey of Israel, Department of Engineering Geology and Geological Hazards

We analyze the Byzantine (6th century) archaeological site of Um el Kanatir, located 10km east of the Dead Sea Transform (DST) in Northern Israel. The site was apparently damaged by an earthquake-induced landslide. We use the landslide mechanical character to constrain historical seismic acceleration in the Northern segment of the DST.

Um el Kanatir is located on the slope of a canyon and its bedrock (the Hordos Formation) makes it susceptible to landslides. A water trough, which collected spring water, is displaced nearly one meter, but no geological fault is found below the site. We realized that the damaged water system is on the southern rim of a landslide that advanced westward; hence the damage is attributed to an earthquake-induced landslide. The archaeological excavations in the nearby village revealed typical earthquake-induced damage in form of aligned fallen columns and walls, horizontal shift of heavy masonry blocks, and complete ceramic pots and farming tools buried beneath fallen ceilings. In order to evaluate the associated ground acceleration, we first measured the bedrock mechanical properties using a direct-shear system. Then we calculated the pseudo-static stability of the slope (using commercial software SLOPE/W) and found the critical acceleration for triggering the landslide. The results show that high values of horizontal seismic-acceleration are required to destabilize the slope, indicating that the slope is statically stable. We conclude that a strong earthquake is required to cause the observed failure of the slope. Indicative archaeological artifacts from the village and the spring area indicate that the site was inhabited until the middle of the 8th century; therefore, the candidate earthquakes are the 749, 1033, 1202 and 1759 AD earthquakes. If we assume that the destruction forced the abandonment of the site, the earthquake of 749 AD is the most likely trigger of the landslide. We used the Newmark displacement method following Jibson et al.'s (2000) empirical equation to calculate the earthquake magnitude as a function of distance from the site needed to cause slope instability. The results show that an $M_W > 6.8$ earthquake up to 50 km from the site could induce the studied landslide.

* N. Wechsler is now at the University of Southern California.

The hydrogeology of submarine groundwater discharge and of seawater recycling in Dor Bay, Southern Carmel coast

Weinstein Y. [1], Swarzenski P. [2], Burnett W. C. [3], Yechieli Y. [4], Shalem Y. [1], Herut B. [5]

1. Bar-Ilan University, Ramat-Gan 52900, Israel
2. U.S. Geological Survey, St. Petersburg, FL 33701 USA
3. Department of Oceanography, Florida State University, Tallahassee, FL 32306 USA
4. Geological Survey of Israel, 30 Malkhei Israel St., Jerusalem 95501, Israel
5. Israel Oceanographic and Limnological Research, P.O. Box 8030, Haifa, 31080, Israel

The Dor Bay is a natural embayment with dimensions of 100x150 m, located at the southern Carmel coast. On its Northern and Western side, the embayment is partly closed to the open sea by a sandstone (Kurkar) ridge, and on its southern side, it is connected to another embayment via sand bars. The relatively slow exchange of water with the open sea makes it an ideal site to study Submarine Groundwater Discharge (SGD). Continuous measurement of radon in the bay, as well as resistivity studies in the sediments showed that groundwater is constantly discharging to the bay on the order of 5-7 m^3/day (see *Shalem et al.*, current volume).

The local aquifer is composed of the Pleistocene calcareous Kurkar sandstone, irregularly covered by loose Holocene sands. A variably thick clay unit is usually found as a confining layer between the two units. Kurkar is exposed at about one third of the bay floor, while the rest is covered by sand. Activities of radon in the Kurkar groundwater are one order of magnitude higher than in the sand (350-400 compared with 20-90 dpm/l).

The composition of the water discharging to the bay was measured in seepage meters deployed on sand-covered bay bottom, as well as at a small seepage site and an old well dug into the Kurkar, both exposed at the inter-tidal zone during low tides. We found that the water discharging from the Kurkar is close to fresh (~3 ppt) and radon-rich (300-400 dpm/l), while the water discharging from sand-covered bay bottom is saline (15-30 ppt) and carries lower radon activities (110-240 dpm/l). Both types of water define a mixing line between the radon-rich Kurkar fresh water and radon-poor seawater. There is almost no contribution of the groundwater in onshore sand. Moreover, stationary resistivity profiles in the bay show that low salinity water (~3 ppt) occur in the submerged Kurkar up to 40 m offshore. On the other hand, saline water (17-25 ppt) is always found at the water table in onshore sand up to 10-15 m from the high tide shoreline, and in March 2006 it was also found 35 m from shore.

The above observations imply that fresh water discharges to the bay derives mainly from the Kurkar unit, while seawater recharge and circulation occur mostly in the shallow, superficial sand. The mid-range radon activities and relatively high salinity of the water discharging in the sand-covered areas of the bay reflect mixing of radon-rich Kurkar water with radon-poor recycled seawater. This is supported by preliminary hydrological measurements, which show that hydraulic heads in a close-to-shore Kurkar borehole are significantly higher than in the sand.

Billow-like folds record turbulent flow in the lacustrine Lisan Formation, Dead Sea basin

Wetzler N., Heifetz E., Marco S.

Department of Geophysics and Planetary Sciences, Tel Aviv University

By quantifying the geometry of soft sediment deformation in the Lisan Formation, we conclude that these structures, which were once under water, are now evidence for the Dead Sea region earthquakes, and a good case study for turbulent behavior.

The various intensities and scales of soft sediment folding reflect various stages of deformation. Our analysis of the billow-like (recumbent) folds shows correlation between the wave number and the energy (kinetic) spectrum with a correlation constant of about -5/3. This result is identical to the theoretical 'Kolmogorov Constant'. This Kolmogorov Constant characterizes the phenomena as a turbulent flow, which is best explained by earthquake-induced shear.

Exploring the physical mechanisms behind radon variations at the Hamei-Tveria hot spring, Israel

Woith H. [1], Steinitz G. [2], Gajewski C. [1], Malik U. [2], Piatibratov O. [2]

1. GeoForschungsZentrum, Potsdam, Germany
2. Geological Survey of Israel, Jerusalem, Israel

Radon is continuously being monitored at the hot spring of Hamei-Tveria (HT; Tiberias) since 2000. The radon signal contains periodic daily and non-periodic multi-day variations as well as periodic seasonal variation patterns.

In the daily variation band tidal effects (O1 and M2 constituents) are absent from the spectra. Spectral analysis shows diurnal (24-hour; S1) and semidiurnal (12-hour; S2) periodic constituents. The amplitudes of these constituents exhibit regular temporal variation having a long-term seasonal pattern. The ratios of co-occurring amplitudes of these constituents define a linear pattern indicating a fundamental statistical property in the frequency domain of the radon time series. Furthermore – the occurrence and observation of such a systematic pattern at the daily scale implies that long term variations in the radon time series are also natural geophysical phenomena.

On a seasonal scale radon is negatively correlated with air temperature and positively correlated with the air pressure. Seasonal radon maxima occur during the rainy winter time. The hot spring waters of Tiberias are a mixture of a shallow and a deep water components: shallow groundwaters are recharged in the west, flow eastward and emerge to the surface along sub-vertical border faults, where they mix with a saline fluid characterized by high temperatures. Rain fall should increase the hydraulic pressure in these conduits and thus should increase the flow velocity. Increased flow means less time for radon to decay and thus a positive correlation between flow rate and radon – at least qualitatively explaining the winter maxima.

Until spring 2003 the average radon concentration was ca. 700 cps, whereas thereafter the average radon concentration dropped to 450 cps. The drop of the radon level in 2003 was accompanied by a significant increase of the seasonal radon amplitude – it doubled from ± 60 cps to ± 120 cps. What happened in 2003? We may rule out rain fall (measured at Hamei Tiberias and kindly provided by Mekorot Ltd.), because the amount of winter rains did not change significantly over time. At this stage we suspect the level of the Tiberias lake as the driving force for the radon drop in 2003. Until 2003 the lake level hovered around -214 m ± 1 m seasonal variation. In spring 2003 the lake level has risen to -210 ± 1.2 m corresponding to the long-term Kinneret lake level (1927-1986).

Mineralization and exploitation of copper in Timna

Wurzburger U.

2 Ben Zion St., Jerusalem

Copper mineralization occurs in the Timna area (Southern Israel) in the Percambrian complex, in the Timna Fm. and the Shehoret Fm. of Cambrian age and in the Avrona Fm. of Aptian age.

Ancient exploitations of copper include: Selective mining of copper nodules in the white sandstone of the Avrona Fm. in the Chalcoilitic-Mamluke period. The minerals are Cu sulfides (Chalcocite) and alteration products, chrysocolla and malachite. Late Bronze age- Early Iron age- intensive exploitation along cliffs of the white sandstone.

Roman period- shaft mining and deep galleries were excavated.

Modern mining concentrated on shales and dolomites of the Timna Fm. The thickness of the ore beds is 4-8m and the copper content 1-1.6%. The Cu minerals are mainly Silicates: chrysocolla, plancheite, bisbeeite and dioptase, carbonates: malachite, phosphate: pseudomalachite as well as chloride and sulfate Cu minerals. Exploitation of copper started in 1959 after reserves of 7 million tons were proven. It started with an open pit mining, followed by "room and pillar" underground mining. Annual production of "copper cement" (containing 80-90% copper) was 10,000-12,000 tons.

Treatment of the ore did not apply pyrometallurgical technologies as in ancient times, but the hydrometallurgical technology. The ore was grinded and milled and the copper was leached by using sulfuric acid produced locally, using imported sulfur. The amount of acid needed is a function of the "parasites" (carbonates and phosphates etc.) in the ore (average of about 90 kg. acid per ton of ore). The copper was solved in diluted brine and deposited by iron scrap. The product was a dark brown mud called "copper cement" containing 80-90 % copper. The cement after drying was exported to copper smelters abroad where it was added to Cu sulfides for production of electrolytic copper.

Due to the deepening of the copper ore southwards, a vertical shaft was excavated to depth of 300m for mobilizing the ore. Due to difficulties in underground mining and the decrease in the ore/overburden ratio in the open pit and tremendous fluctuations in copper prices it was decided in 1976 to stop the operation. A few years later the works were renewed on a smaller scale but in 1983 the operation was stopped again. At this stage more reserves were known than at the beginning of the exploitation in 1959.

Pre-collapse detection and location of brittle failure in instable cliffs by nanoseimic monitoring

Wust-Bloch G. H.

Department of Geophysics, Tel Aviv University, Israel
hillel@seismo.tau.ac.il

Nanoseismic monitoring techniques were applied to detect brittle failure generated at the top of an unstable 40 m-high sandstone cliff. Three small-aperture sparse arrays (Seismic Navigation Systems-SNS) were deployed with an imbricated geometry on top of an overhanging cliff section, which was left after a 1000 m^3 mass failure. The SNS recorded in continuous mode at 200 and 500 Hz under favorable SNR conditions.

Dozens of high frequency spiky signals were detected during a 12-hour period at slant distances varying between 7 and 51 meters. Waveform characterization by sonogram analysis shows that signals have very similar frequency contents (10-80 Hz). Event magnitudes corrected for extremely short distances (Wust-Bloch & Joswig, 2006) range from $-3.7 < M_L < -2.1$. The 3-D mapping of these nanoseismic events produces clusters and bands whose extension to the surface matches tensile cracks observed in the soil. These features also corroborates predictions for the linear down-scaling of surface rupture length, whereby the size of the nucleation zone is expected to be in the order of 1-10 cm for M_L -2.0 events.

This feasibility study demonstrates that nanoseismic monitoring can be applied to detect and locate, with high accuracy, brittle failure generated within cliffs before failure and collapse take place.

Pre-collapse sinkhole hazard assessment by integrated nanoseimic monitoring and GIS techniques along the Dead Sea shores in Jordan

Wust-Bloch G. H. [1], Al-Zoubi A. [2], Ben-Avraham Z. [1], Al-Ruzouq R. [3], Abueladas A. [2], Joswig M. [4]

1. Department of Geophysics, Tel Aviv University, Israel
2. Engineering Geophysics, Al-Balqa University, Jordan
3. Surveying & Geomatics Engineering, Al-Balqa University, Jordan
4. Institute für Geophysics, Stuttgart University, Germany

Sinkhole hazard has been affecting the Jordanian Dead Sea shores for over a decade, adversely affecting the agriculture, tourism and the natural resources industry. An innovative hazard assessment approach has been developed here that integrates nanoseimic monitoring with GIS techniques. A test-project was set up in the Ghor Al-Haditha - Lisan area.

The GIS-supported model for the Ghor Al-Haditha - Lisan region consists of a custom DTM, calibrated by high-density GPS benchmarks. It also includes old aerial photos, orthophotos and recent satellite images. Additional information layers comprise geology, lithology, hydrology, geophysical surveys and lifelines. The model shows a high correlation between sinkhole distribution, tectonic and hydrological features.

Nanoseismic techniques, which were developed to detect extremely low-energy signals generated by cavitation processes taking place in the unconsolidated, layered media (Wust-Bloch & Joswig, 2006) were applied in strategic locations to determine the true activity of the subsurface. The detection of nanoseismic signals and the ensuing signal waveform characterization by sonogram analysis identified two main groups of nanoseismic events: impacts on dry material and impacts in liquid. When correlated to local geological constraints, this discrimination can be used to assess the maturity of the sinkholes since it indicates whether failure is still confined to the groundwater or is progressing towards the surface.

The integration of both techniques results in the design of innovative hazard maps that include a detailed mapping and quantitative assessment of pre-collapse invisible subsurface cavitation and sinkhole activity.

Estimation of PGA values from back analysis of a large landslide in the eastrens margins of the kineret

Yagoda G.[1,2], Katz O. [2], Amit R. [2], Hatzor Y. H. [1]

1. The department of geological and environmental sciences, Ben-Gurion University of the Negev, P.O. Box 653, Beer-Sheva, 84105.
2. Geological Survey of Israel, 30 Malkhe Israel St., Jerusalem, 95501.

The eastern margins of lake Kineret, situated along a Northern segment of the Dead Sea transform, have been subjected to high seismicity associated with normal faults. Examination of old and recent air photos reveals numerous lineaments striking north-south, as well as several old landslides, in the study area between Haon cliffs and Susita. Resolving the interaction between those morphological elements is not obvious, and can be a key factor in understanding the level of local seismic hazard and the relative timing of the events.

The largest landslide observed in the field, 500m wide and 1500m long, was selected for analysis. A very detailed mapping of the area around the slide was preformed, and the rock unit along which sliding took place, a horizon within the Ein-Gev sands formation, was identified in the field. Samples of Ein-Gev sands were tested at the laboratory in direct shear to determine characteristic shear strength properties including both peak ($c = 376kPa$; $f = 43^{\circ}$) and residual ($c = 0$; $f = 39^{\circ}$) values. Tests were performed on dry samples in drained conditions. The topography of a stable slope next to the studied slide was used for limit equilibrium analysis utilizing the strength properties obtained at the laboratory. Both static and pseudo-static analyses were performed with a commercial software package SLOPE/W 2004.

Results of limit equilibrium analyses indicate that the slope is stable under static gravitational loading both with peak and residual shear strength values. Pseudo-static analyses results indicate that a horizontal PGA of ~ $0.8g$ would be required to drive the observed failure if peak strength values are assumed; a horizontal PGA value of ~ $0.3g$ would be required if residual strength values are assumed. Interestingly, the GII seismic hazard map predicts a PGA value of $0.3g$ for this location, in basic agreement with our results assuming residual strength conditions for the material.

A trench was excavated on the landslide, crossing a fault clearly detected both in air photos and in the field on both the Northern and Southern boundaries of the slide. The 3m deep trench exposed three soil profiles developed in the colluvium composing the landslide, two paleosols overlain by an upper, recent, soil. The development of the three soil profiles implies cyclic down-slope movement of material and quiescent periods between movement episodes, allowing soil formation. Time relationships between the slide and the fault are yet not clear, although sedimentary and pedogenic disturbances detected in the trench may be associated with faulting.

Existence of seismic anisotropy in the Eastern Mediterranean sea

Yelin G., Reshef M.

Department of Geophysics and Planetary Sciences, Tel Aviv University.

In recent years, it has been shown that seismic anisotropy exists in almost every geological province which is characterized by massive shale formations. Detailed studies of anisotropy were performed in places such as offshore West Africa, the Gulf of Mexico and the North Sea, all known as major oil and gas provinces. These studies clearly showed that if anisotropy is not taken into account during seismic data processing and imaging, significant errors can be expected in the geological interpretation phase. Similar to these provinces, the young sedimentary sequence offshore Israel is known to consist of shales and clays which may indicate that anisotropy should be considered while processing seismic data from this area.

In most seismic exploration projects, the subsurface is assumed to be isotropic. The reason for this assumption is the simplified data processing and interpretation procedures that are implemented. Such a wrong assumption may lead to erroneous time to depth conversion, lack of accuracy in events positioning, poor data resolution, miss-ties between seismic and well log data and erroneous geological parameters.

In this study, seismic data from the Eastern Mediterranean have been re-processed in the time domain, assuming an anisotropic medium. Special velocity analysis algorithm was used, in which travel time curves follow a non-hyperbolic trajectories, and an extra parameter, related to the medium's anisotropy is determined. Our analysis provides evidence for the existence of anisotropy in the young sediments above the well known "M" horizon. The determined parameters are used to perform an anisotropic time migration which is compared to the traditional isotropic time migration.

Radon transport within rocks along the Dead Sea Transform in relevance to the study of earthquake related phenomena - model and field results

Zafrir H., Piatibratov O.

Geological Survey of Israel, Malkhe Israel 30, Jerusalem, 95501

The basic assumption underlying monitoring of radon along the Dead Sea (DS) Transform is the capability of radon to emanate to the porous media and be available for further transfer by diffusion via the pore content (fluid or gas) or to transport by these carriers, to a limited (half life = 3.8 days) range. To this end the correlation between the temporal variations of radon at daily, multi days and yearly scale is investigated versus other geophysical parameters: pressure, temperature, precipitation, gravity, and geodynamic processes (local and regional). A central issue in such an investigation relates to the transport of radon in the geogas system.

An advanced model for radon transport in porous media accounts for known physical parameters assumed to control the transport of radon within the rocks, usually from depth to the surface. The general equation for time dependent radon transport from the air-filled part of the porous media is:

$$\beta\frac{\partial Ca}{\partial t} = \nabla\bullet(D\nabla Ca) + \frac{k}{\mu}(\nabla p\cdot\nabla Ca) - \beta\lambda C_a + \Phi$$

Where: Ca is the radon concentrations in the air-filled part, $\nabla\bullet(D\nabla Ca)$ is the bulk flux density of radon from diffusion and it is proportional to the bulk radon concentration gradient ∇Ca, $\frac{k}{\mu}(\nabla p\cdot\nabla Ca)$ is the radon advective flux density produced by local gradient in pressure ∇p (deviation from the aerostatic absolute pressure) and is calculated from Darcy's law, $-\beta\lambda C_a$ is the radon radioactive decay with decay constant λ, and Φ is the radon production rate from its immediate parent radium. β is the partition-corrected porosity, D is the bulk diffusion coefficient, k is the isotropic gas permeability and μ is the geogas dynamic viscosity.

Defining the relation between a time varying radon signal and eventual geophysical parameters adds further complexity. The results from the Amram tunnel (Bloch Geophysical Observatory) and from shallow sites at the NW DS indicate that: No correlation occurs between radon and atmospheric pressure variations at the Amram site. The pressure in the subsurface and outside is the same. Therefore no local pressure gradient exists to produce an advection that can account for the radon anomalies. In addition, there is no connection between the temporal variation of radon and the stable subsurface temperature ($28^0 \pm 0.3^0$ in tunnel).

Nevertheless, an apparent correlation in the time domain occurs between the radon at depth and the temporal variation of the outdoor temperature at Amram. The radon follows the temperature variation with a delay of about 10 hours, consistently. Furthermore, the multi-day and the seasonal variation of the radon emanation also indicate the same similarity with the external temperature. Similar relations occur at the NW DS, between part of the radon signals and the temporal variation of the environmental temperature. The rest of the radon signals (anomalies) could be related to other geophysical processes such as geodynamic ones (earthquakes; Geology, v. 31, 505-508).

Radon response to seismic calibration explosion experiment at Bet-Alfa

Zafrir H. [1], Malik U. [1], Gazit-Yaari N. [2], Haquin G. [2], Steinitz G. [1]

1. Geological Survey of Israel, Malkhe Israel 30, Jerusalem, 95501
2. Soreq Nuclear Research Center, Yavne, 81800

Radon measurements were performed at shallow levels during an in-land 20 ton seismic calibration explosion experiment, simulating a 2.6 M_L earthquake. The experiment was conducted at a basalt quarry in the Northern margin of the Beit Shean valley (Israel). The measurements were conducted in order to investigate the influence of the explosive blast and the transitory seismic wave fields on the radon transport in the fractured rocks, adjacent to the focus of the explosion. Five gamma-ray sensors were placed, at a depth of 2 meters, along a transect located 17 to 150 meters from the edge of the explosion boreholes. Measurements commenced 4 days before and continued for 9 days after the explosion. 15 minute integrations were used throughout and 10-second recordings were collected in an interval of several hours before and after the explosion.

Typical diurnal variations of radon, reflecting the typical variation pattern of radon in the shallow environment, were recorded at all measurement points before and after the calibration explosion. No change in the radon concentration was recorded as consequence of the main explosion as well as three smaller experimental shots 0.5 ton, 0.5 ton and 2 tons that were conducted also at the same day and site, before the calibration blast. The seismological data indicate that the transient excess pressure at the farthest sensor was above 70 bars per meter during 0.2 to 0.4 seconds, and evidently much higher at the nearest sensors. None of the sensors responded by recording a change in radon concentration. The general equation for time dependent radon transport in the air-filled part of porous media is:

$$\beta \frac{\partial Ca}{\partial t} = \nabla \bullet (D \nabla Ca) + \frac{k}{\mu} (\nabla p \cdot \nabla Ca) - \beta \lambda C_a + \Phi$$

Where: Ca is the air-filled radon concentrations (Bq m^{-3}), $\nabla \bullet (D \nabla Ca)$ is the bulk flux density of radon from diffusion, $\frac{k}{\mu}(\nabla p \cdot \nabla Ca)$ is the radon advective flux density produced by local gradient in pressure ∇p (deviation from the aerostatic absolute pressure calculated from Darcy's law) $\nabla p = -\frac{\mu}{k} u$, $(-\beta \lambda C_a + \Phi)$ is the radon radioactive source terms (decay with constant λ and production rate from the immediate parent radium). β is the partition-corrected porosity, D is the radon diffusion coefficient in air-filled ($m^2 s^{-1}$) , k is the isotropic air-filled permeability (m^2) and μ is the air-filled dynamic viscosity ($kgm^{-1}s^{-1}$).

From Darcy's law **the calculated air-filled bulk velocity is** $|u| = \nabla p \frac{k}{\mu} = 3 (ms^{-1})$ (based on the literature parameters μ=17,4 x 10^{-6}($kgm^{-1}s^{-1}$) and k= 10^{-11}(m^2)).

Radon level in geogas is probably enhanced due intense fracturing disintegration at the focus of the explosion. But, the model suggests that radon movement in the vicinity of each sensor could not exceed about 1 meters during the 0.4 seconds of exposure to the seismic wave - a value that is not capable to produce a radon anomaly at the loci of the sensors. This is supported by the experimental observations.

Site effect investigation for seismic hazard assessment: The town Petah Tikva and around areas

Zaslavsky Y., Ataev G., Gorstein M., Kalmanovich M., Perelman N., Aksinenko T., Giller D., Giller V., Dan I., Livshits I., Shvartsburg A.

Seismology Division, Geophysical Institute of Israel, P.O.Box 182, Lod

For microzoning goals about 550 microtremor measurements across the study area of 128 km^2 including the towns of Petah Tiqwa, Hod-Hasharon and Rosh HaAyin, partially Ramat Hasharon and Qiryat Ono and adjoining settlements Elishma, Neve Yerek, Givat Ha-Shlosha, Kefar Sirkin, Nahshonim, Givat Shemuel, Ganey Tiqwa and others, have been done on different grid scales. Majority of measuring sites were spatially distributed each 500 meters. High variations in the observations led us to increase the density to a grid spacing of 250 m and in some sites even 150 m.

Measurement results indicate site amplifications ranging from 2.5 up to 7-8 units decreasing from the west to the east within the frequency band 0.4-13 Hz. In the first approximation the resonance frequency has general trend to increase toward the east. Owing to a higher resolution, the frequency map not only identifies and traces the structural blocks and faults detected in the structural map of the top Judea Gr. but also reveals the new tectonic features.

Data from representative boreholes and two refraction profiles integrated with H/V observations at corresponding locations were used to develop models of the subsurface at the measurements sites. By comparison of the Uniform Hazard Acceleration Spectra calculated for 100 selected sites and considering the subsurface models constructed across the investigated area, we divided the area into number of zones. Each zone is characterized by a generalized seismic hazard function representative the sites within that zone. For many zones the Israel Standard (IS-413) underestimates the acceleration in the broad period range.

Seismic hazard assessment by ambient noise measurements for new constructions: The Check Post test site (Haifa)

Zaslavsky Y., Kalmanovich M.

Seismology Division, Geophysical Institute of Israel, P.O.Box 182, Lod

Local variations of soil conditions can increase ground motion generated by earthquakes and the consequential damage. The dramatic collapse of the Cypress Street Viaduct on Nimitz freeway during the 1989 Loma Prieta earthquake demonstrates importance of providing experimental estimation of local site effect for design of new bridges. This study is focused on estimating the seismic hazard to Qrayot Interchange bridge designed in Check Post, Haifa. This process of hazard assessment involves: detailed mapping of the fundamental and other natural frequencies and amplitudes of H/V spectral ratios from ambient noise; compiling geological, geophysical information and well data and integrating it with H/V observations to construct subsurface models for different sites. The subsurface model serves as input for computing linear and non-linear site-specific acceleration response spectra at the investigated sites.

For the 29 locations in the area of about 0.4 km^2 H/V spectral ratio were derived. Based on the observed resonance frequencies, we divided the study area into fife zones as follows:

Zone I. Characterized by two resonance frequencies: first, near 0.9 Hz and second about1.3 Hz with amplification factors within the range of 5-6.

Zone II. Soil sites exhibited significant peak between 1.3 and 2.0 Hz. with amplification of up to 6.

Zone III. Amplification effects of factor 3-3.5 are at frequencies 3-3.5 Hz band.

Zone IV. Amplification levels of 3-3.5 are observed in the frequency range 5-8 Hz.

Zone V. No amplification in the entire frequency band.

The linear and non-linear Uniform hazard site-specific acceleration response spectra calculated for I and II zones were significant different from ones prescribed by the current building code IS-413, in that IS-413 underestimates the accelerations in the period range from 2 to 0.2 s.

The middle to Late Pleistocene sand sheets sequence of Kerem Shalom, Western Negev - a record of sand incursions to the coastal plain of Israel

Zilberman E. [1], Porat N. [1], Roskin J. [2]

1. Geological Survey of Israel, 30 Malkhe Israel St., Jerusalem 95501, Israel.
2. Dept. of Geography and Environmental Development, Ben Gurion University in the Negev, Beer Sheva, Israel

A 15 m thick sequence of calcic sandy paleosols was exposed in a trench excavated in the Western Negev flat sand sheet that extends between the Agur dune field in the south and the kurkar ridge of the Gaza Strip in the northwest.

Seven calcic paleosols, separated by erosional contacts, were identified in the sequence. Most of the paleosols developed to stage III-IV and they are intensely bioturbated, with abundant burrows and rhyzolites traces.

We used the optically stimulated luminescence (OSL) method to date the time of sand deposition and soil formation. By separately dating the medium-sand fraction and the very-fine-sand fractions, we could distinguish for some units between the event of sand incursion and the subsequent dust accumulation, which contributed to the formation of the calcic soils. The ages of the sand units range from more than 400 ka at the base of the section (Units 1, 2) to about 13 ka at its uppermost part (Unit 7), with large time gaps between the units. The age of Unit 6 is similar to that of Ramat Gan and Dor kurkar members in the Sharon coast, and the age of unit 5 is similar to the lower Kurkar unit in the Carmel coast. However, the major Late Pleistocene phase of sand incursion into the Negev, which formed the Agur and Haluza dune fields, is missing from this sequence.

Since the source of the sand in this area is the Mediterranean coast, each unit of sand sheets in the Western Negev reflects an event of sand incursion to the coastal plain of Israel and formation of Kurkar ridges. Each break in sand supply is represented in the Western Negev by calcic soil and in the Sharon coast by Hamra soil.

The Western Negev sand sheets sequence reflects the Pleistocene history of sand incursions to the coastal plain of Israel and as such it can be used to reconstruct climatic fluctuations in the Eastern Mediterranean. The calcic soils developed under a climatic regime not much different from the present, with annual precipitation of at least 200-250 mm. The time span between each sand accumulation event indicates that in this region, where the only source for carbonate and silt is in dust, the development of mature calcic soil takes several tens thousands years.

Geomorphologic - lithologic mapping along the Israel coastline

Zilberman E., Ilani S., Netser-Cohen H., Calvo R.

Geological Survey of Israel, 30 Malkhe Israel St., Jerusalem

In the framework of validating the "Beach Law" by the Ministry of Environmental Protection, the GSI was asked to prepare a geomorphologic map of the coastal belt, up to ca one kilometer from the shore. This map is part of the coastal geodatabase, retained in the GIS of the Geological Survey and the Ministry of Environmental Protection, for use in future infrastructure planning.

The maps include several layers:

1. Layer presenting the morphologic – lithologic units exposed along the coast (on a scale of 1:5000).
2. Layer presenting the topography of the shore, the coastal cliffs, the drainage systems and the kurkar ridges.
3. Layer presenting the kurkar and sand quarries, some of which serve as garbage dumping sites, causing environmental hazards.

Built-up areas where the original landscape was disturbed and restricted areas were not included in the maps.

The coastal belt was divided into three segments, according to geomorphologic and lithologic affinities:

1. The Southern coastal area (from Ziqim in the south to Bat Yam in the north), characterized by wide sandy beaches, with sand dunes east of the backshore.
2. The central coastal area (from Bat Yam in the south to Nahal Hadera in the north), characterized by steep, high (up to 30 m.) continuous kurkar cliffs.
3. The Northern coastal area (from Nahal Hadera in the south to Rosh Ha'Niqra in the north), characterized by shores without cliffs, some of them sandy and some rocky (kurkar and beach-rocks), forming embayments.

Sixteen mapping units were selected, based upon lithologic and morphologic characters:

(0) Built-up areas; (1) Kurkar (Dor and Ramat Gan); (2) Sandy soils (Natanya Hamra and reddish calcic soils); (3) Holocene calcarenite (Tel Aviv Kurkar); (4) Stable sand units (Ta'arucha and Hadera); (5) Stable Dune fields (Hadera dunes); (6) Stable sand sheets; (7) Active coastal sand dunes (8) Archaeological sites; (9) The swash zone (the flat backshore); (10) Beach-rocks; (11) Abrasive plates (in sea); (12) Stream channels (including the flood plains); (13) Fine clastic flood-plain and marsh sediments and soils; (14) Coarse alluvial sediments and soils; (15) Garbage dumping areas.

Brines in the sinkholes along the Dead Sea coast: Origin and geochemical evolution

Zilberman T. [1,2], Gavrieli I. [2], Yechieli Y. [2], Katz A. [1]

1. Institute of Earth Sciences, The Hebrew University, Jerusalem 91904, Israel
2. Geological Survey of Israel, Jerusalem 95501, Israel

Sinkholes first appeared along the Dead Sea shores in the 1980s and have been developing at an ever increasing rate since then. The origin of these sinkholes has been attributed to dissolution of a salt layer at depth that is being dissolved by freshwater which flow eastwards following the decline in the Dead Sea water level. Many of the sinkholes are filled with saline waters, whose origin and relationship to their development is not known. The present study aims at identifying the source of these brines and their geochemical evolution. The Samar and Shalem (Mineral Beach) sites, containing waters of 5-550 and 181-508 g/L, respectively, have been selected as the focus of the study.

Field observations and chemical analyses indicate that evaporation plays a major role in the brine's evolution. Hence, evaporation experiments were conducted in the field with two relevant water types, the Dead Sea brine and the brines from the thermo-saline springs (e.g. En Kedem) which discharge along the coast of the Dead Sea, including at Mineral Beach site. Comparison of the composition of the evaporated brines and the fluids in the sinkholes indicates that a) All of Samar and most of Mineral Beach waters follow the evaporation path of Dead Sea brine. b) A few of Mineral Beach solutions follow the En Kedem evaporation path, while others display an intermediate composition between the Dead Sea and En Kedem paths, indicating mixing between these two water types.

The low Na/Cl ratios (< 0.33), as well as the ionic load and ratios typical of the investigated waters, suggest that they were not involved in the dissolution of halite that was responsible for the sinkhole formation, but reflect on-site evaporation. Salt precipitates encrusting the bottom of many of the sinkholes support this conclusion.

Plot of Ca vs. Li in the evaporated Dead Sea brines and in Samar waters exhibit excellent linear evaporative concentration path (R^2=0.998) passing through the origin, indicating a conservative behavior of Ca and Li. However, the plots of Br vs. Ca and Br vs. Li are non-linear implying significant co-precipitation of bromide with evaporitic minerals that precipitate from the brines. Hence, Ca and Li may readily serve as indicators for the degree of evaporation for Dead Sea waters and their evaporative derivatives while bromide exhibits a more complex behavior.

The possible uplift of Western Mount Carmel since the middle Pleistocene

Zviely D. [1], Galili E. [2], Ronen A. [3,4], Ben-Avraham Z. [5]

1. Recanati Institute for Maritime Studies, University of Haifa, Haifa, 31905, Israel.
2. Israel Antiquities Authority, POB 180, Atlit 30300, Israel.
3. Zinman Institute of Archaeology, University of Haifa, Haifa 31905, Israel.
4. The Max Stern Academic College of Emeq Yezreel, Emeq Yezreel 19300, Israel.
5. Department of Geophysics and Planetary Sciences, Tel Aviv University, Tel Aviv 69978, Israel.

Tabun Cave is located on the western slope of Mount Carmel, some 20 km south of Haifa. Its entrance faces north-west at elevation of 45-63 m above the present sea level (asl) (Zviely and Ronen, 2004). Excavations revealed 25 m thick cultural layers ranging from at least 630,000 years (630 kyr) (MIS 16) to about 100 kyr before present (BP). A horizon at mid-fill was dated to about 400 kyr BP (MIS 11) (Rink et al., 2004). The cave's bedrock is at 45 m asl. No marine sediments were found in the cave sediments, indicating that the sea had never penetrated the cave. Current studies indicate that Pleistocene high sea stands in the last 630 kyr reached maximum elevation of about 10 m asl, as last interglacial high sea stand of MIS 5e (about 125 kyr BP). Therefore, the cave's entrance could not have been below about 15 m asl throughout its occupation. Hence, the maximum range of uplift possible for Tabun Cave and the Western Mount Carmel within the last 630 kyr is 30 m, or a rate of 20 mm/kyr. It follows that from the Middle Pleistocene to the present, Western Mount Carmel may be considered tectonically stable [relative to the hilly backbone of Israel, were minimum uplift rates of more than 400 mm/kyr were proposed]. This is in good agreement with recent study, suggesting that since the last 125 kyr the possible vertical displacement of the Carmel coast could have been maximum 40 mm/kyr (Galili et al. 2006). These finds support the results of the current study for the Late Pleistocene. This means that the marine terraces found by Michelson (1970) above 60 m asl, must antedate the occupation of Tabun Cave.

Galili, E., Zviely, D., Ronen, A., Mienis, H.K., 2006. Beachrocks of the last interglacial, as indicators for tectonic stability of the Carmel coast in the last ca. 125,000 years. In: Mart, Y., (ed.), The Israeli association of aquatic sciences, 3rd annual conference, abstracts, University of Haifa, Israel, pp.22-26 (in Hebrew).

Michelson, H., 1970. The geology of the Carmel coast. Tahal, Report HG/70/025, 61 p. (in Hebrew).

Rink, W.J, Schwarcz, H.P., Ronen, A., Tsatskin, A., 2004. Confirmation of near 400 ka age for the Yabrudian industry at Tabun Cave, Israel. *Journal of Archaeological Science* 31, pp.15-20.

Zviely, D., Ronen, A., 2004. Garrod's spring in Tabun Cave, Mt. Carmel (Israel): 70 years later. In: Maos, J.O., Inbar, M., Shmueli, D., (eds.), *Contemporary Israeli Geography (Special Issue of Horizons in Geography*, Vol. 60-61, pp.167-176.

תקצירים

נווה זוהר 2007

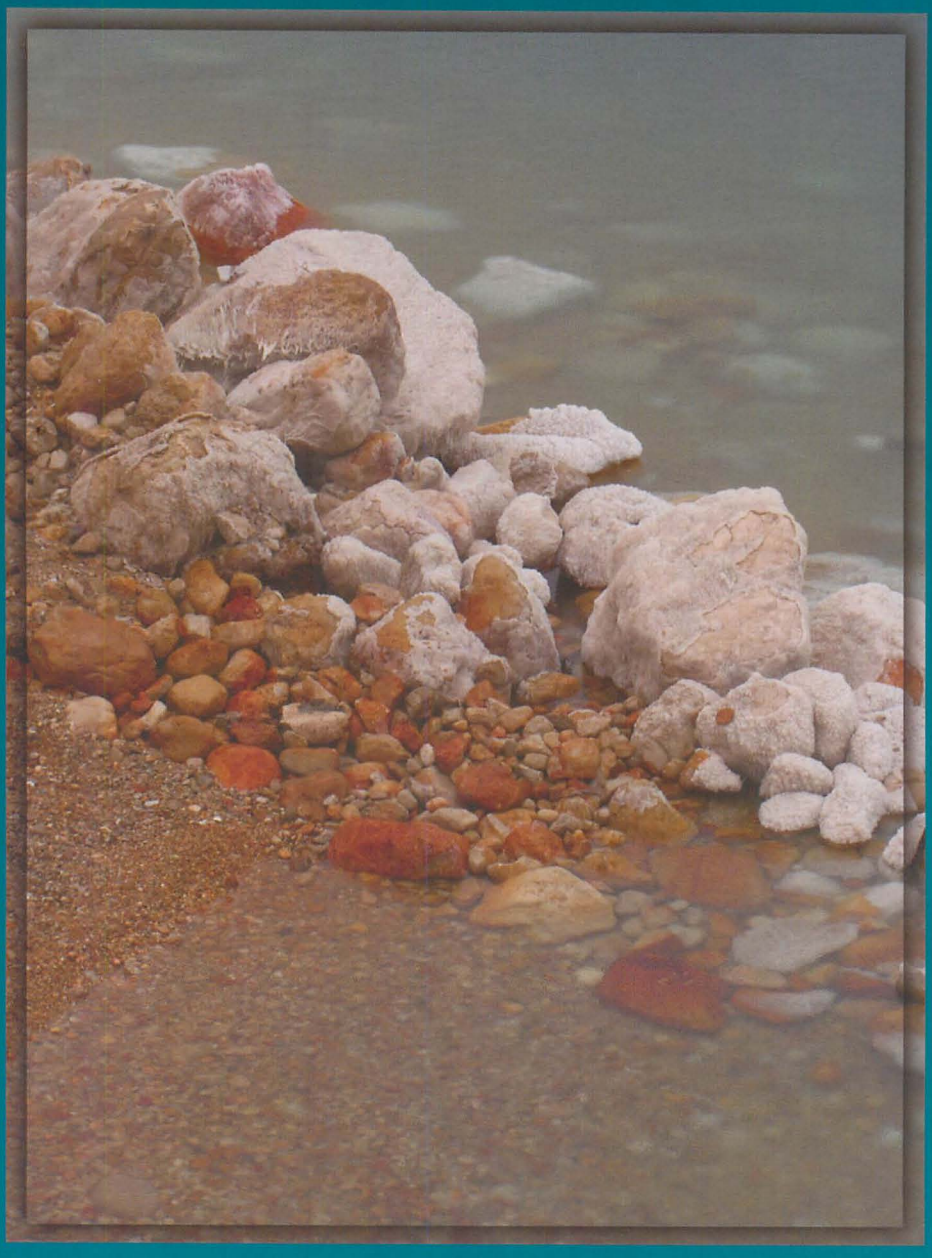

כנס החברה הגיאולוגית הישראלית